Investigation of Surface Chemistry, Micro-Topography, and Wettability Alteration of Calcite-Asphaltene Interface in Presence/Absence of NiO and MgO Nanoparticles using Atomic Force Microscopy and X-Ray Photoelectron Spectroscopy

By

Alisher Rakhmetullin

Thesis submitted to the School of Mining and Geosciences of Nazarbayev University in Partial Fulfillment of the Requirements for the Degree of

Master of Science in Petroleum Engineering

Nazarbayev University

April 2023

ORIGINALITY STATEMENT

I, Alisher Rakhmetullin, hereby declare that this submission is my own work and to the best of my knowledge it contains no materials previously published or written by another person, or substantial proportions of material which have been accepted for the award of any other degree or diploma at Nazarbayev University or any other educational institution, except where due acknowledgement is made in the thesis.

Any contribution made to the research by others, with whom I have worked at NU or elsewhere is explicitly acknowledged in the thesis.

I also declare that the intellectual content of this thesis is the product of my own work, except to the extent that assistance from others in the project's design and conception or in style, presentation and linguistic expression is acknowledged.

Signed on **15.04.23**

_____

ABSTRACT

Calcite is the main constituent of a large class of petroleum reservoirs namely carbonate rocks. Fundamental researches on effect of changes in surface topography, wettability alteration, and surface chemistry of calcite-asphaltene interface in presence/absence of nanoparticles (NPs) are scarce. To address this research gap, a comprehensive experimental research plan was designed in three stages of NP characterization, preparation of asphaltene deposited smooth calcite surfaces followed by X-Ray Photoelectron Spectroscopy (XPS) surveys and Atomic Force Microscopy (AFM) probes. Asphaltene was extracted from a Kazakhstani crude oil using indirect IP-143 standard method. Then, NiO and MgO NPs were characterized using scanning electron microscopy (SEM), Transmission Electron Microscopy (TEM), and Energy Dispersive X-ray Spectroscopy (EDAX) to determine NPs' surface morphology, particle size and distribution, and elemental composition. Then, XPS was used to survey elemental orbitals C1s, O1s, S2p, N1s, Mg2p, Ni2p, and Ca2p on each sample to identify the level of adsorption. An overall XPS survey was conducted to determine elemental composition of the samples. Contact angle measurements were conducted in each stage to check the wettability alteration of each sample. AFM probes were used to investigate micro-topographical features of the surfaces in presence and/or absence of NPs. The analytical methods used, confirmed the authenticity of the NPs used. Contact angle measurements showed that MgO and NiO NPs changed the contact angle of the surfaces to a more water wet state. AFM probes revealed that both MgO and NiO NP reduced the height of asphaltene agglomerates the amount of aggregates on the surface, notably. However, NiO performed better than MgO, significantly. All of the elements of calcite + asphaltene + MgO + heptane sample were detected by XPS. The surface (Ca2p) and Mg2p NP elements were detected at high resolution. Ca and Ni atoms were not detected at high resolution in the Calcite + asphaltene + NiO + heptane sample. This implies that Ni was not absorbed onto the calcite's surface and adsorption kinetics of NPs and calcite-asphaltene interface depends on the type of NP. The results obtained from this research work shed some light on understanding changes of surface topography, surface chemistry, adsorption, and wettability alteration of MgO and NiO NPs at the calcite-asphaltene interface. The research results have applied implications in design of nano agents for alteration of surface chemistry of calcite's surface and adsorption and inhibition of asphaltene.

***Keywords*:** Asphaltene, nanoparticles, calcite-asphaltene interface, AFM, XPS, micro-topography, wettability alteration, surface chemistry, asphaltene adsorption.

ACKNOWLEDGMENTS

I would like to express my deepest gratitude and appreciation to my supervisor, Dr. Ali Shafiei, for his invaluable support, motivation, and guidance throughout the entire research and writing process of this thesis. Without his persistent help and involvement, this work would not have been possible.

I also would like to thank Dr. Sohrab Zendehboudi (MUN, Canada) and Dr. Changhong Gao for serving in my thesis committee. I appreciate their constructive feedback, which contributed to the improvement of quality of this dissertation.

I also wish to extend my sincere appreciation to Dr. Simin Tazikeh, postdoctoral fellow and research group member, for her invaluable and timely assistance in laboratory work and helping me to make sense of my data.

The present work was a part of Collaborative Research Proposal Faculty grant project (091019CRP2103) entitled: “A comprehensive study on asphaltene characterization and screening asphaltene deposition inhibitors for Kazakhstan crude oils”. I would like to acknowledge the financial support I received from Nazarbayev University through this grant.

Furthermore, I would like to acknowledge Nazarbayev University, specifically the SMG faculty and staff, for their constant willingness to help and provide knowledge in a variety of subjects. Their invaluable assistance during my studies is greatly appreciated.

Lastly, I would like to express my gratitude to my family for their constant support throughout my academic pursuits. I owe my achievements to my family, who provided me with opportunities and experiences that have shaped me into who I am today.

LIST OF FIGURES

LIST OF TABLES

1 INTRODUCTION

The term “flow assurance” is coined in the literature to refer to all flow blockage issues caused by asphaltene deposition in oil reservoirs, tubing, other production and surface facilities, and pipelines. Asphaltene deposition in oil reservoirs can lead to formation damage due to blockage of pores and wettability alteration towards more oil-wet state and eventually reduced oil flow rate and oil recovery. Various mitigation measures are suggested to either lessen the deleterious effect of asphaltene deposition or prevent its occurrence.

With an emphasis on special features and capabilities of NPs as adsorbents for effective adsorption and removal of asphaltene from surfaces and inducing favorable surface chemistry changes, and wettability alteration, a brief background on relevance of asphaltene precipitation and deposition as well as flow assurance in oil industry is provided at the beginning of this. Then, the statement of problem is established followed by proposed research objectives and the proposed research methodology. The chapters end with a description of this dissertation’s organization and structure.

1.1 Background

Crude oils are complex mixtures of hydrocarbons, various organic molecules, and small amounts of metals. The petroleum fractions with the largest molecular weight are called asphaltene (Speight, 2004). Asphaltene is the most polarizable fraction and consist of polycyclic aromatic groups with lateral alkane bonds. Asphaltene molecules are found in a wide range of concentrations, ranging from insignificant levels in volatiles to tiny quantities in vapors. It controls the viscosity and affects the extraction, transportation, and refining the crude oil. It took several decades for scientists to understand the precise composition and structure of asphaltene molecules that self-associate into various types of aggregations. A good representation of asphaltene molecules is the model proposed by Yen-Mullins that is widely accepted and used in asphaltene research (Mullins, 2010). Nevertheless, this is still a controversial area of research and differences in view exist among the researchers on various aspects of asphaltene research.

Asphaltene deposition is one of the major issue in the petroleum industry also known as “flow assurance”. Asphaltene molecules deposit on the surface of reservoir rocks altering its wetting state and lowering its permeability due to blockage of pores. Deposition of asphaltene

during oil production especially gas injection processes can also lead to formation damage. This undesirable consequence can harm boreholes and casings; two important production-related elements. (L. Nabzar, 2005). The quantity of organically deposited asphaltene particles during the flow of hydrocarbons is significantly impacted by variations in formation pressure. According to Aquino-Olivos et al. (2001), asphaltene molecules do not deposit in the formation if the pressure is greater than the saturation pressure. In addition, asphaltene precipitates in the reservoir and wellbore if the pressure is less than saturation pressure. When pressure and temperature are reduced, asphaltene deposition occurs (Karambeigi & Kharrat, 2014).

The amount of asphaltene found in crude oils does not correlate with asphaltene instability leading to its precipitation and deposition. Asphaltene precipitation and deposition is controlled first by asphaltene molecule's features and rest of the petroleum fractions that exist in the crude oil. Crude oil's composition and chemistry are crucial factors controlling stability of asphaltene. Stable asphaltene molecules have high hydrogen concentration and moderate aromaticity (Pereira et al., 2007). The impact of temperature on stability of crude oil is very complicated and influenced by a number of factors. Solubility of asphaltene that rises with temperature is the primary contributing factor. The second factor is the compositional changes in the crude oil caused by increase in temperature leading to a poor solubility of asphaltene and its rapid agglomeration and then precipitation. The third aspect is how viscosity affects the pace of agglomeration. As the temperature rises, the viscosity drops increasing diffusivity of asphaltene molecules rises that speeds up their accumulation (Maqbool, 2011).

Asphaltene-surface contacts are occasionally a manifestation of the adsorption processes that drive asphaltene molecules to aggregate and asphaltene and resins to combine. Adsorption is a harmful phenomenon that needs to be prevented in formations, tubing, and producing equipment. Asphaltene strongly favors self-association and formation of clusters (K. Ichikawa, 2004). Two distinct models for asphaltene adsorption are widely used by researchers are Langumir (Kokal et al., 1995), forming a single coverage on the substrate (i.e., monolayer adsorption model) and Freundlich's multilayer adsorption model. Adsorption isotherms represent variations in asphaltenic particles' states in the solutions and on the rock surface (Marczewski & Szymula, 2002). The development of aggregates and bulk deposition of asphaltene are strongly connected processes (Castillo et al., 2001). For such a tendency, there is yet no satisfactory justification.

Factors affecting asphaltene adsorption include: the origin and chemical composition of the crude oil where distinct origins produce asphaltene with varying qualities, the quantity of asphaltene adsorbed depends on its molar weight where molecules with higher molecular weights are predominantly adsorbed onto surfaces in polydisperse settings, the proportion of resins in the asphaltenic samples because of various isolation techniques (Mclean & Kilpatrick, 1997), the solvent's polarization upon being redissolved (Simon et al., 2009), pre-wetting of the molecules (a hydrophilic molecule that has been wet with water adsorbs less asphaltene compared to dry ones), and the type of replaceable cations in the clay matrix and the substrate's elemental composition, and temperature, and duration of the contact.

In situ upgrading crude oils to increase fluid outputs can be accomplished by in situ adsorption of asphaltenic particles inside the wellbore by NPs of metal oxides on silica (Cortés et al., 2012). It was shown that metal-impregnated NPs such as NiO can enter into porous medium, adsorb troublesome asphaltene molecules, and restart the flow (Franco et al., 2013). The aromaticity of the solvent used for adsorption tests has an impact on asphaltenic adsorption, as well. According to the literature, reducing the shape of aggregations causes a decrease in quantity of asphaltene that is adsorbed onto rock substrate (Zahabi et al., 2012). Using chemical agents like surfactants (Kashefi, Shahrabadi, Jahangiri, et al., 2016), polymeric inhibitors (Kashefi, Shahrabadi, Lotfollahi, et al., 2016) is the most efficient ways to reduce asphaltene precipitation. Asphaltene has been removed from crude oil using a variety of adsorbents including rock substrates (Marczewski & Szymula, 2002)**,** clays and formation rocks, metal surfaces (Abdallah & Taylor, 2007), and various metal-based NPs (Hashemi et al., 2016).

The exceptional characteristics of NPs such as their small size (1-100 nm), functionalizable substrate, and large surface to volume proportion that enables them to access very small pore throats in the reservoir and improve the flow and production makes them an ideal candidate for inhibition of asphaltene precipitation (Mirzayi & Shayan, 2014). The nature of asphaltene and composition of NP and the substrate have a significant impact on how much asphaltene is adsorbed onto them (Nassar et al., 2011a). Various factors are involved in adsorption of asphaltene onto NPs including the substrate charge, the acid-base contact of surfaces of NPs and asphaltene particles (Mirzayi & Shayan, 2014).

1.2 Statement of Problem

Precipitation and deposition of asphaltene is a widespread problem in petroleum industry. Application of NPs has yielded promising results in adsorption and inhibition of asphaltene from precipitation and deposition with direct implications in flow assurance and EOR strategies. The deleterious effects of asphaltene precipitation and deposition in oil reservoirs and the importance of flow assurance in carbonate reservoir rocks is prominent. Further fundamental research is needed to delineate the interaction between calcite-asphaltene interface in presence and/or absence of nanoparticles (NPs) using the state-of-the-art analytical research facilities. Such fundamental level research is key to further the current understanding of factors controlling changes in surface micro-topography, chemistry, and wettability characteristics of the calcite-asphaltene interface in presence or absence of NPs. Outcomes of such research work will directly impact our ability in design, evaluation, and deployment of more effective inhibitors to enhance the flow of oil and improve the recovery of oil from carbonate reservoirs. It might have other implications in other areas of applied sciences such as environmental engineering research.

1.3 Research Objectives

The main objectives of the current research work are:

- To confirm authenticity of NiO and MgO NPs and characterize them using scanning electron microscopy (SEM), Transmission Electron Microscopy (TEM), and Energy Dispersive X-ray Spectroscopy (EDAX) to determine their surface morphology, particle size and distribution, and elemental compositions.
- To conduct contact angle measurements on each sample at each stage to investigate wettability alteration of the samples considering the surface roughness effect.
- To conduct XPS surveys on pure asphaltene, pure calcite, calcite + asphaltene and calcite + asphaltene + MgO NP + heptane and calcite + asphaltene and calcite + asphaltene + NiO NP + heptane samples to determine the elemental composition of the samples under investigation. Furthermore, to conduct an elemental survey of orbitals via using XPS C1s, O1s, S2p, N1s, Mg2p, Ni2p, and Ca2p on the samples to identify the level of adsorption of NP on calcite’s surface.

- To conduct AFM probes on the special surface samples prepared to delineate micor-topographical features of the calcite surfaces in presence and/or absence of NPs and analyze the height and surface coverage of asphaltene aggregates deposited on the surface of the calcite.

1.4 Research Methodology

This is an experimental research conducted using state-of-the-art research facilities in Nazarbayev University's Core Facilities, SMG labs, and Dr. Shafiei's lab. The details of each method, the materials used, and their step-by-step experimental procedures are described in detail in Chapter 3. The work was divided into 5 main stages as the following:

- Asphaltene extraction from a paraffinic Kazakhstani crude oil using indirect IP-143 standard method and its characterization using FTIR, BET, NMR, and XPS,
- Characterization of NiO and MgO NPs using scanning electron microscopy (SEM), Transmission Electron Microscopy (TEM), and Energy Dispersive X-ray Spectroscopy (EDAX) to determine NPs' surface morphology, particle size and distribution, and elemental compositions,
- Sample preparation for XPS and AFM probes: Special calcite + asphaltene + MgO + heptane and calcite + asphaltene + NiO + heptane samples according to specific sample preparation procedures for XPS and AFM surveys,
- Sample preparation and contact angle measurements for calcite surfaces under various conditions in line with the XPS and AFM sample preparation and testing programs. The calcite surface samples preparation by polishing and cutting specimens to meet the requirements of each equipment, especially the surface roughness that must be below 5 μm,
- Conduction of XPS survey on pure asphaltene, pure calcite, calcite + asphaltene and calcite + asphaltene + MgO NP + heptane and calcite + asphaltene and calcite + asphaltene + NiO NP + heptane. Based on the method of sample preparation, conduction of elemental orbitals C1s, O1s, S2p, N1s, Mg2p, Ni2p, and Ca2p on each sample to identify the level of adsorption. Moreover, conduction of an overall XPS survey on each sample to determine the elemental composition of the samples under investigation.

1.5 Thesis structure

The following are the chapters that make up this thesis. The background information about asphaltene, its precipitation and adsorption, problem statement, aims and study techniques are all included in Chapter 1. A thorough survey of the literature is presented in Chapter 2 with particular attention paid to the significant scientific works reported in the literature with emphasis on crude oil fractions, asphaltene management techniques, and factors affecting deposition and inhibition. A detailed overview of the methods used in this research is provided in Chapter 3 along with a step-by-step procedures and equipment used to carry out the planned investigation including asphaltene extraction, surface preparation, AFM, XPS, and contact angle measurements. The outcome and discussion of the abovementioned equipment and methods is presented in Chapter 4. The findings of the calcite surface features are provided in a number of images and tables. Chapter 5 includes a summary of the conclusions as well as some suggestions for additional research work.

2 LITERATURE REVIEW

In this chapter, first an overview of common definitions for asphaltene is provided with a brief review of different features of asphaltenes such as their aromaticity and molecular weight and its measurement techniques. Then, consequences of asphaltene precipitation and deposition in reservoirs with special reference on wettability alteration and permeability impairment are discussed. Various mitigation measures suggested in the literature to counter negative effects of asphaltene precipitation and deposition in oil reservoirs are discussed, briefly. This chapter ends with relevant literature on effect of asphaltene precipitation and deposition on wettability alteration, surface morphology and micro-topography of rock surfaces, and adsorption of asphaltene by NPs.

2.1 Definition of asphaltene

Asphaltene is the heaviest fraction of crude oil mainly characterized as a compound of C and H atoms with a low number of heteroatoms such as S, O_2, and metals such as Ni and Fe (Dickie et al., 1969). Asphaltene molecules consist of several of polyaromatic rings and aliphatics within other natural chemical groups. Since petroleum does not include as many heteroatoms asphaltene fraction does, these heteroatoms will accumulate in the asphaltene fraction. Gaweł et al. (2014) described the compositional assessment of several distinct hydrocarbons together with associated subsequent fractions, such as saturates (S), aromatics (A), resin (R), and asphaltene (A) fractions. As anticipated, the listed substances showed the greatest H-to-C rations. A relationship between the H-to-C ratios and the aromaticity components could be determined, which may be used to determine the degree of ring condensing. Sulfur is distributed roughly evenly amongst aromatics, resins, and asphaltene. Sulfur is not present in saturates indicating that the majority of the sulfur is found in chemicals that are connected to polycyclic aromatic molecules (Sharma et al., 2002). Additionally, asphaltenes have much larger O_2 and N_2 levels compared to different portions, which accounts for their stronger polarity. In comparison to various components, asphaltenes have a substantially higher metal composition. Asphaltenes include metals mostly in two types. Metalloporphyrins, characterized as heterocyclic molecules in which metals may attach to internal receptors to generate combinations, are the primary possible formation of metals. Another type is through flaws, metals could potentially be included in the aromatic center of asphaltene particles (Mullins, 2007).

2.1.1 Aromaticity

Understanding the aromaticity features and composition of asphaltene is required to comprehend the aggregating behavior and ability to self-associate. Aromaticity is a feature of interconnected cyclo-alkenes where the stability of the atoms is influenced because of electrons' ability to be dispersed in the pi-orbital. Aromaticity is a significant component in determining stability of crude oil. Bouhadda et al. (2010) reported that aromaticity of asphaltenes vary between 0.4 and 0.7. Whenever the aromaticity of asphaltene is strong, it tends to agglomerate and be deposited. It rises when both mentioned factors rise (Speight & Moschopedis, 1982). Moreover, the rheology of asphaltenes is affected due to increased temperature. According to Kayukova et al. (2016), several compounds such as carboids and coke could be formed because of polymerizing and condensing, which increases the level of aromaticity. The aromaticity value can be calculated using a variety of methods including nuclear magnetic resonance, infrared spectroscopy, elemental composition, and other methods. Calculating the index of aromaticity involves dividing the total quantity of aromatic carbons by the total sum of aromatic and aliphatic compounds (Y. J. Liu & Li, 2015).

2.1.2 Molecular Weight

Molecular weight is among the most essential characteristics required for developing correlation of physical parameters of asphaltenes. Asphaltene is a polydisperse mixture of a variety of atoms of various shapes and molecular properties. The typical molecular weight of asphaltene monomers ranges between 500 and 1,000 g/mol. For aggregates, the range of molecular weight goes up to 10,000 g/mol (Yarranton, 2005). During the calculation of molecular weight, there could be several problems such as self-association of molecules into nanoaggregates. In terms of molar mass, it is dependent on the temperature, solvents, and concentrations. The molar mass of asphaltenes increases when the abovementioned factors of the solvents are increased.

Three techniques are commonly used to measure the molecular weight, which are:

1) Gel permeation chromatography (GPC),
2) Vapor pressure osmometry (VPO),
3) Mass spectroscopy (MS).

2.1.2.1 Gel permeation chromatography (GPC)

Gel permeation chromatography sorts molecules according to their size. The volume of the sample in the liquid is the sole factor used to determine the separation. As in traditional high-performance

liquid chromatography, no contact with the packaging of the row is necessary. The method of splitting depends on the substance's volume. Moreover, the material should be dissolved in the appropriate solution for a proper chromatography analysis (Lambert, 1971). The chromatography includes PSS-SDV sections with pore diameter of 100 Å, 1000 Å and 10000 Å. They serve as filtration points for molecules and might be small or big. The small sized columns block bigger molecules. On the other hand, smaller molecules enter into majority of columns and remain in place for a longer period of time (Lambert, 1971). GPC procedure is shown in Figure 1. In this case, Tetrahydrofuran (THF) is used as mobility agent because of its low viscosity. The solute sample is injected into a channel of solvents that is constantly running in GPC system. Masses of very porous, stiff grains are all stacked closely in columns as THF passes past. The procedure is remotely controlled by data-collectors, which also keep track of the outcomes and determine the average molecular weight (Hendrickson & Moore, 1966).

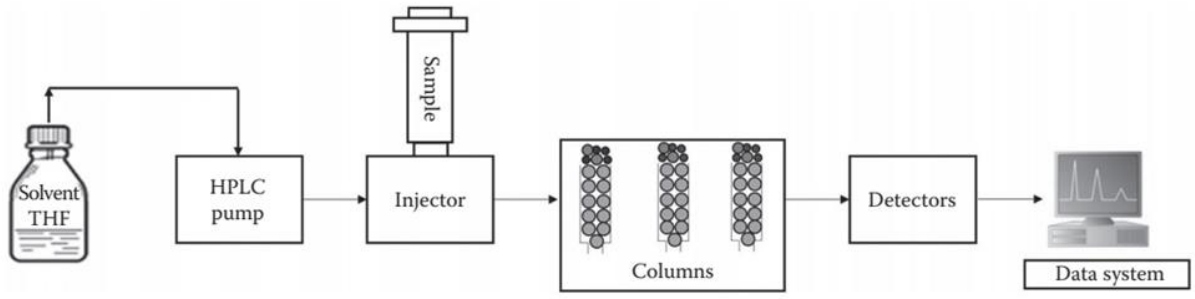

Figure 2-1: Gel permeation chromatography procedure (Walker & Rapley, 2008).

Chromatography measures polydispersity. Polydispersity, itself, is the ratio of average molecular weight to the number average molecular weight. According to Buenrostro-Gonzalez et al. (2002), it gives information about the tendency of the asphaltene molecules to aggregate. The average molecular weight depends on particles with various weights. On the other hand, number-averaged weight depends on the molecular agglomerations, by which physical characteristics of asphaltene particles are influenced. Average weight should be higher compared with the numbered-average molecular weight; otherwise, asphaltene aggregations are totally monodispersed. The significant disadvantage of the GPC techniques is the use of polystyrene as the benchmark. Since crude oil with peri-condensed polyaromatic structures is likely to dissolve longer compared with linear polymers with equal molecular weight. Meanwhile, Sato et al. (2005)

argues that the number-averaged weight measured for asphaltene molecules is lesser than anticipated. It is believed that the molecular weight found using this approach is a polystyrene similar molecular weight instead of the true indication. One more issue is that part of the aggregations must be removed by filtering the solution using 0.2 μm filtration papers. Consequently, this chromatography cannot be used to quantify asphaltene's molecular weight at various ratios.

2.1.2.2 Vapor pressure osmometry (VPO)

Vapor pressure osmometry is another technique used to calculate molecular weight of asphaltenes. It is a typical approach for determining the weight, but one of its biggest limitations is that it is unable to accurately estimate the molecular weight of asphaltene particles in a liquid due to the tendency of asphaltenes to aggregate. The primary benefit of using VPO over GPC approach is its ability to determine the molecular weight of asphaltene particles with various concentrations, according to (Yarranton et al., 2000). Calculations of the asphaltene molar mass depending on the VPO technique have a reproducibility of about 15%. VPO techniques are focused on the variations in vapor pressure produced when a little quantity of the solution is mixed with a solvent. In VPO, a couple of thermistors containing a purified solvent and a droplet of solute are put into a camera. The varied pressure of the vapors brought on by the differing solute compositions causes every thermistor to display various temperatures. The resistivity changes in accordance with the solution's molar mass due to changes in temperatures (Barrera et al., 2013).

2.1.2.3 Mass spectroscopy

Mass spectroscopy is widely used for determining molecular weight of asphaltenes. Evaporation of samples and ionizing form the foundation of this approach. This is a potent technique for identifying and quantifying compounds in common and complicated solutions by measuring the mass-to-charge ratio of ions. It involves vaporizing the crude and ionizing it with a generator of ionization. External forces will divert the generated ions. Afterwards, ions will reach a sensor after being diverted. A detector identifies ions then each moment depending on intensity of the magnetic force. Relying on the comparative presence on the y-axis and the supposing that ion is charged positively, it is feasible to determine the weight proportion of every ionic fraction (Ana Varela Coelho & Catarina de Matos Ferraz Franco, 2013).

An analytical method is applied to distinguish between organic and several inorganic substances is known as Fourier transform infrared (FTIR) spectroscopy. Its basis is the absorbance of mid-infrared light. The various connections in a molecule typically receive infrared light of frequencies while subjected to it that alters its dipole moment and, consequently, the stimulated vibrational condition. The enthalpy changes among the basal and stimulated vibrational conditions determine the wavelength of beam that a particular link will absorb. Hence the wavelengths absorption by the samples are a trait of its molecular structure. The resulting representation of radiational absorption against wavenumber is known as the FTIR spectrum (Silverstein Robert M., 2014). A few properties of petroleum and asphaltene fraction such as the quantity of asphaltenes in a petroleum, their aromaticity, the presence of heteroatomical clusters against aliphatic substances, and the extent of evaporation in the polyaroma have been defined using the functional groups' ability to be defined and radioactivity absorption spectrum to be documented (Asemani & Rabbani, 2016). The listed variable are applied to describe the dynamics of asphaltene fraction in petroleum as well as the geochemical development and connection of hydrocarbons from various places (Asemani & Rabbani, 2016).

Nuclear magnetic resonance (NMR) is a characteristic of an atom's nucleus that is connected to nuclear rotation. A magnetic force is created, once an atomic nucleus rotates. If there is also an exterior magnetic signal, the nucleus will coordinate alongside or opposing the outer magnetic signal. In petroleum engineering, NMR is primarily applied to determine the aromatic and aliphatic carbonic parts, as well as the converted aromatics of asphaltene fraction (Castro, 2006).

2.2 Consequence of asphaltene precipitation

Precipitation and deposition of asphaltenes on surfaces can lead to a variety of issues in petroleum engineering applications. In this section, the detrimental consequences of asphaltene precipitation and deposition and some solutions to mitigate these challenges in the oil and gas industry are discussed.

The effects of asphaltene precipitation in the formation, casings, and infrastructure are significant. The formation, where it can have a considerable effect on the flow rate, is of particular importance. The asphaltene deposition is caused by asphaltene's adherence on the rock's substrate and the obstruction of the flowing route caused by deposition. Therefore, the permeability is

decreased and the mineral's wetness condition is changed to a more unfavorable state. In both static and dynamic asphaltene adherence studies, several mineral types with various grain shapes were used to explore this idea. This was done in an effort to measure and link any relationships between mineralogy, grain shape, and speed of precipitation. The temperatures and frequency of asphaltene dissociation for the nanometric adsorption are linearly related according to investigations on the effects of adsorption scale, temperatures, and pressures.

Disrupting asphaltenes' aging procedure is an effective way to avoid asphaltene accumulation. As seen in Figure 2-2, as asphaltene particles continue to agglomerate, they started adhering and building on top of one another. This model is called Yen-Mullins model and it demonstrates the predominant asphaltene molecules and colloidal forms in fluids and hydrocarbons (Mullins et al., 2012). Whenever the layering process among various asphaltene particles starts, the contacts between molecules create a phase of greater stability by causing the particles to produce nanoaggregates by adhering to one another. Each asphaltene compound consists of polyaromatic bonds connected by rigid aliphatic bonds, replacement of aliphatic bonds, various heteroatoms, and at least single polar components. The polarity of particles may differ significantly based on the many components attached to it. Furthermore, the kind of asphaltene might alter the discipline of the resulted layering. In identical thermodynamic circumstances, heptane-plus asphaltenes inclined to exhibit orderly layering than pentane-plus asphaltenes.

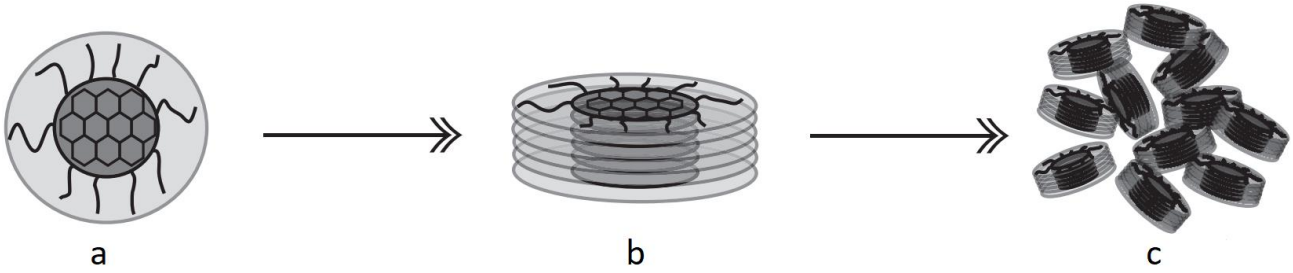

Figure 2-2. Asphaltene agglomeration process (a – asphaltene molecule; b – asphaltene nano-aggregate; c – cluster) (Hoepfner, 2013)

Once the oil medium undergoes a shift in equilibrium that promotes deposition, asphaltene nano-aggregates start to expand in size. Since the asphaltene phases separate out of an oil-rich state to an asphaltene-rich state, bigger groups are created with additional nano-aggregate layers (Figure 2-c) as microscopic agglomerations. When the aging procedure begins, the composition of asphaltene groups faces a microscale alteration. During deposition, different compounds such as

aromatics and resins also precipitate along with asphaltene keeping them viscous and in liquid-like state. Asphaltenic particles, as the heaviest and polar constituents of hydrocarbons, are retained in crude by resins at optimum settings. The following variables could be thought as of significant influences on asphaltenic precipitations: pressure, temperature, chemical content, volume, and fraction of gas injection for EOR (Davudov & Moghanloo, 2019), the form of flow in porous medium, and the features of the pipes where fluid moves (Buenrostro-Gonzalez et al., 2004). The most crucial factor in precipitation of asphaltene is pressure, with other variables coming next. The most asphaltene are deposited in near wellbore area because of the pressure drops caused by increased flow rate (Kord et al., 2019). The method that prevents the precipitations of asphaltene in boreholes effectively is possibly reservoir pressure control (Lobanov et al., 2020). Asphaltene particles precipitated during the extraction phase, followed by a corresponding reduction in pressure and temperature, create sludge-like and strongly adhesive aggregates (Mullins, 2007).

2.3 Mitigation measures for asphaltene precipitation and deposition problem

To guarantee the greater performance of the petroleum production procedure, invention of a cost-effective method for managing asphaltene precipitation is of vital economic relevance. Accurate laboratory tests and computational assumptions may give crucial insights on asphaltene deposits avoidance and removal procedures. Generally, there are two main types of techniques have been created and used to deal with precipitates, which are inhibition and treatment (Figure 2-3). Using inhibitors and manipulating cumulative product rate circumstances and characteristics are two examples of inhibition methods. Overall, there are five widely used techniques based on treating exist, such as mechanical, thermal, chemical, biological, external (Gharbi et al., 2017).

Two basic approaches are used in the field to address the problem of asphaltene precipitation and deposition: treatments and cleanup. The typical deposition cleanup techniques fall into one of three classifications: mechanical, chemical, and thermal procedures (Shedid, 2004b), with thermal approach being the least effective. Chemicals used frequently include solvent and acid injections that both may mainly dissolve precipitations and cannot stop their accumulation. Additionally, the requirement for chemical treatments on a regular basis during the course of about a year likely to lead to higher cost and more regular shutdowns (Zoveidavianpoor et al., 2013). Consequently, wherever possible, avoidance is often preferable to therapy. In reality, when the producing

procedure cannot be changed to avoid precipitation, chemicals and use of other approaches are typically adopted (G. Ali Mansoori, 2010). One more intriguing method to avoid or reduce precipitation is to apply specific layers to the interior substrates of pipelines. Controlling precipitation in surface facilities by altering the conditions is the proven way to prevent its depositional phenomena. For example, by lowering shear rate, decreasing difference in pressures, managing unsuitable materials, and adding an insulating agent to prevent heat loss are the common measures to avoid precipitation of asphaltene in oil reservoir (S. L. Kokal & Sayegh, 1995).

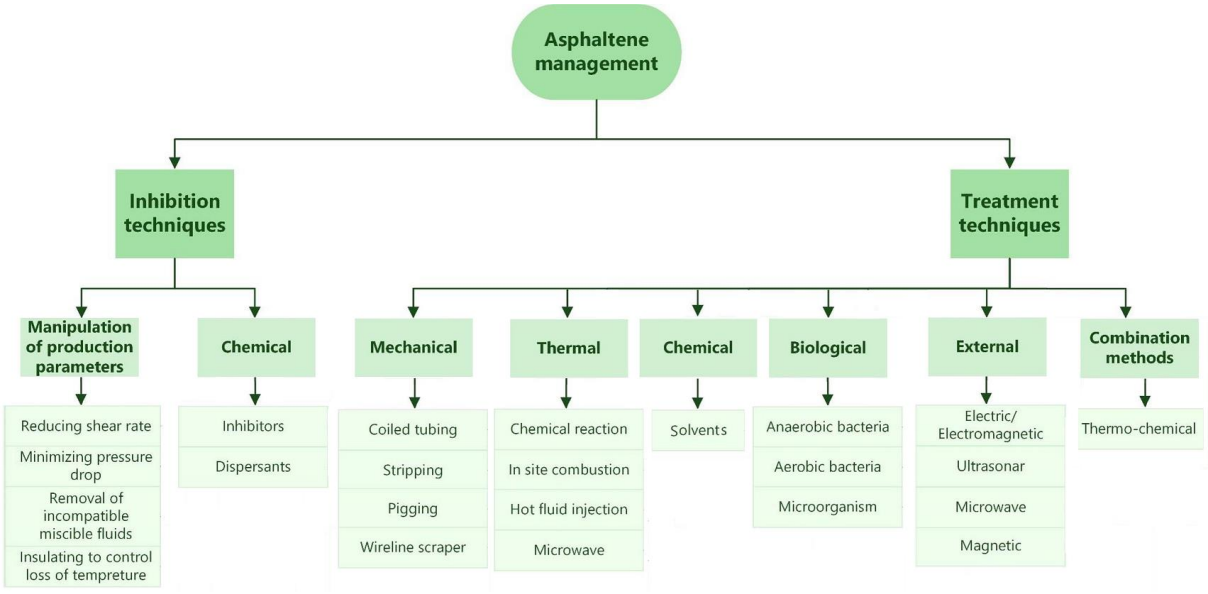

Figure 2-3. Asphaltene management classifications (Alimohammadi et al., 2019)

2.3.1 Chemical inhibition

Asphaltene precipitation inhibition using chemicals is one of the most frequently used methods for controlling asphaltene precipitation and deposition (Leontaritis, 1989). Asphaltene dispersers, a kind of asphaltene inhibitor, are compounds that designed to avoid asphaltene from forming in the producing tube. The dispersants are to peptize asphaltene aggregates by connecting asphaltene to own polar categories and extending the aliphatic chain into the solid solution, generating a steric stabilizing layer surrounding them (Stephenson & Chemical, 1991). The polar compounds generally comprise of heteroatoms that may adhere to asphaltene's surfaces; while, the alkyl group relates to the aliphatic tails that can inhibit asphaltene particles from aggregating (Goual et al., 2014). Connections among aromatic rings, hydrogen groups, acid-base contacts, dipole-dipole interrelations, and complicated metal ions are all potential relationships of asphaltene and

dispersants. Non-ionic amphiphiles, ionized fluids, nano-fluid, polymers, and other chemicals have varying degrees of efficiency in preventing asphaltene deposition. A great deal of researches reported in the literature addressing factors affecting effectiveness of mixtures.

Asphaltene properties, solvents parameters, additive compounds, and the quantity of molecules adsorbed on surface of asphaltene have been documented to have a role in efficiency of the suppression of asphaltene deposition (Kelland A., 2009). The efficiency of three asphaltenic dispersants, based on 4-dodecyl, in precipitation process, emulsification, and NP development was investigated by Kraiwattanawong et al., (2009). Applying dispersing agents causes asphaltenic agglomerations to be stable or to be divided into relatively small particles, postponing the start of deposition (Kraiwattanawong et al., 2009). Higaki et al. (2014) investigated the asphaltene precipitation's adsorption behaviors, adhesion, and detaching on various polymeric surfaces.

2.3.2 Mechanical methods

Mechanical methods of asphaltenic deposit removal from surface facilities include coiled tubing operations, tripping, and pigging. All of the mentioned methods have both their own strengths and weaknesses. These procedures are effective and do not contribute to skin appearance, but they are not cheap, take a lot of time, and are challenging to use (Al-Yaari, 2011). Precipitation that has built up in manifolds that can transport pigs can be removed via pigging. For asphaltene, pigging equipment with cups is effective during removing the depositions. Its removal effectiveness depends on how often it is used and needs proper optimization. The equipment can be easily trapped if the procedure is carried out too quickly or slowly, which leads to notable precipitation (Al-Yaari, 2011). The latest breed of pigs known as "smart pigs" is used for heating process, distance viewing, and controlling. The internal surfaces of tubing can be cleaned from asphaltenic deposits using scraping and coiled tubing, as well. However, the ability of coiled tubing is limited due to the long distance between the deposits and the equipment (Guo, 2014).

2.3.3 Thermal methods

Asphaltenic deposits can be remedied thermally via injection of fluids, in-situ combustions, heat (enthalpy) change for negative points, and microwave. A prompt reaction is anticipated because this type of treating is quite effective. However, it is possible for skin to happen, which suggests that repeated treatments are required (Bernadiner, 1993). Using circulation of fluids in the system,

the precipitates are dissolved. However, it is necessary to control the dissolved asphaltene from redeposition (Bernadiner, 1993).

2.3.4 Chemical methods

Another technique to deal with precipitates is application of aromatics (G.Ali Mansoori, 2010). The solvents break up the weaker compounds of deposits, which also eliminates bulk deposits. Several research studies reported on crude oil solvents, methanol, paraffins (Miadonye & Evans, 2010). Moreover, xylene and toluene were used more frequently to remove asphaltene deposits. In some cases, chemical treatments are not suitable because of environmental issues, human factors, and possible corrosion occurrence (Shedid, 2004a).

2.3.5 Biological methods

Biological methods mainly include treatments with microorganisms such as fungi. One of the methods is based on biodegradation process, where asphaltenic solids become lighter in terms of composition. The lengthy procedure takes up to a year. By consuming the precipitated asphaltene, microorganisms create carbon, heat, and a number of other substances (Xue et al., 2015). Biological approaches are favorable, since they are not flammable and toxic, no damage to the environment, and not combustible. They do have significant downsides, such as their aggressive behavior for tubing, like corrosion occurrence and difficulties in controlling the treatment. Additionally, the limitation of this approach is that it is applicable for water production wells only (Abdulrazag Y. Zekri, 2001). However, it is important to evaluate the hazards connected to these kinds of therapies.

2.3.6 External methods

The deposited asphaltene is treated using methods that use external forces including magnetic, ultrasonic, and electrostatic/electrodynamic power. The majority of the listed techniques can be used in modest ranges (G. Ali Mansoori, 2010). Kaushik et al., (2012) reported using ultrasonic aided cavitation to strengthen hydrocarbon splitting under atmospheric conditions for cleanup processes. As a result, their team investigated how ultrasound affected the residue content and reported that the asphaltenic composition and viscosity of the residue was greatly decreased proving that the ultrasonic technique (Kaushik et al., 2012).

2.3.7 Combination methods

Organic deposits can be removed by combining chemicals with thermal methods. The method uses energy generated by an enthalpy decrease to dissolve and remove the precipitates. A blend of esters and surfactants is created because of melting and dispersion of organic precipitates. Additionally, the use of chemicals can slow the process in the harmed near wellbore area (Sheykh Alian et al., 2013). It is crucial to remember that to mitigate the problem, the treatment must be continued until the plug has fully formed. The effectiveness of the treatment is restricted to dispersion if carried out when the precipitates formed (Civan, 2007). The treating method consists of three stages: a process of preflush, in which precipitates are soaked in a special organic liquid; after the flush stage, in which energy is generated and a combination of solutes are used to remove the precipitates. The last stage is a procedure of asphaltene cleanup and removal. To prevent production of deposits during the treatment operation, chemical compatibility studies are typically carried out (Al-Ibad & Civan, 2013).

2.3.8 Dispersion

The precipitation of asphaltene occurs because of destabilization of asphaltene nano-aggregate depositing as tiny agglomerations and then, assembling them into bigger ones throughout the process. Abovementioned microscopic agglomerations, also known as primary particles, are typically vary in hundreds of nanometers in size. In addition, there is a term for micro-aggregates, which are bigger groups of asphaltene, substantially bigger than microscopic clusters. According to Vargas et al. (2014), asphaltenes move through several steps on their way to reach a solid like phase as depicted in Figure 2-4. Nanoaggregates deposit from the liquid state into microscopic clusters once asphaltene is destabilized. The initiation of asphaltene deposition might be reached because of variations in affecting parameters such as pressure, temperature, or liquid properties of the reservoir.

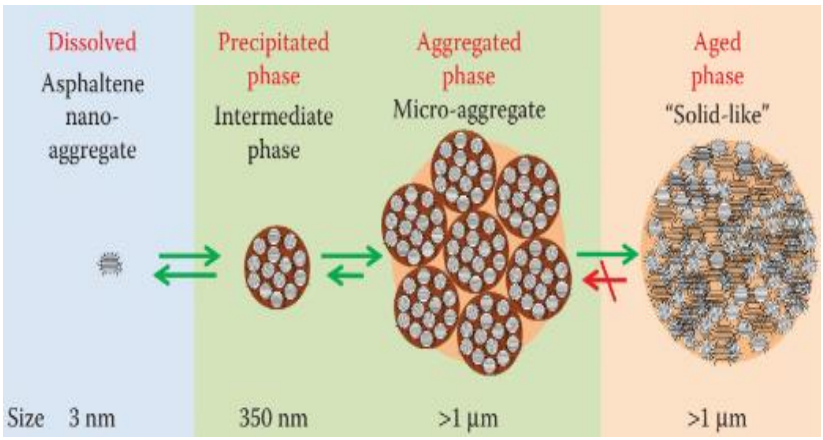

Figure 2-4. Stages of asphaltene precipitation (Vargas et al., 2014)

Chemical dispersants are amongst extensively used ways for minimizing asphaltene precipitation. They usually act as an inhibitor by postponing the accumulation of asphaltene particles. Chemical dispersants are created to peptize and stabilize asphaltene molecules in solutions. Kelland A. (2009) suggests that the major stabilizing process consists of contacts involving dispersants and asphaltene particles. The composition of asphaltene particles may change based on the crude oil samples, with distinct asphaltene including heteroatoms, aromatic compounds that differ. It is assumed that the perfect chemical dispersants performs same as resins, which is able to stabilize the asphaltene molecules. Injection of inhibitors is driven by the notion that it can avoid asphaltene from aggregation and deposition. A difficulty while using chemical dispersants as precipitation regulators is that they are not always efficient in reducing dimensions of asphaltenic agglomerates and not always reduces the precipitation of asphaltene. This happens because tiny molecules have a great surface area that might lead to increase in the potential for precipitation. In addition, some dispersants can generally worsen asphaltene precipitation in the oilfield according to Melendez-Alvarez et al. (2016). Low effectiveness of inhibitors used in the industry is attributable to inadequacy of the commercialized procedures presently used to evaluate such compounds.

2.3.9 Electrostatic interactions

Exposing asphaltene systems to electric currents was found to change their adsorption nature that provides a means to discourage precipitation. In 1975, Lichaa et al. demonstrated similar phenomena with an electrode test. In their arrangement, the electrode of steel was separated by 2 mm's inside the equally divided mixture of crude oil and electro-resistant diluent. The mixture

itself was subjected to a certain indication of voltage for three to five days. As a result, the electrodes with negative charges were invariably covered the crude oil full of asphaltene; while, the electrodes with positive charge covered with just a small coating of the crude oil. Lichaa et al. examined the ability of electromagnetic field to transport asphaltene in mixtures. By progressively raising the voltage in a mixture monitored with microscope, it was determined that 120 volts is enough to generate considerable displacement of asphaltene in liquids with minor electrical effect responses. Khvostichenko (2009) reported that the solid asphaltene particles in crude oil have a clear negative charge, but the particles destabilized by positively charged *n*-heptane. These results are encouraging since they provide a good strategy for preventing asphaltene precipitation. According to Vargas et al. (2010), the interaction between surfaces and varying circumstances enhances the adhesion and the potential accumulation of asphaltenic nanoscale categories. Manipulating the electrostatic mechanisms related to precipitation processes enables control of electrode charges intrinsic to asphaltene structurally controlled by various asphaltenes. With further refinement, an inhibitory approach that regulates the mobility of asphaltenes in mixture might provide significant advantages.

Methods for managing asphaltene deposits are essential for economics of oil production. Identifying the appropriate control solutions for precipitation problem is quite difficult because treatment and removal methods have certain disadvantages (Ovalles et al., 2016). Both human and nature protection dangers issues should be taken into consideration when applying chemical approaches (Samuelson & Schlumberger, 1992).

2.4 Effect of asphaltene precipitation on wettability

Surface chemistry of reservoir rocks influences wettability, which is defined as the tendency of liquids to adhere to a surface (Morrow, 1990). Wettability is regarded as a significant factor in EOR affecting oil recovery. The key elements influencing wettability modification include surface chemistry of the reservoir rock, energy availability, and characteristics of liquid. (Otitoju et al., 2017). For example, sandstone reservoirs are often water or mixed wet. After adsorption of polar material or precipitation of organic components contained in hydrocarbons, these surfaces become more oil wet (Kaminsky & Radke, 1997). The process of precipitation of asphaltene has the ability to transform homogeneous surfaces to heterogeneous by changing the wetness of the rock from its neutrally wetting condition to a highly oil-wet one. As a variety of elements determines the

condition of a surface, wettability has a very complicated character. Nassar et al. (2012) reported that asphaltene molecules affect affinity and adsorption capacity and there is a clear correlation between molar mass and quantity of adherence. Additionally, adsorption affinity is relatively poor for lesser molar mass despite a high adsorption capacity.

Characteristics of a surface, different hydrocarbon components, content of brine and environmental factors are a few of the variables that influence wettability. According to Wang & Gupta, (1995), pressure has no discernible impact on contact angle between crude oil and a surface made of calcite or quartz. In addition, when temperature is increased, quartz's wetting parameter's changes to oil wet and calcite gets water wet. M. Rajayi & A. Kantzas (2011) showed the effect of pressure on contact angle between bitumen and water. They reported that the interaction's contact angle rises with temperature at a particular pressure value. The state is mostly water-wet at reduced temperatures, and as the temperature rises, the state's wetness shifts approaching neutral wet state. Najafi-Marghmaleki et al. (2016) showed how temperature affects the wetness of different carbonate surfaces. According to Andersson et al. (2016) inclusion of divalent transition metal particles increases the hydrophilicity of the calcite substrate. To improve recovery factor, they suggested using divalent ions like Mg and Fe, for the lowest and highest temperatures of carbonate reservoirs respectively (Andersson et al., 2016).

Various methods for measuring wettability are available including measuring contact angle, imbibition approaches using the Amott Cell technique, and USBM index (Anderson, 1988). Significant features of solid surface wettability include contact attributes such as roughness and heterogeneity of the surfaces (Buckley, 2001). Researchers use these features to correlate surface attributes with observed wettability indexes. One of the convenient and frequent methods to gauge wettability characteristics is measuring contact angle. This approach disregards the impact of roughness on wettability.

According to Craig's criteria, the wetting state changes from oil to water-wet state if the residual water saturation rises, the relative permeability shifts, and the crossover point moves to the right following NPs usage (Giraldo et al., 2013). Coreflooding can be used to capture wettability changes by correlating the differences between several rock and fluid parameters. The impact of different nanofluids on change of the wettability of several kinds of minerals has been the reported in the literature. To determine the wetness Li et al. (2015) used Amott tests. They reported that SiO_2 NPs converted oil-soaked sandstone samples to moderate wetness. In addition,

Roustaei et al., (2015) conducted an analytical investigation to determine how SiO_2 NPs affected a carbonate formation's wetting properties. The outcomes also showed that SiO_2 NPs might be used to improve wetness of carbonate samples. Al-Anssari et al. (2016) reported that the SiO_2 NPs caused wetting parameter changes in oil and mixed wet calcite surfaces.

Hendraningrat & Torsaeter (2014) examined the impact of Al_2O_3 NPs on wetting state change and reported that the wettability of sandstone samples can easily be changed by spreading Al_2O_3 NPs from a completely oil-wet to a completely water-wet state. After that, TiO_2 and Al_2O_3 NPs were used by Hendraningrat (2014b) and TiO_2 NPs made the quartz substrate strongly water wet. Karimi et al. (2012) reported alteration of wettability of a carbonate rock by using ZrO_2 NPs-based fluid. Li (2013) measured contact angle between crude oil within different percentages of SiO_2 NPs on synthesized SiO_2 and reported that a variety of variables including NP type and volume as well as brine might influence the wettability change brought on by fluids. Hendraningrat, Li, & Torsaeter (2013) used the Amott-test to determine how nanoparticle shape affected clearly wetting states. As NPs volume shrank, the contact angle of the water state shrank, as well. This is because once the number of NPs is high and their size is smaller, their electrostatic repulsion is greater. Additionally, (Hendraningrat & Torsaeter 2014) reported that the period of NPs' contacts in the fluids complex, the starting wetness of the porous media, and the amount of brine all affect wetness changes. Al-Anssari et al. (2016) investigated the redox potential of NP adsorption revealed that the process remained primarily irreversible, despite presence of a partly reversed response following the application of acetic and purified water to the substrate.

2.5 Effect of asphaltene deposition on surface's micro-topography

Surface morphology of reservoir rocks can affect a number of the fundamental attributes of substances including their tendency for liquids to adhere onto the substrate or wetness. The topography's degree of roughness is regarded as a crucial surface characteristic that alters significantly, as deposition of organic compound such as asphaltene occurs. The precipitation of organic elements can change a homogeneous rock substrate into a heterogeneous state if it was homogeneous before asphaltene deposition. An illustration of a heterogeneous substrate is asphaltenic deposition on solids. This alters micro-topographical feature of mineral's morphology and change in wetness termed as "wettability alteration".

During petroleum extraction operations, particularly EOR, wetness change is a significant event that affects hydrocarbon production (Buckley, 2001). Fractal dimension, a suitable representation of micro-topography data, is able to characterize complex substrates surface roughness (Feninat et al., 2001). Fractal dimension is a useful representation of substrates due to the idea of surface self-similarity at various ranges (Othman et al., 2006). The fractal dimension was previously demonstrated to be a key metric for characterizing substrate. Single fractal dimension was used in nearly all the substrate investigations recently conducted using fractal concept (J. M. Li, 2003). Bi-fractal analysis, in combination with conventional fractal methodology, may be a highly effective method to investigate heterogeneous substrates. The deposition or separation of phase 2 on the substrate prevented the detection of a homogeneous state across the entire substrate. A bi-fractal technique can represent the heterogeneous substrate effectively compared to a mono-fractal type (Bénard et al., 2005). The division of the substrate into several separate varieties is a common technique to measure roughness. This covers both macro-asperity and micro-asperity areas. In the bi-fractal technique, the two various sized areas are represented by two differing dimensions. On the other hand, topographical features can be analyzed and described using a variety of techniques (Zhang et al., 2005). Several of these techniques have been developed in response to substrate picture processing.

Atomic force microscopy (AFM) is a scanning probes microscope technique. The two phases of the AFM's functioning mechanisms are contact and non-contact. In the contact type, a probed point is directly touched to measure parameters (Meyer, 1992). The interval separating the tips and the samples is regulated around 10 and 100 nm in the non-contact type (Meyer, 1992). The substrate is examined while the tips or the samples are moved in relation to one another. For generation of a topographical view of samples, stresses involving the tips and the samples are subsequently estimated by observing deformations in cantilevered strings connected to the tips (Meyer, 1992). The advantage of this approach is its capability in scanning an object's surface through three directions (x, y, z), as opposed to more traditional methods which exclusively work in two planes such as optical or electron microscopy. The AFM method additionally offers quantitative data on surface structure. This approach offers an insightful way to examine how the surface is altered by substance adhesion and deposition (Shi et al., 2019). The samples need to be minimally or not treated prior the examinations, which is another noteworthy benefit of the AFM (Meyer, 1992). The rate at which AFM scans restricts the scope of the inquiry, which is a

drawback. AFM is frequently impractical to use for substrates greater exceeding 100 m. Tazikeh et al. (2020) used AFM to examine micro-topography of quartz surfaces following asphaltenic adherence on them both with and without NPs. According to their findings, asphaltenes adhere to NPs' surface and precipitates or adhere to quartz surfaces with less intensity. As a result, the substrate will become uniform when NPs are present.

Scanning Electron Microscopy (SEM) technique is among the electron microscopic techniques that offer pictures of the target object with a precision between 1 nm and 1 m (Vernon-Parry, 2000). This technique offers detailed substrate data. SEM can provide evidences on sample content, crystalline morphology, and electronic characteristics. It also has several benefits compared to traditional optical microscopy including increased depth of focus, greater attainable growth, and greater quantities of information that could be collected overall (Vernon-Parry, 2000). Compared to transmission electron microscopes (TEM), SEM allows for quicker processing times and greater studied sampling methods (Vernon-Parry, 2000). SEM's vulnerability to other electrical, magnetic, and vibrating disturbance are its disadvantages (Scheu & Wayne D. Kaplan, 2012). The SEM outputs offer more qualitative substrate data than the AFM.

Fractal theory is used to investigate morphology of the surfaces and their roughness and irregular microstructures. Its theoretical model highlights similarity and affinity at various scales (Benoit B. Mandelbrot, 1982). Fractal dimensions may define complex surfaces since it is a suitable proxy for topographical data. The fractal dimension, that promotes the idea of surface identity at various ranges, is a suitable surface variable and can be connected with other layer roughness factors. Different scholars have also used it to examine the heterogeneous qualities (Mahovic Poljacek et al., 2008). Fractal dimensions are established using data from computerized photographs of substrate morphology. Various methods including X-ray, SEM, AFM, and many different substrate can be used to offer diagnostic pictures. SEM is a widely used method to identify surface changes, whereas AFM is a sophisticated scanning tool. AFM has lately become a potent and significant instrument in surface heterogeneity and structural characterization research. Surface roughness data such as root-mean-square and mean roughness is frequently thought of as a criterion for topographical measurements in the AFM approach. This approach itself, said to have a beneficial quality that allows for quantitative evaluation of surface roughness (Mohanty et al., 2006). As a result, this technique is typically used to observe how compounds that attach to a surfaces affect the substrate (Nikooee, 2009). Additionally, there is a strong relationship

between fractal dimensions generated using this technique and those produced using alternative approaches (Fujisawa et al., 2006). SEM pictures are used to identify fractal characteristics. A high level of focus in SEM observation offers deeper in-depth details on surface topography. Differences in picture intensities cab be used to determine the surface topography when interpreting SEM photos. Imaging fractal analysis has the potential to be used to gather quantitative data. This technique provides better fractal data compared to other methods such as electrochemical impedance spectroscopy (Risović et al., 2009). Several investigations are reported on comparing fractal dimensions found using AFM and SEM outputs. During application to heterogeneous substrates, a bi-fractal study can generate noticeable results once contrasted to a straightforward mono-fractal approach.

There are two commonly used methods to determine surface roughness, which are root mean square roughness (RMS) Rq and mean roughness Ra. However, they typically are not reliable in terms of correct description of the roughness. A multifractal technique is more capable of depicting the variance more effectively in surface's roughness, as demonstrated by Gan and team (2007). Given the clear relationship between both roughness index and contact angle it is possible to predict whether changes in wettability can seen in multifractal properties or not. The structure properties may be represented using multifractal formalism in its spectra. Its spectra itself, displays the fluctuation in fractal properties in a broad variety of scales influencing the reaction of the system. By way of explanation, compared to a standard fractal analysis, the multifractal technique can provide more extensive data. It is a viable method for studying features of a surface across subjects because of the abovementioned qualities. Multifractal properties are usually found from different surface information. Main topographic characteristics of complex surfaces are found in pictures and are used to identify the desired multifractal characteristics. Several methods such as domain modification (Serrano, 2009) are used to accomplish multifractal analysis.

2.6 Adsorption of asphaltene on surfaces and nanoparticles

A great deal of research is reported in the literature on adsorption of organic elements of petroleum fractions like asphaltenes (Xia et al., 2019). According to several experimental research results, where the static and dynamic tests were conducted, it was observed that asphaltenes have a great level of adherence on calcite surface. As minerals, crude oil, and brine are all present in porous

medium, their contact with each other is unavoidable. The process of asphaltenes adherence in the existence of a water layer does not involve the diffusion of asphaltenic particles via water. Instead, asphaltenes actually immediately adheres to the substrate once the water coverage ruptures. Asphaltenes encounter a mechanistic barrier of the substrate and a large, constant water coating, which reduces adsorption. On the contrary, a small water layer might become unstable and burst, that increases the adsorption of asphaltenes (Buckley J., 1989). Asphaltene can pierce a shaky water layer between the oil and brine and adhere on a flat surface (Joonaki et al., 2018). The pH and ionic concentration of an aqueous layer affect its stability (Buckley et al., 1998). Asphaltenes are classified as a one coverage adsorbate, according to the findings on its ability to bind to clay when exposed to toluene concentrations of asphaltene (Collins & Melrose, 1983). The primary cause of the wetness change of crude oil formation minerals is thought to be the adherence of asphaltenic particles and resins.

A significant issue in extraction oil is deposition of asphaltenic particles in reservoirs and its adsorption on various surfaces (including reservoir minerals, bottom hole equipment). Asphaltene precipitation onto the formation minerals decreases the permeability concurrent with pore plugging, which lowers petroleum extraction rates and raises operational expenses. Deposition of asphaltenes can be brought on by property modifications in the formation. These two most significant elements are the decrease in formation pressure and the difference of hydrocarbon's chemical makeup because of injection. The wetness of formation minerals is changed by asphaltenic particles precipitation. It was demonstrated that following the adherence, originally hydrophilic adsorbents changed to hydrophobic as the number of hydrocarbons in the porous media rose (Maravilha et al., 2021). Thus, it can have a detrimental effect on the flow rate of petroleum. Asphaltene adherence activity is significantly influenced by the state of a substrate. Although asphaltene is typically not readily adhered on a hydrophobic substrate, their symmetrical parts are likely to do so. However, if certain asymmetrical elements are adsorbed, it can be challenging to remove them from the substratum (F. Liu et al., 2021).

Over the decades, scientists have faced difficult questions regarding the deposition of asphaltenes from hydrocarbon compounds and its adherence on diverse surfaces (Ahooei et al., 2020). Bantignies et al. in 1998 reported practical research on adsorption of asphaltene on kaolinite in presence and absence of water. The research outcomes showed that there were differences between the adherence procedure with no water presence and with it. Dudášová et al. in (2008)

investigated the adsorption on several rocks, particularly hydrophilicity and hydrophobicity of SiO_2, was investigated by. Asphaltenes N_2 concentration correlates with percentage of asphaltenes adhered on the adsorbents. The tendency of dolomite, quartz, and mica to adsorb asphaltenes was investigated by Syunyaev et al., (2009). Mica showed the best level of adherence compared to all of the examined adsorbents. Nassar et al. (2011) looked at how adsorbent grain shapes affected the adsorption of asphaltenes. In comparison to micro- Al_2O_3, the nano-Al_2O_3 shows a higher adherence capability depending on the substrates. The potential of SiO_2, ZrO_2, TiO_2 NPs to adsorb and stabilize asphaltenic elements in hydrocarbons were investigated by Mohammadi et al. (2011) and the scientists reported that TiO_2 in an acidic medium can significantly increase the stability of asphaltenes. Stability of water layer on rock surface and quantity of asphaltenic adherence might be affected by variations in mineralogy of rocks, the makeup of the asphaltenes, and the chemical composition of the saline (Saraji et al., 2013).

The primary cause of change in wetness of formation rocks is considered to be coverage of the rock substrate by polar particles such as asphaltenes or sometimes resin (Buckley et al., 1997). Therefore, research on adherence of asphaltenic particles onto reservoirs containing mineral surfaces and the contact of solids and fluids with tocks is crucial in understanding how to regulate flowrate in formations more effectively (Garrouch & Al-Ruhaimani, 2005). The surface morphology and chemistry of asphaltenes have a significant impact on how they precipitate. Asphaltenes have properties that influence the stability of petroleum and hydrocarbons' polarity, aromaticity, and heteroatomic functional groupings which all help them to adsorb onto the substrates of formation containing rock grains (Ahooei et al., 2020). A primary phenomenon of the adherence of asphaltene particles influences reservoir mechanisms like movement of charged particles in porous medium, rock dissolution, and movement of microelements (Wesolowski et al., 2000). Stimulation, post-drilling remediation, LSWF are examples of procedures that change the formation's pH and affect the substrate. The contact of fluids and rocks and the deposition of particles are caused by this phenomenon. As a result, it alters the chemical composition of the surface and encourages the rock to absorb hydrocarbon particles (Mohammed, al Shehri, et al., 2021b).

Scientists have long recognized the adhesion of asphaltenes to diverse surfaces as a significant phenomenon (Mohammed, al Shehri, et al., 2021b). Gonzalez & Middea, (1988) demonstrated that asphaltenes adsorbed on calcite at a faster rate than for resins. The asphaltenes

adherence concept is determined by the asphaltene content as shown by Marczewski (2002). Increasing the original content of asphaltenes enhanced the adherence on sandstone and carbonate minerals, and the existence of asphaltene regulators decreased the quantity of asphaltene adsorption, according to research results reported by Khormali et al. (2018). Dynamic adherence studies by Monjezi et al. (2019) demonstrated that the existence of a saline aqueous coating creates a mechanistic barrier at the interaction of adsorbent's substrate and asphaltenic particles and significantly reduces adsorbing (Monjezi et al., 2019). A computational study and laboratory research of asphaltene precipitation on metal flat substrates is reported by Ahooei et al. (2020) revealed that the morphology and content of asphaltenes have a significant impact on volume of precipitation. Mohammed et al. (2021) investigated the role of iron containing rocks in altering the wetness. They showed that iron minerals increased scaling development and asphaltene adherence, which led to changes in the substrate. Magnetite has been described as the important iron mineral and presented as a significant threat (Mohammed, al Shehri, et al., 2021a). Additionally, it was demonstrated that Magnetite NPs can be used for EOR by offering colloidal element adherence spots in addition to certain qualities including magneto-responsiveness and a decrease in the oil-water IFT. In the investigations, the structural content and chemical condition of the components existing at the surfaces of samples were identified and quantified using sophisticated substrate description method known as X-ray photoelectron spectroscopy (XPS). XPS is reasonably simple to use and requires only minor sample pretreatment. The content of components with an amount of atoms larger than three in the 10 nm outer layers can be detected and measured using XPS. The investigated material is irradiated with a focused X-ray beam while being held in a strong vacuum. Electrons are ejected from the initial strata as a consequence of the contact of the sample's atoms with the X-rays. The detectors then find the escaping electrons, and the electron energy spectrometer measures their kinetics. The binding power of the thrown electron is a property of the emitted electron and its related component due to the power of the electrons that are linked to atoms is particular and distinct based on the electronic structure of the atom. The classification and measurement of the components could be done using the quantity of expelled particles and the numbers of corresponding interaction energies, respectively.

3 MATERIALS AND METHODS

The materials used and the experimental procedures followed tightly for sample preparation and testing the samples using various state-of-the-art analytical instruments are presented and described here in detail in this chapter.

3.1 Materials

MgO and NiO NPs (Table 3-1), calcite slices are the materials used to prepare smooth surfaces to be used in the experiments. Crude oil from the Karaturun oilfield was used to extract the asphaltene and the results of SARA analysis is presented in Table 3-2. Asphaltene is extracted and purified using *n*-heptane (Merck, >99%) and toluene (Merck, >99%) based on ASTM-D6560 method also known as indirect IP-143 standard method. Calcite surfaces were used after preparation to deposit asphaltene on their surface for the purpose of further tests designed for the purpose of this research work.

Table 3-1. Specification of the NPs used in this research work.

Name of NP	Purity (%)	Size (nm)	Manufacturer
MgO		≤ 50 nm	Aldrich
NiO	≥99.9%	< 80 nm	Nanoshell

Table 3-2. SARA analysis for the crude oil.

Saturates, %	37.14%
Aromatics, %	32.07%
Resins	24.87%
Asphaltenes	5.65%

3.2 Preparation of Calcite Surfaces

First, some thick slices of calcite were cut (Figure 3-1) using a cutting machine (Figure 3-2). The slices range from 1.5 to 2 cm in length and 1.5 mm to 3 mm in thickness.

Figure 3-1. The prepared calcite slices

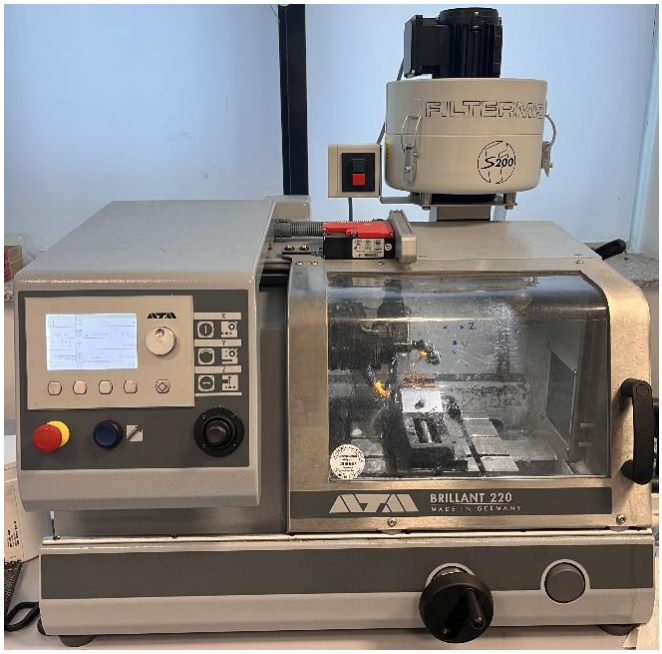

Figure 3-2. Cutter (Brillant 220)

The surface of the cut calcite surfaces was very rough with small number of visible macro-pores. This creates problems for AFM probing. Hence, the sample surfaces were polished to meet

the AFM tests requirements. The polishing machine (Figure 3-3) that uses special nozzles of different hardness enabled preparing smoother surfaces suitable for AFM probing.

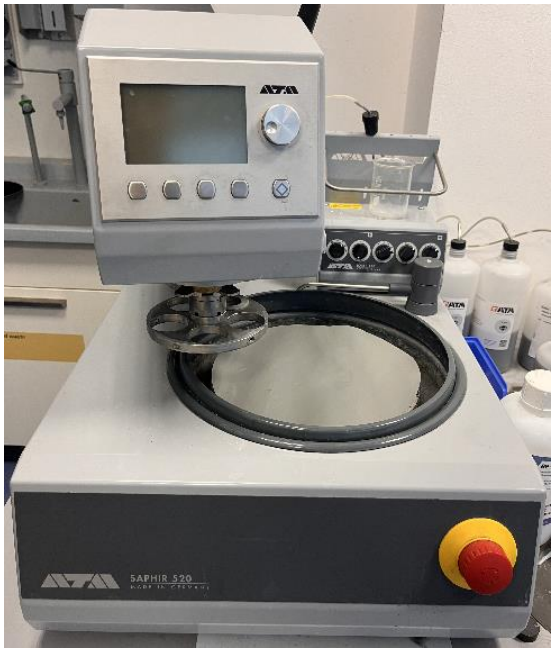

Figure 3-3. Polishing Machine (Saphire 520)

3.3 Asphaltene extraction

Asphaltene was extracted from a paraffinic heavy crude oil obtained for an oilfield located in West of Kazakhstan. According to the procedures described in the indirect IP-143 standard method, crude oil was mixed with *n*-heptane with a ratio of 1 to 40 using a magnetic stirrer for four hours at 600 rpm. The reason for mixing the crude oil with *n*-heptane is to make the crude oil unstable resulting in precipitation of asphaltene. All other fractional components of the crude oil were dissolved in *n*-heptane. Then, the mixture was left to sit for a while to let the asphaltene particles to precipitate. This step was followed by filtration of the precipitated asphaltene particles out of the solution using Whatman filter paper #42. However, the filter paper filters not only asphaltene fractions, but some other fractions such as wax and resin present in the crude oil. Hence, the only method to dissolve them in *n*-heptane is at high temperature. Therefore, Soxhlet extraction apparatus (Figure 3-4) was used to purify the asphaltene. The filter paper was put into the Soxhlet extractor while the flask containing *n*-heptane was boiled. The vapor was then cooled at the condenser where small drops of *n*-heptane fall onto the filter paper and start to dissolve the impurities inside until the fluid in the extractor becomes colorless. The next stage is to replace the

n-heptane from the boiling flask with toluene. Toluene is used to dissolve the pure asphaltene from the filter paper, until all dissolved asphaltene at high temperature are mixed with toluene in the boiling flask. The toluene must then be evaporated by heating the final solution to roughly 100°C. The last step is to dry the remaining asphaltene fractions in the oven at a certain temperature to achieve solid asphaltene particles (Figure 3-5).

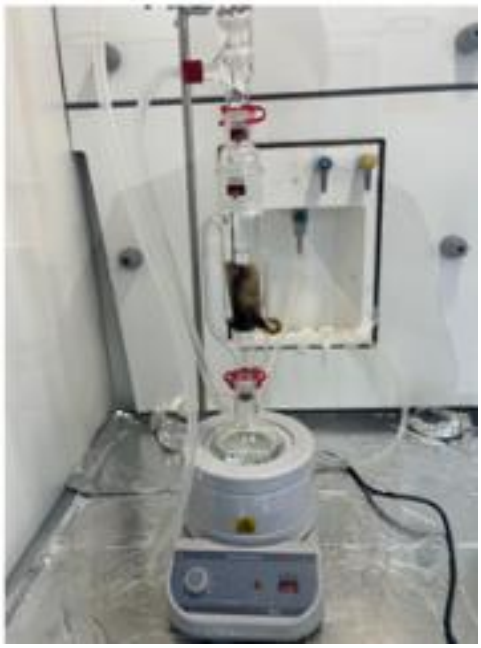

Figure 3-4. Soxhlet apparatus

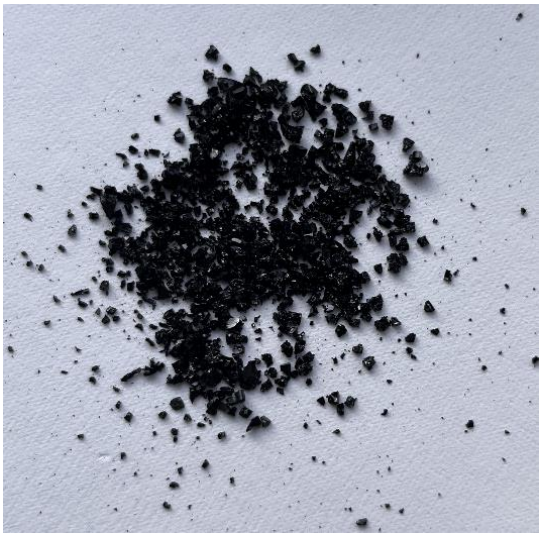

Figure 3-5. The extracted asphaltene

3.4 Nanoparticle Characterization

3.4.1 Scanning Electron microscope (SEM)

The high-resolution scanning electron microscope (SEM) is a great tool for determining the size and form of NPs (Figure 3-6). SEM image presents a two-dimensional (2D) depiction of the three-dimensional (3D) objects. The secondary electrons (SEs) produced once the material is hit by the primary electron (PE) beam provide the signals necessary to produce a SEM image. High-resolution SEM images with excellent surface morphological contrast can be created by the SEs. Powdered substances or suspensions samples are commonly used for testing.

The morphology and shape of the NPs were examined on a ZEISS Crossbeam 540 scanning electron microscope (SEM). Onto a spotless glass slide, a small quantity of the NP powder was placed and left to dry under ambient conditions. The SEM was operated at a certain accelerating voltage and a working distance of 2.4-2.5 mm. The sample was imaged at various magnifications ranging from 10-20 KX and electron high tension of 5 kV.

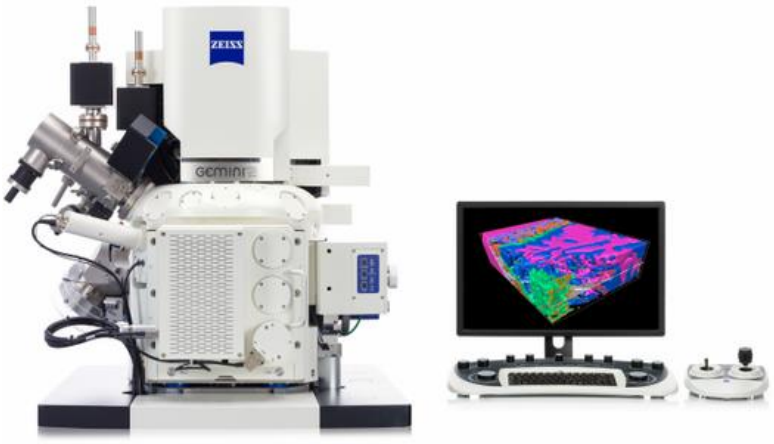

Figure 3-6. SEM (ZEISS Crossbeam 540)

3.4.2 Transmission Electron microscope (TEM)

Transmission electron microscopy or TEM was used to determine particle's size and their distribution, and morphology quantitatively. Compared to SEM, TEM has a pair of benefits: it can offer higher spatial resolution and more quantitative results. There are several TEM methods used to analyze nanoparticles' size, which are high resolution TEM, Scanning TEM, Energy dispersive X-ray etc. TEM works by transmitting a beam of electrons through a sample, which interacts with the electrons to produce an image of the sample's internal structure at high magnification.

Using TEM, the NPs' shape and structure were examined. A JEOL JEM-1400 Plus apparatus running at 120 kV of accelerating voltage was used to do TEM imaging (Figure 3-7). After mounting the already assembled grid with the NPs onto the TEM holder, the microscope was adjusted to focus on the grid. Employing a high-resolution camera, the TEM pictures were captured at different magnifications that ranged from 10 to 100 kX.

Figure 3-7. TEM (JEOL JEM-1400 Plus)

3.4.3 Energy Dispersive X-ray (EDAX)

EDAX was used to examine the physical and chemical characteristics of MgO and NiO NPs. The SEM-EDAX technique, which enables the investigation of the elemental content and shape of the particles, was used to investigate the nanoparticles.

3.5 Calcite surface samples' preparation

The sample preparation for various tests including XPS, AFM, and CA measurements involved using synthetic oil, MgO and NiO NPs, pure calcite, and ultrasonic homogenizer equipment (Figure 3-8). Slightly different procedures were followed for sample preparation for each test, which are described here in this section. Synthetic oil was prepared using the extracted asphaltene powder and toluene. Its concentration can be defined using the formula below:

$$t\% = \frac{m}{m + w_{sol} \times \rho} \times 100\% \qquad 3\text{-}1$$

where w is the weight of the solvent, ρ is the density of the solvent, and m is the mass of powder. During the experiments, 0.5 wt% solutions were prepared using 0.435 grams of asphaltene and 100 ml of toluene. As for NPs, the solution of 0.1 wt% was prepared using the same procedure.

Figure 3-8. Ultrasonic homogenizer (FS-300N)

Two scenarios were considered when preparation of the calcite surface samples so that a comparison can be later made between asphaltene adsorbed on the surface of the calcite substrate in presence or absence of NPs. To begin with, synthetic oil was prepared by dissolving asphaltene in toluene. Special calcite + asphaltene + MgO + heptane and calcite + asphaltene + NiO + heptane samples were prepared according to specific sample preparation procedures for XPS and AFM surveys. For the first case, flask was filled only with synthetic oil; while, the second flask contained synthetic oil with different NPs inside which was homogenized using a homogenizer. The subsequent sample preparation procedures are identical. Asphaltene was deposited on the surfaces as a result of destabilization of asphaltene in the oil where *n*-heptane serves as a destabilizer and was added to the solution at the volumetric ratios of 40-60%.

Depending on the type of the experiment conducted (i.e., CA measurements, XPS, or AFM), the calcite surface samples were aged in the prepared solutions. The aging time for AFM

and CA measurement was 2 hours, whereas for XPS 7 days. For AFM and CA measurement, the samples were prepared as the following:

1) 60 ml of synthetic oil with (0.5 wt%) of asphaltene with NPs (0.1 wt%) was prepared;
2) The solution was then homogenized using an ultrasonic homogenizer for 15 minutes at 20°C;
3) 40 ml of *n*-heptane was then added to the solution;
4) The calcite samples were placed into the solution horizontally for 2 hours for aging;
5) The solution was then removed allowing calcite to dry.

The preparation of samples for XPS was done as the following procedure:

1) Two solutions with and without heptane were prepared (keeping the concentration of 60% solution, 40% heptane) each of X ml of synthetic oil with 0.5 wt% of asphaltene with 0.1wt%NPs;
2) The solution was then homogenized using an ultrasonic homogenizer for 15 minutes at 20°C;
3) The solutions was poured onto the surface of the calcite samples while placed vertically and was let to age for 7 days;
4) After draining the solution, the samples were placed it in a vacuum oven set at 50°C for one day to inhibit calcite surface oxidation due to exposure to air.

The alterations in surface chemistry, micor-topography, and wettability then were measured and investigated by using three separate techniques - he contact angle measurement, and state-of-the-art analytical equipment namely Atomic Force Microscopy SmartSPM 1000 (AFM) and X-ray Photoelectron Spectroscopy NEXSA (XPS).

3.6 Atomic force microscopy (AFM)

AFM probing has been proved an effective tool (Figure 3-9) for imaging of substrates from atomic to micron scale (Maurice et al., 1996). A sharp tip that connected to or a component of a cantilever used in AFM to scan samples positioned on a piezoelectric tubing. There are many ways to observe the cantilever's deflection; while, the samples are rotated underneath it. However, the best method used includes optical levers that use lasers reflecting lights off the cantilever's end to illuminate a photodiode. AFM functions according to the idea of surface sensing using a very tiny tip. The tip type and characteristics are provided in Table 3-3. The procedure involves vector scanning a sample's substrate line by line to capture it. The process can change greatly depending on the operational regime. The AC mode was used during imaging micro-topography of the surfaces in this research work first in presence of asphaltene and then in presence of asphaltene + NPs. The outputs are 2D and 3D images of the surface probed. A 3D micro-topographic representation of the investigated surface is created by combining the values that the AFM tip records throughout the probing. Moreover, it can provide material properties, roughness, and magnetic and electrical characteristics of the investigated surface. The surface images are captured in both 5 and 10 micrometers (μm).

Figure 3-9. Atomic Force Microscope SmartSPM

Table 3-3. Tip types and their characteristics used in AFM probing in this research work

SPM Probe – Part # TM300-A-10

Material type	Si, N-type, 0.01 – 0.025 ohm/cm
Material origin	Single Crustal Silicon Cantilever
Length	115 – 1.45 μm
Width	35 – 4.5 μm
Thickness	3.5 – 4.5 μm
Tip - Radius	<10 nm
Height	12 – 16 μm
f	200 – 400 kHz
k	25 – 75 N/m
Coating	Al (Reflex Side)
Wafer #	1470
PD	180905

3.7 X-ray Photoelectron Spectroscopy (XPS)

XPS (Figure 3-10) is a special surface-sensitive method for elemental evaluation since the measured electrons come through mainly the top several atomic layers due to the extremely limited mean free pathway of electrons in materials. A spectrum is created by plotting the quantity of the observed electrons against respective kinetic energy for each energy interval. The spectrum of each components is different. The spectrum of an elemental combination is roughly equal to the combined amount of the peaks of its components. Peak levels and zones can provide quantifiable information and precise measurements of peak locations and breakups along with specific spectral properties. X-ray Photoelectron Spectroscopy is able to survey surface chemistry of the investigate

surfaces via using monoenergetic soft x-rays to irradiate a material in vacuum oven measuring the released electrons from the surface due to the photoelectric effect. Such information can be used to identify chemical conditions and provide statistical data along the surface investigated.

Figure 3-10. X-ray Photoelectron Spectrometer NEXSA (XPS)

Typically used x-rays include Mg or Al. Such rays can only penetrate solids up to 10 micrometers thick due to their restricted penetration power. The photoelectric effect is a result of their interactions with the ions in the substrate area. The observed kinetic energy of the released electrons expressed as follows:

$$KE = hv - BE - \phi_s \qquad 3\text{-}2$$

where the hv-photon energy [eV] , BE-binding energy [eV], and ϕ_s-work function [eV].

The BE of every component differs allowing spectroscopy to be used to distinguish the components on the substrate and estimate their content. The chemicals potentials and polarity of combinations vary causing changes in the compositional binding energy. To determine the chemical phase of the surfaces under investigation, the mentioned chemical variations can be used. Sample preparation and installation is generally an important and sensitive issue in XPS operations. The sample is fastened to the experiment plate (Figure 3-11) and the surveying starts with the material in its original state to avoid changes in the substrate's makeup.

A broad scanning and surveying spectrum must be collected first in a standard XPS surveying in which the surface chemistry is unclear to determine the components contained. To obtain a more complete understanding of the chemical structure, smaller quantitative scanning of chosen peaks may be used after the elemental compositions were established. Despite the fact that

the content of the specimens is known before the survey this method was used to compile the information for the conducted surveys.

Figure 3-11. Sample installation for the XPS surveys

Table 3-4. Investigated orbitals of each sample using XPS

Sample	Orbitals
Calcite	Ca 2p3/2; O 1S; C 1s
Asphalteane (powder)	C 1s; S 2p 3/2; N 1s; O 1s
MgO (powder)	Mg 2p; O 1S
NiO (powder)	Ni 2P 3/2; O 1S
Calcite + Asphaltene	Ca 2p3/2; O 1S; C 1s; S 2p 3/2; N 1s
Calcite + Asphaltene + Heptane	Ca 2p3/2; O 1S; C 1s; S 2p 3/2; N 1s
Calcite + Asphaltene + MgO (NP)	Ca 2p3/2; O 1S; C 1s; S 2p 3/2; N 1s; Mg 2p
Calcite + Asphaltene + MgO (NP) + Heptane	Ca 2p3/2; O 1S; C 1s; S 2p 3/2; N 1s; Mg 2p
Calcite + Asphaltene + NiO (NP)	Ca 2p3/2; O 1S; C 1s; S 2p3/2; N 1s; Ni 2p3/2
Calcite + Asphaltene + NiO (NP) + Heptane	Ca 2p3/2; O 1S; C 1s; S 2p3/2; N 1s; Ni 2p3/2

3.8 Contact angle measurement method

Changes in surface chemistry and the surface roughness affect the wettability state of the surface. As a proof of concept and additionally investigating the effect of asphaltene deposition of on the calcite surface and later inhibitory effect of presence of NPs, contact angle measurements were conducted on the prepared samples before and after addition of the NPs on the calcite's surface.

A liquid drop that contacts a solid object creates a contact angle, which is typically observed via the denser phase (i.e., the liquid). Using the Young-Laplace's equation a contact angle can be measured which is a measure of how receptive a solid substrate is to a liquid. Mathematically, Young-Laplace's equation is expressed as follows (Nakajima, 2011):

$$\gamma_{sv} = \gamma_{sl} + \gamma_{lv} \cos\theta \qquad 3\text{-}3$$

where γ_{sv} is IFT of the substrate with solid and vapor, γ_{sl} is IFT of the substrate with solid and liquid, γ_{lv} is IFT of the substrate with liquid and vapor, and θ is contact angle which can be used to determine wettability of a surface (Figure 3-11). The Young-Laplace's equation does not take into consideration the influence of surface roughness on wettability of a surface and therefore it is suitable for homogenous surfaces. The Young-Laplace to consider the effect of material complexities and roughness, the contact angle measurements must be modified using available models such as Wenzel; and the modified Wenzel models.

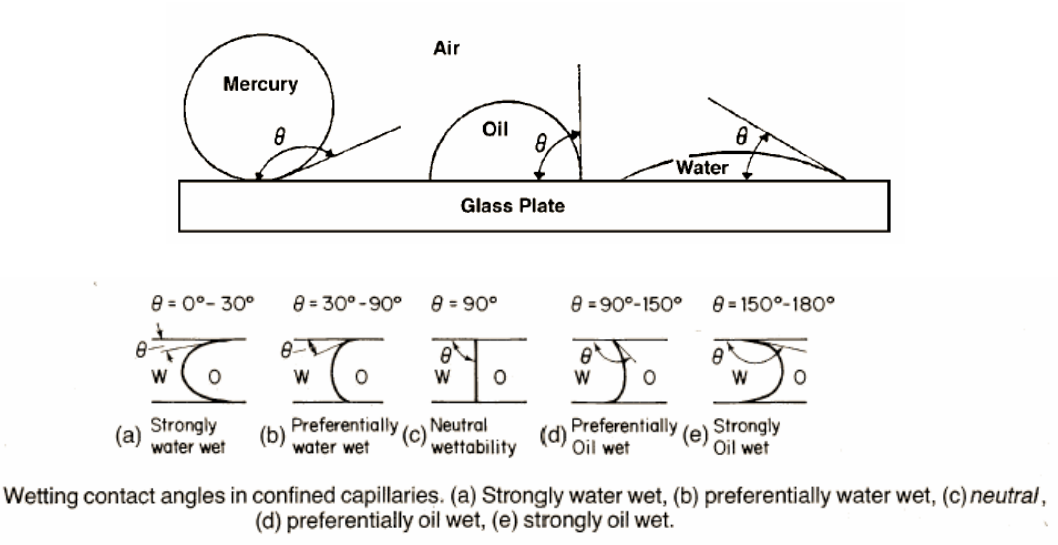

Wetting contact angles in confined capillaries. (a) Strongly water wet, (b) preferentially water wet, (c) *neutral*, (d) preferentially oil wet, (e) strongly oil wet.

Figure 3-11. Classification of wetting states (Zolotukhin A. & Ursin J, 2000)

The investigated contacts in this research work are particularly susceptible to contaminations. Therefore, the measurements are conducted multiple times to get repeatable results. A drop entirely spreads out on a substrate if the particles of the drop are firmly drawn to the molecules of the substrate, which corresponds to an angle of 0°. A solid substrate is regarded as hydrophilic if the contact angle is less than 90° and hydrophobic if it is more than 90°. The contacts on strongly hydrophobic substrates constructed of negligible surface energy substances can reach up to 120°. Because of the air gaps below the droplet, certain surfaces with extremely rougher substrates can have an angle larger than 150°. Such materials are known as highly hydrophobic ones. In contrast, a liquid with a slow adsorption takes up the most volume in the porous media, primarily in the centers of big pores (Roach et al., 2008).

In this research work, changes in surface wettability in presence or absence of the NPs were measured at standard temperature and pressure using the contact angle measurement (equipment shown in Figure 3-12) approach. This approach provides a specific angle between a drop of distilled water and the calcite surface. Four calcite surfaces with different sampling methods were prepared and used to measure the CA after several hours of saturation by synthetic oil and NPs. A droplet of distilled water was poured onto the calcite surfaces. A digital camera connected to digital microscope with high-quality zoom was used to capture images. The images were then analyzed using a software program to determine the CA with three distinct techniques namely ellipse, circle, and Young-Laplace model.

Figure 3-12. Contact angle measurement apparatus (OCA 15EC LMS instruments) used in this research work

4 RESULTS AND DISCUSSION

In this section, results obtained from various experimental sections of this research work are presented and discussed. First, the results obtained from various state-of-the-art analytical techniques used for characterization of the NPs such as SEM, TEM, and EDAX are presented and discussed. Then, the results obtained from AFM, CA measurements, and XPS are presented and discussed in detail.

4.1 Characterization of nanoparticles

A material is considered to be a NP if at least one of its dimensions falls between 1 and 100 nm. Scanning Electron Microscopy (SEM), Transmission Electron Microscopy (TEM), and EDAX techniques were used to characterize the NPs. As a result, surface morphology, particle size, and chemical composition of the NPs were determined.

4.1.1 SEM and TEM Analysis

Scanning Electron Microscopy (SEM) and Transmission Electron Microscopy (TEM) methods of electron microscopy were used to obtain images of the surface of NPs. While, the TEM offers high-resolution 2D picture of the sample's inside, the SEM offers a 3D image of the sample's surfaces. In SEM, a beam of electrons is moved along the sample's substrate and the dispersed or released electrons are recorded and used to build images. In TEM, an electron beam is passed through the sample and the measured electrons are used to build a picture. Both methods can reveal details about the NPs' dimensions, morphology, and shape.

Both SEM and TEM were used in this research to analyze MgO and NiO NPs to identify their sizes, shape, and dispersion. The substrate coverage per unit weight of the NPs can be calculated using specified surface area studies. It is important to remember that these methods support one another, and that to completely define the NPs, a combination of several methods is required.

Figure 4-1 was captured with a magnification of 13.2 kx and was then increased in size to a maximum of 10.00 kx. Because of the extreme magnification, the NPs seem relatively small in the picture but are still discernible. For TEM scanning, the accelerating voltage used was 80kV, which is a comparatively low voltage. This voltage was selected to avoid damage to the NPs given the fact that high accelerating voltages can harm the sample. The exposure period was 0.469

seconds, which is a brief amount of time. Additionally, this lessens the sample's deterioration. The MgO NPs appear in the photograph as tiny, black particles, which shows that they are electron-dense and absorb the beam's electrons. By matching the dimensions of the NPs on the picture to the given magnification, their size can be determined. The synthesis process and prospective uses of the NPs can be inferred from the size and shape of the particles. For instance, a high-quality synthesizing process could be indicated by a limited size range and consistent form, but irregular shapes or a large size distribution may point to contaminants or other problems.

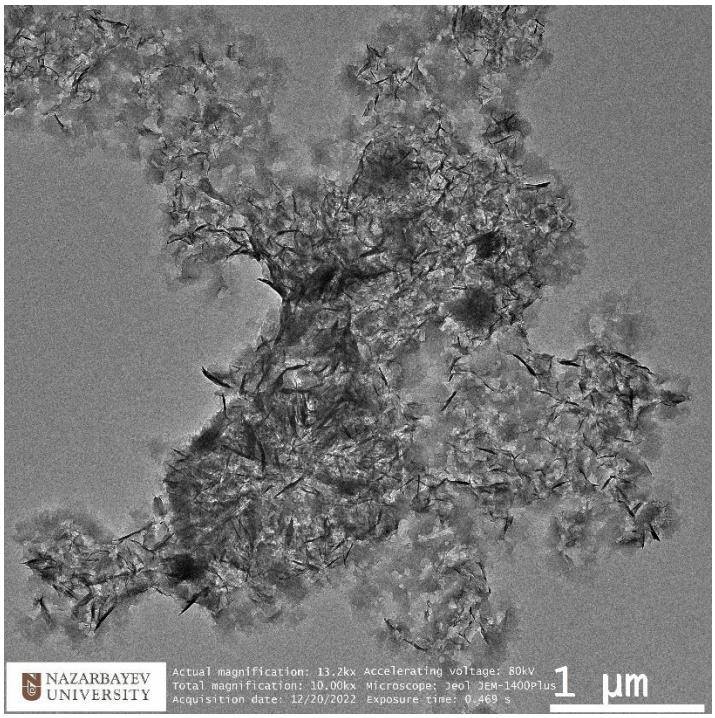

Figure 4-1. TEM image of the MgO NP.

A transmission electron microscopy picture of NiO NPs is shown in Figure 4-2. The volume, shape, and aggregation status of NiO NPs were revealed by using the TEM images. As shown in Figure 4-2, the NiO NPs have circular oval form and are poorly distributed with a range of sizes resulting in small agglomerations that are joined together. The incredibly small sizes and strong surface energies of few microscopic particles prevent them from aggregating into secondary NPs. The actual magnification of the image is 99.9kx, which means that the magnification is high and allows for visualization of the NPs at a very high resolution. The accelerating voltage used for this image was 80kV, which is a common voltage used in TEM imaging. At this high magnification, the image provides a detailed view of the morphology and size distribution of the

NiO NPs. The particles appear to be roughly spherical in shape, and their size ranges from a few nanometers to several tens of nanometers in diameter. The size distribution of the NPs can be determined by analyzing the TEM image and measuring the diameters of a large number of particles. The TEM image also provides information on the crystal structure of the NiO NPs. By examining the lattice fringes and diffraction patterns in the image, it is possible to determine the crystal structure of the NPs. NiO is known to have a rock salt crystal structure, which is characterized by a face-centered cubic lattice with Ni and O atoms occupying alternate lattice sites. Overall, the TEM image of NiO NPs provides valuable information on the morphology, size distribution, and crystal structure of the particles. This information can be used to better understand the properties and behavior of these NPs in various applications. TEM analysis results showed that the average particle of size of the MgO and NiO NPs are 50 nm and 70-80 nm, respectively.

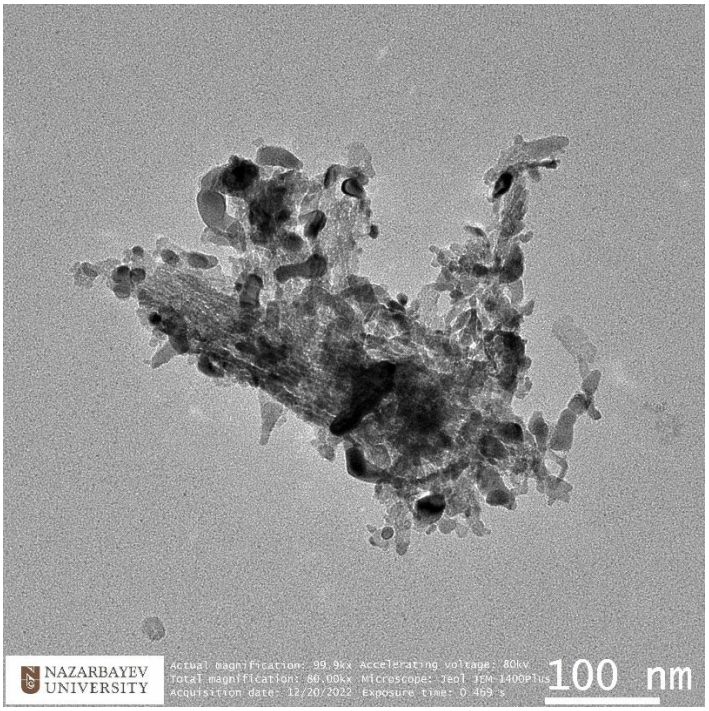

Figure 4-2. TEM image of the NiO NP.

Figure 4-3a is a SEM images from surface of MgO NPs at certain magnification. It is evident from the image that the spherical granules in the microstructure of MgO shown in the figure are not distributed uniformly and they are made up of a single component or a group of fragments with the MgO NPs present as aggregates. The confined image of the spherical nanomaterials has shown that the powder grains are moderately agglomerated. The NP's

morphology is shown in Figure 4-3b. It is obvious from the SEM image that the granules are naturally strongly coalesced. There are certain larger particles because of the aggregation or overlapping of tiny ones. The SEM images clearly display bigger, irregularly scattered grains, as well as uniform, spherical-shaped granules.

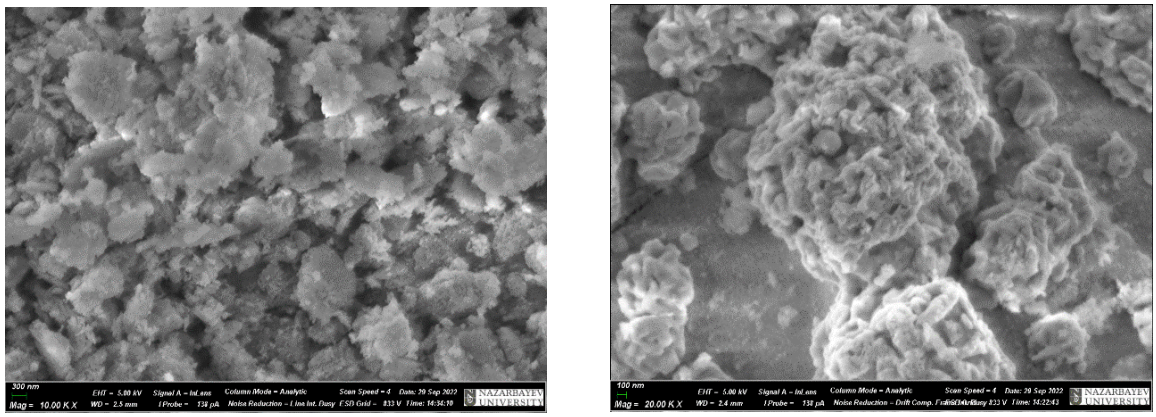

(a) (b)

Figure 4-3. SEM images of NPs: (a) MgO and (b) NiO

4.1.2 Energy Dispersive X-ray Spectroscopy

Energy Dispersive X-ray Spectroscopy, or EDAX, is an effective analytical method for determining a compound's elemental analysis. It operates by irradiating a material with high-energy X-rays that causes the sample's molecules to release distinctive X-rays that are particular to every component. NPs are particularly difficult to evaluate using conventional analytical methods due to their small size; however, the EDAX can be used to determine the elemental composition of specific NPs giving important information on molecular characteristics and behavior.

4.1.2.1 MgO NP

The EDAX spectrum of the investigated MgO NP (Figure 4-4) shows two large peaks, with the first peak located at 1.2-1.4 keV on the x-axis and a corresponding intensity of more than 85 cps/eV on the y-axis, indicating a high concentration of Mg in the sample. The second peak corresponds to O_2 and is located at 0.4-0.6 keV on the x-axis with a corresponding intensity of around 70 cps/eV on the y-axis. The presence of C is also detected with a peak located at 0.2-0.4 keV on the x-axis and an intensity of 10 cps/eV on the y-axis. The weight percentages and sigmas of each element in the sample are also provided by the EDAX analysis. The results show that the sample contains

50.3 wt% O_2, 32.1 wt% Mg, and 17.6 wt% C, with sigmas of 0.2, 0.2, and 0.3, respectively. These values provide a quantitative measure of the elemental composition of the sample and allow for a more detailed analysis of the sample. In addition to the primary peaks corresponding to Mg, O, and C, the EDAX spectrum also shows several small peaks corresponding to trace amounts of Au. The gold peaks are located at energy levels higher than 1.6 keV on the x-axis, with the highest peak having an intensity of around 5 cps/eV on the y-axis and the lowest peak having an intensity of around 0 cps/eV on the y-axis. The presence of gold suggests that the sample may have been contaminated or prepared using equipment that was not properly cleaned.

Overall, the EDAX analysis confirms the presence of Mg, O_2, and C in the investigated MgO NP with trace amounts of gold also detected. The weight percentages and sigmas provide a quantitative measure of the elemental composition of the sample and the presence of gold suggests that contamination may have occurred during preparation or analysis.

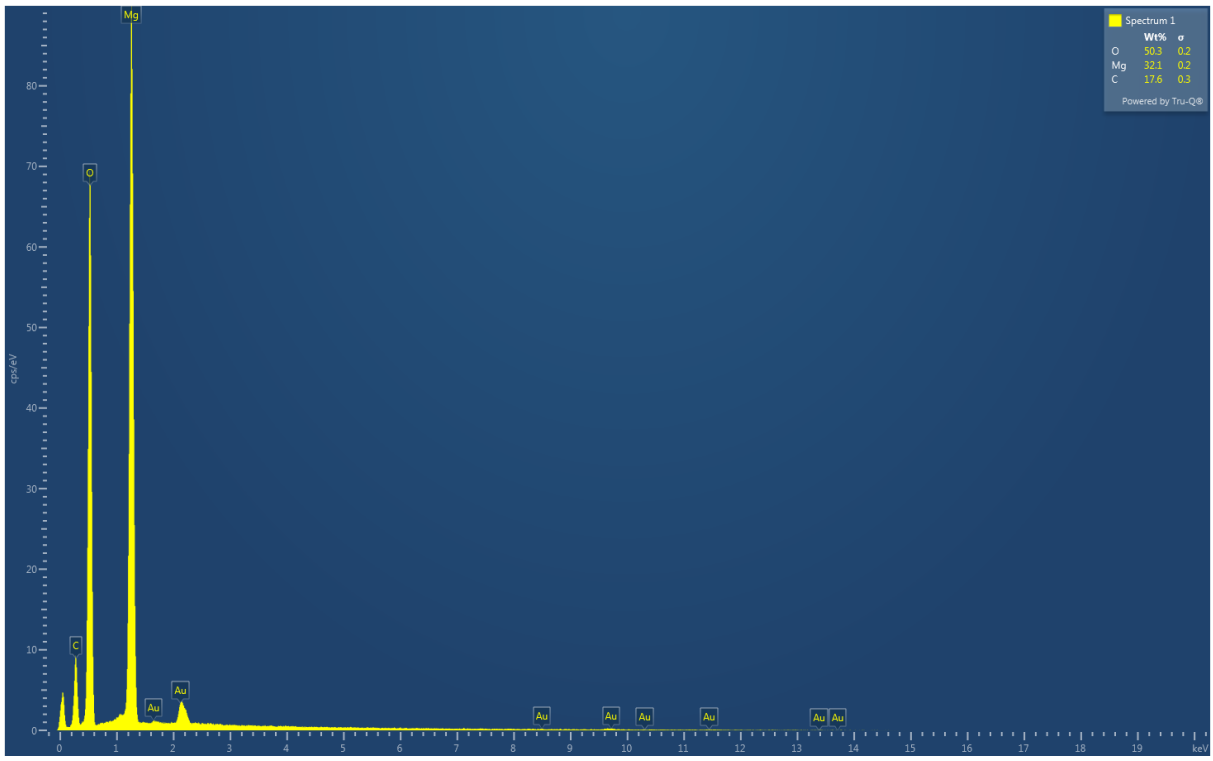

Figure 4-4. MgO NP's EDAX spectrum

4.1.2.2 NiO NPs

The NiO NPs were analyzed by using the EDAX experiment (Figure 4-5). The presence of Ni is evident from the highest peak detected at 50 cps/eV (y-axis) and 0.6-1 keV (x-axis), which is consistent with the characteristic peaks of Ni. The second and third highest peaks are also attributed to Ni, confirming the presence of Ni in the sample. The oxide peak detected at around 25 cps/eV (y-axis) and 0.4-0.6 keV (x-axis) is indicative of the presence of O_2, further confirming that the sample is NiO. The presence of other elements, such as Al, C, Si, Au, and Cr, is also detected. The single Al peak detected at almost 15 cps/eV (y-axis) and 1.5 keV (x-axis) indicates the presence of Al. The highest peak of Cr is detected at a little more than 1 cps/eV (y-axis) and 0.8 keV (x-axis), while the highest peak of gold is detected at 4 cps/eV (y-axis) and 2-2.4 keV (x-axis), with other peaks detected at higher keVs (x-axis) and not exceeding 2 cps/eV (y-axis). The presence of C and Si can also be detected, though the intensity of their peaks is lower than that of Ni and the other elements. Overall, the EDAX results confirm the presence of NiO NPs and provide information about the elemental composition of the sampl including the presence of Ni, O_2, Al, C, Si, Au, and Cr. The results of the analysis indicate that the NP is composed of 73.1 wt% Ni, with a standard deviation (sigma) of 0.3, and 13.9 wt% NiO, with a sigma of 0.2. Carbon is present at a concentration of 6.7 wt%, with a sigma of 0.3; while, Al is present at a concentration of 5 wt% with a sigma of 0.1. Finally, Cr is present at a concentration of 0.9 wt%, and Si is present at a concentration of 0.4wt%.

The presence of Al, C, Si, Au, and Cr in the sample suggests that the NP may have been synthesized or processed using materials that contain these elements. Moreover, the presence of multiple peaks for Ni and other elements in the EDAX spectrum indicates the presence of various phases and/or chemical states in the sample, which may affect its physical and chemical properties. The accuracy and precision of the EDAX results (as indicated by the reported sigmas) provide confidence in the reliability of the analysis and the representativeness of the sample.

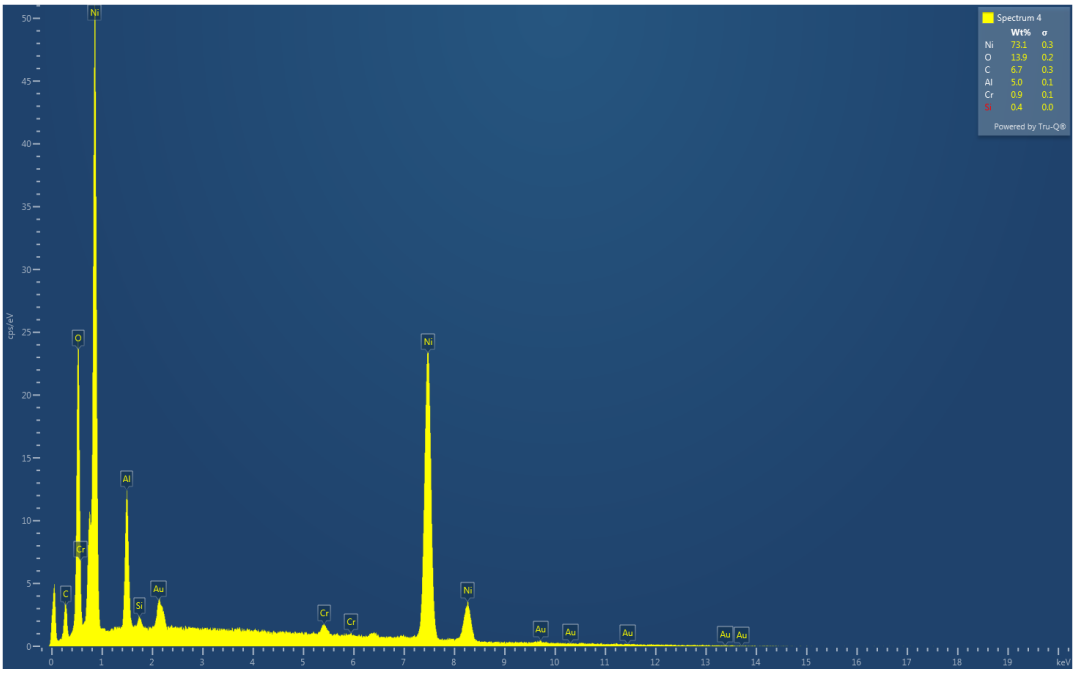

Figure 4-5. Nickel Oxide EDAX results

4.2 AFM results

The AFM was used to examine the calcite samples that have asphaltene deposited on the surface in presence or absence of NPs. The roughness and micro-topography of the surface following asphaltene deposition can be better understood using AFM probes. AFM images for pure calcite together with ones with asphaltene deposition with and without MgO NPs are presented in Figure 4-6. It is important to note here that during AFM probe of the calcite substrate, the shade of the NPs differs from asphaltene and the surface without NP can be easily distinguished. The variation in size is one of the important features that must be highlighted during the AFM probes. The AFM images are provided in both 2D and 3D. The Z bar shows the level of deposition. The image after asphaltene deposition (4-6b) shows the rise in thickness of the asphaltene layer for about 20 times, which is 600 nm, although the initial height difference in irregularities on the surfaces was 30 nm. The panel (4-6c) shows the impact of NPs; the maximum point is 300 nm, which is twice as small as the case with deposited asphaltene. Moreover, the decrease in surface area of light spots in presence of NPs can be clearly seen compared to the image taken in absence of the NPs. This indicates that MgO NPs affected decrease of asphaltene agglomerations and deposition.

The functional groups (e.g., pyridine, thiophene, carboxylic) of asphaltene adhered onto the calcite substrate's surface. As a result, the characteristics of the surface are impacted by asphaltene deposition. The surface of the substrate of pure calcite was rough and not smooth initially. Once the asphaltene was deposited on the substrate, its roughness changed. Due to the NP's greater adherence ability, the amount of unstable asphaltene on the surface decreased. The asphaltene is absorbed by NPs, effectively reducing the amount of unstable asphaltene present in the synthetic oil medium. By reducing the amount of unstable asphaltene, the overall stability of the crude oil is improved making it easier and safer to transport and process.

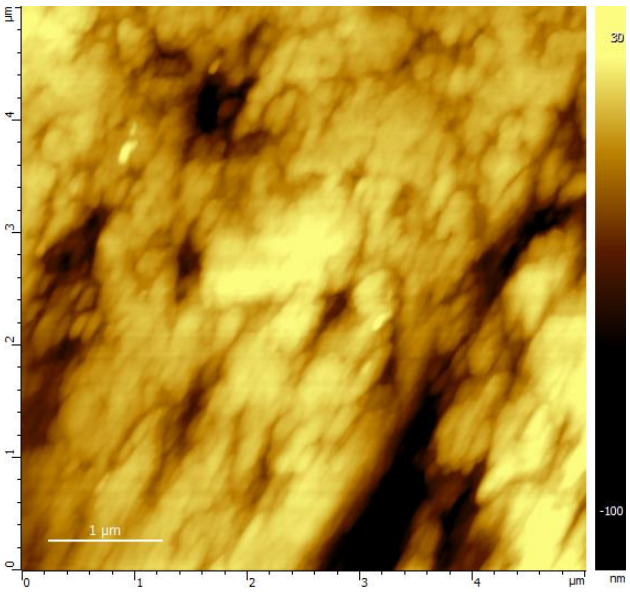

(a)

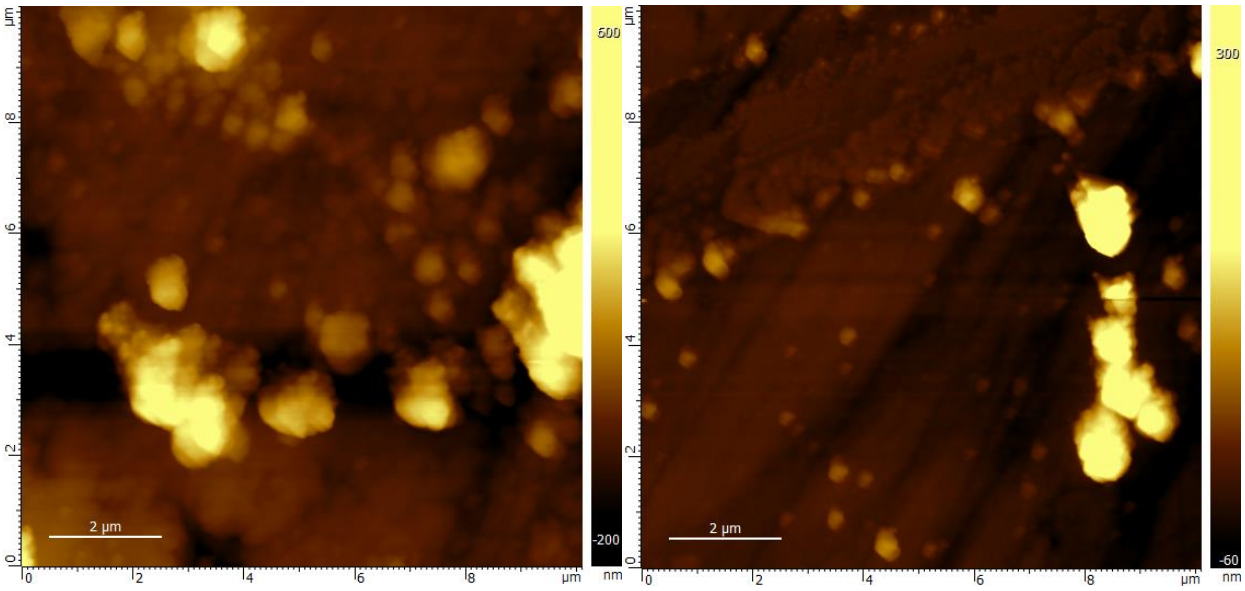

(b) (c)

Figure 4-6. 2D AFM images of the calcite surface for MgO. (a) Pure calcite; (b) Calcite deposited with asphaltene (slight spots); (c) Calcite deposited with asphaltene (slight spots) plus MgO NP. The distribution and size of the asphaltene agglomerates is reduced n presence of MgO NPs.

The calcite surface with the asphaltene deposited and the effect of NiO NPs is presented Figure 4-7. The precipitation of organic materials such as asphaltene is depicted by a light tone on the AFM images. NiO NPs cause small asphaltene to deposit on the calcite substrate reducing the size of the light tones, which initially were asphaltene. Since the Z bar's starting height in this example is 20 nm, it clearly displays the surface imperfections prior to deposition making it particularly notable. Asphaltene aggregates are tall because during the aging process, the height of the deposited asphaltene reached 1,000 nm. As can be seen in panel (4-7c), there are a lot of affected aggregations and very few large aggregations are remaining. The adsorption of asphaltene onto the NP surface dramatically reduced the height of the aggregations and deposition of the asphaltene. In addition, NiO NPs have affected the surface area of organic depositions gradually as it can be observed from the images. NiO NPs could introduce functional groups that directly affect to the surface area.

The substrates' arithmetic average roughness (S_a), and surface dimensional ratio (S_{dr}) are decreased when NPs are present as shown in Table 4-1. In comparison to the absence of the NP, a more uniform substrate with fewer asperities is established.

Table 4-1. Surface characteristics (roughness, fractal dimensions)

*	S_a	S_{dr}	D
Pure calcite	0.175	16	2.460
Calcite and asphaltene	0.141	10.32	2.626
With MgO	0.153	12.55	2.557
With NiO	0.154	10.53	2.769

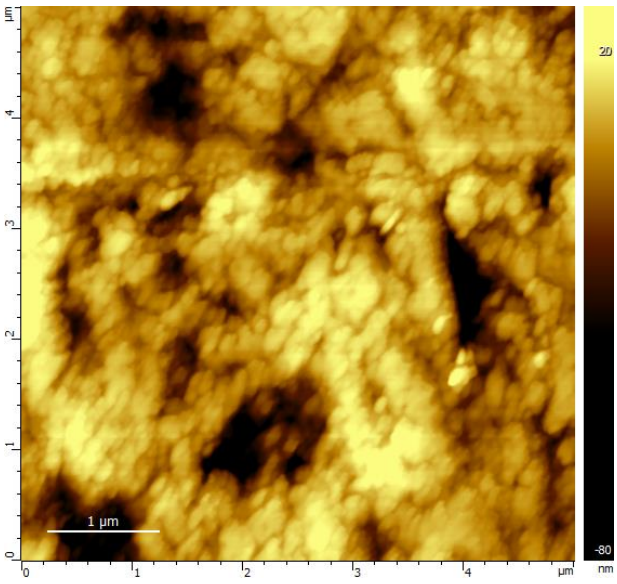

(a)

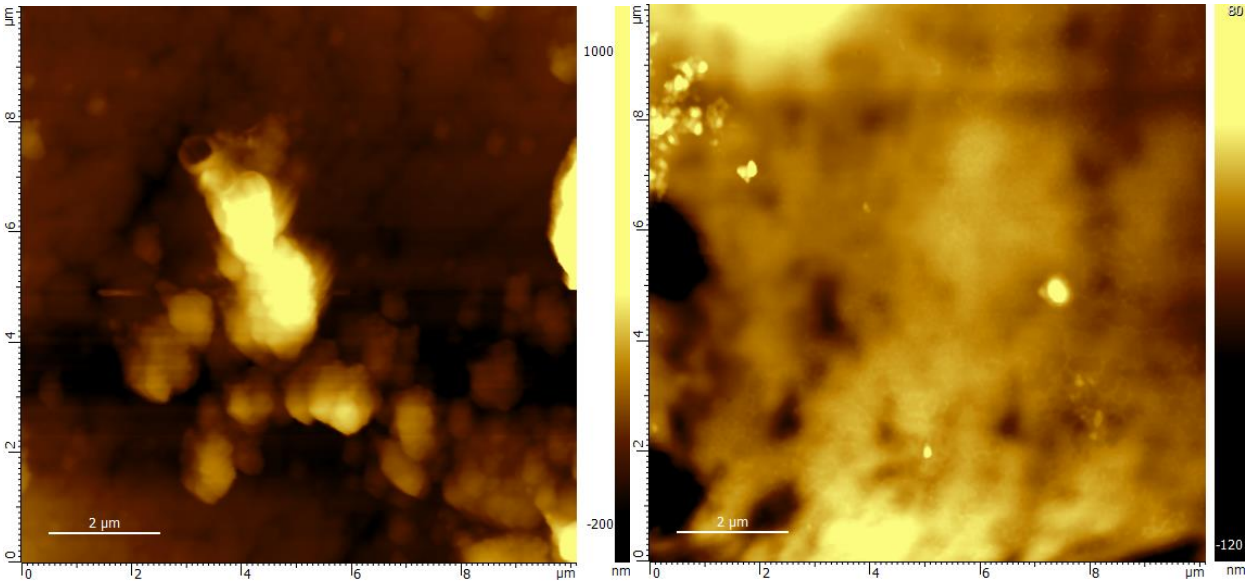

(b) (c)

Figure 4-7. 2D AFM images of the calcite surface for NiO. (a) Pure calcite; (b) Calcite with asphaltene (light spots); (c) Calcite with asphaltene plus NiO NPs. The organic materials has become barely noticeable in terms of surface coverage and distribution after the application of NiO NPs.

The surface roughness in this research work was characterized by two parameters: arithmetic average roughness and surface dimensional ratio; while, the fractal dimension (D) was used to characterize the surface complexity or irregularity. Surface dimensional ratio is used to describe the degree of roughness or irregularity of a surface. A high S_{dr} value indicates a surface with a high degree of roughness or irregularity; while, a low S_{dr} value indicates a smoother surface (Brown et al., 1998). Contrary to the statistical parameters, the fractal dimension is a reliable indicator to examine the micro-topography. A crucial characteristic to define the micro-topographic features and substrate complexity throughout all dimensions is fractal dimension. The fractal dimension can be used to gain a thorough understanding of all facets of surface morphology. A substrate's fractal dimension falls between 2 and 3. A smooth surface is implied when D equals to two; while, a rise in D's values indicates a rise in the roughness of the substrate. As can be seen from Table 4-1, the quantity of fractal dimension rises in presence of NP due to deposition of asphaltene agglomerations on the calcite substrate. Thus, the substrate will become more complicated and fractured. The decrease in height of the asphaltene aggregations represents the absorption of asphaltene by the NPs. The first sample, which was a pure calcite, showed a fractal dimension of 2.46 indicating a relatively smooth and regular surface. In contrast, the calcite with asphaltene deposition showed a higher fractal dimension of 2.626 indicating a more complex and irregular surface because of asphaltene deposition onto the calcite's surface. This sample also showed a lower S_a of 0.1410 suggesting some layers of asphaltene cover roughness onto calcite surface and decrease the S_a. This observation is consistent with some previous studies that showed asphaltene adsorption on solid surfaces can cause surface roughening due to formation of aggregates or clusters (Khodja et al., 2013). The third sample, which was calcite with asphaltene deposition and affected by MgO NPs, showed a fractal dimension of 2.557 that is slightly lower than that of the second sample. This result suggests that the addition of MgO NPs may have reduced the surface irregularity or complexity induced by decreasing size of asphaltene deposition. The S_a of this sample was 0.1533, which is higher than sample in absence of MgO. The fourth sample, which was calcite with asphaltene deposition and affected by NiO NPs, showed the highest fractal dimension of 2.769 indicating a highly irregular or complex surface because of less and small size of asphaltene precipitation onto the calcite surface. The S_a this sample is 0.1539, which is similar to those of the third sample. In addition, the fractal dimension of the surface increased to 2.769. These results suggest that the surface roughness of calcite can be affected by various

factors such as precipitation with different materials and addition of NPs. The surface complexity or irregularity, as characterized by fractal dimension, generally increased with asphaltene deposition on the surface and further enhanced by the addition of NiO NPs. The observed changes in surface roughness and complexity are likely due to adsorption and interaction of different molecules or particles on the surface, which can induce surface restructuring or aggregation. Additionally, the variety of NPs used in the adsorption affects the sort of chemical reactions that occur (Mazloom, 2020). The influence of temperature, according to the different studies, is evident in quick reacting times but has no general influence the adsorption processes (J. Adams, 2014).

3D AFM images of the effect of MgO NPs on an asphaltene-deposited calcite surface are shown in Figure 4-8. Although the surface irregularities were compensated after deposition of asphaltene, a slight uplifts and large settlements can be seen on the surface of the calcite. The NP more or less levels the surface and affects the large depositions of asphaltene. This NP reduced the volume and height of the deposited asphaltenes more than two times. Precipitates that were initially small turned into point and barely noticeable aggregates. The thickness of asphaltene layers covering the calcite surface is decreased in presence of NPs allowing the original scratches on the calcite surface to be seen. In absence of NP, the thick layers of asphaltene restrict the original calcite surface scratches from being seen.

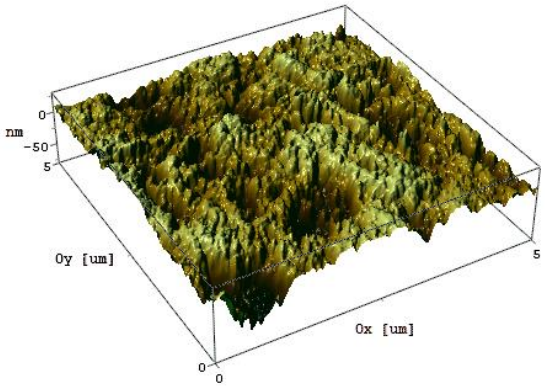

(a)

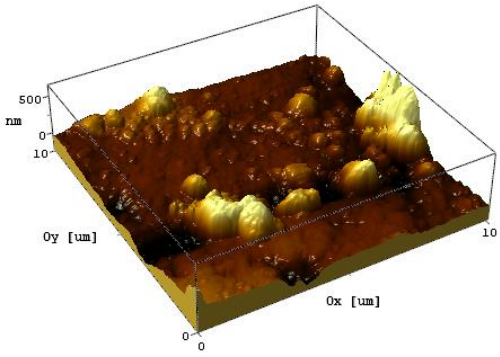

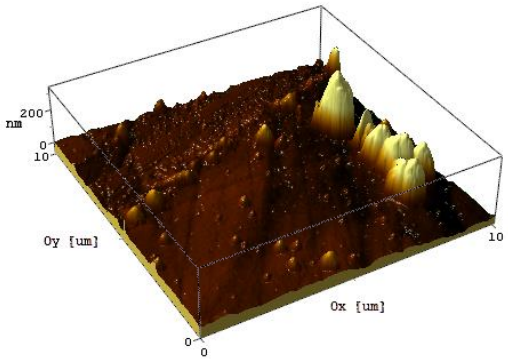

(b) (c)

Figure 4-8. 3D AFM images of the calcite surface for MgO. (a) Pure calcite; (b) Calcite with asphaltene deposition; (c) Calcite with asphaltene deposition plus MgO NPs. The height of agglomeration has reduced from 500 nm to 200 nm in presence of the MgO NPs due to the NPs' functional groups introduction.

3D views of the calcite surface of the calcite surface for the case of NiO are shown in Figure 4-9. Initially, the abnormalities were many. After that, synthetic oil solution entirely coated the region under investigation leaving only the deposited asphaltenes in place. Finally, the amount, thickness, and surface coverage of the deposited asphaltene was decreased by the NiO NPs leaving behind tiny precipitated stacks.

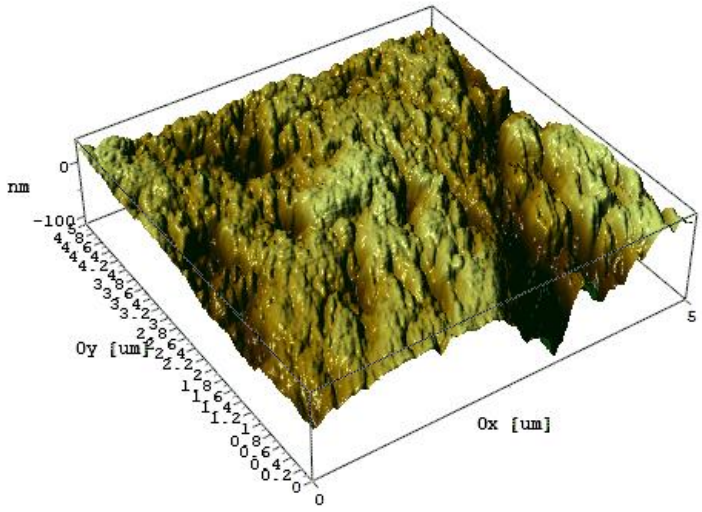

(a)

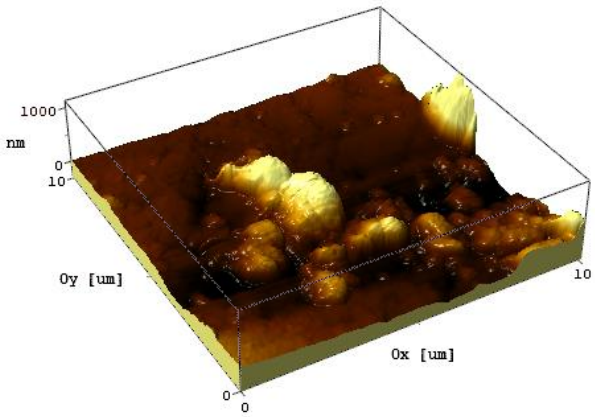

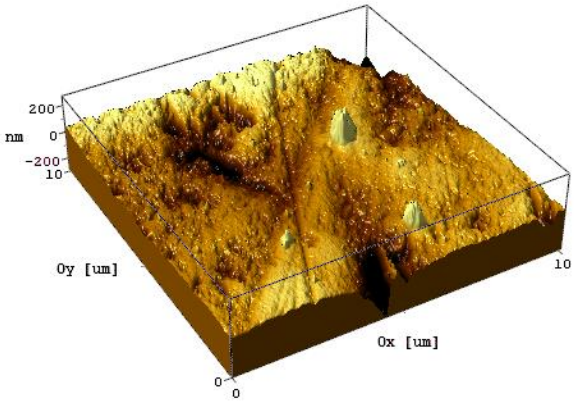

(b) (c)

Figure 4-9. 3D AFM images of the calcite surface for NiO NPs. (a) Pure calcite; (b) Calcite with asphaltene deposition; (c) Calcite with asphaltene deposition plus NiO NPs. The organic materials almost disappeared (decreased height of five times) due to the high adsorption capacity of NiO NPs.

The 3D AFM images of the asphaltene precipitation on the calcite substrate are shown in Figure 24 and Figure 25. According to the images, it can be clearly seen that the samples affected by NP have lower precipitation of asphaltenes compared to the samples without NP. It explains why larger asphaltene agglomerations tend to form in the solutions with no NPs. Both figures present clear changes of the volume of asphaltenes after the effect of NPs. Figure 24 features the effect of Mg oxide NP, which affected big and tall precipitates of asphaltenes. As a result, the precipitation is minimized after exposure of NPs. As for figure 25, the nickel oxide NPs coped flawlessly with the precipitated asphaltene, leaving a barely noticeable oil residue, Moreover, the surface of the calcite is also affected leading to almost full removal of asphaltenes.

NPs adsorb unstable asphaltene in the medium. As a result, assuming non-equilibrium circumstances, lesser and smaller asphaltene agglomerations occur. When asphaltene precipitates, it leaves behind many asperities on the substrate. Bigger mountains and troughs develop when NPs are absent. Additionally, the probability of asphaltene precipitation is higher when there is no NP. Tiny peaks are minimized when massive agglomerations form, which lowers the substrate's micro asperity. The formation of more uneven forms of substrate roughness is caused by the deposition of tiny aggregates of asphaltenes with the involvement of NPs. Accordingly; there are more tiny formations on the substrate after NPs compared to the case without them.

4.2.1 Comparison of MgO and NiO nanoparticles effect

Figure 26 is presented in order to compare the effects of both NPs. The results show that the influence of NiO NP on the surface of calcite is superior to that of MgO NP. The deposition of MgO NP on the surface of calcite leads to a reduction in height and volume, and the formation of smaller aggregates compared to NiO NP. This observation is in agreement with previous studies that have reported that the size and morphology of NPs play a crucial role in their interaction with surfaces (Ibrahim et al., 2019). Furthermore, after the effect of NiO NP on the asphaltenes, very small aggregates of asphaltenes are observed, which indicates the interaction between NiO NP and asphaltenes. Asphaltenes are complex organic molecules that are known to interact with mineral surfaces, and their deposition on the surface of calcite can affect the wettability and adhesion properties of the surface. The interaction between NiO NP and asphaltenes can be attributed to the chemical properties of NiO, which has a high surface energy and is known to form strong chemical bonds with organic molecules. In contrast, the interaction between MgO NP and the surface of calcite seems to be weaker, as the aggregates are arranged in a heap, which suggests that the effect of MgO NP on the surface is not significant. This examination is in line with previous studies that have reported that the interaction between MgO NP and surfaces is mainly governed by physical adsorption rather than chemical bonding (Hu et al., 2016). It is also worth noting that the location of the precipitation aggregates differs between MgO and NiO. In the case of MgO, the aggregates are arranged in a heap, whereas after the deposition of NiO, almost single aggregates with a small size remain. This consideration suggests that the aggregation behavior of NPs on the surface of calcite is influenced by their size, morphology, and chemical properties. Generally, NPs are divided into three metal oxides, based on their origin, which basic, acidic, amphoteric. NiO NPs are known as amphoteric metal oxides, while MgO are basic metal oxide NPs. Basic metal oxide NPs have lower adsorption capacity compared to amphoteric, because of the absence of surface functional groups (Nassar et al., 2011a). On the other side, NiO NPs can provide a favorable condition for asphaltene precipitation removal and modify the surface functional groups, which enhance the adsorption capacity.

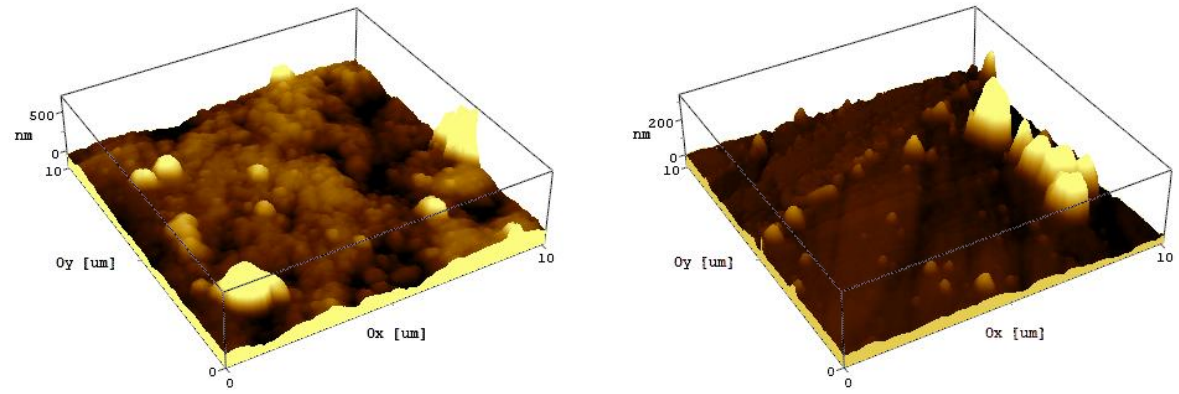

(a)

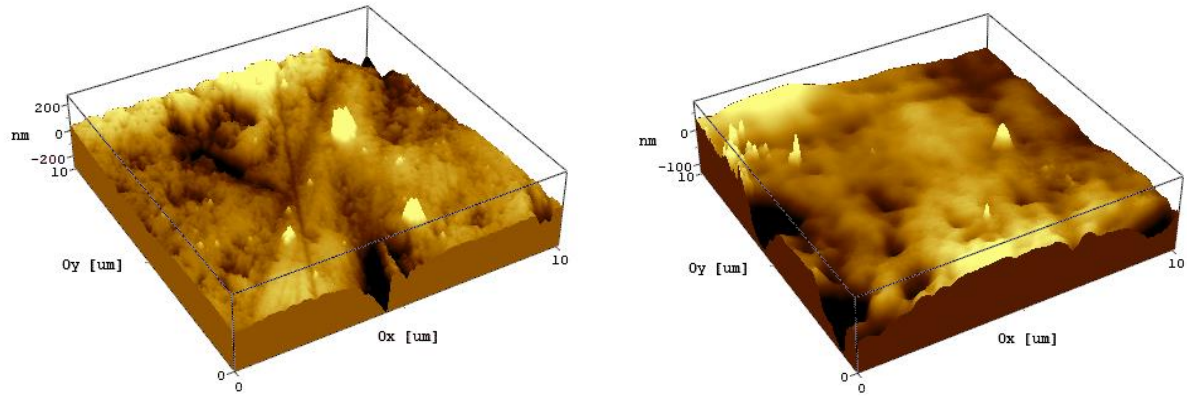

(b)

Figure 4-10. AFM height map images after adding the NPs (a) MgO; (b) NiO

4.3 Contact Angle measurement

Contact angle measurements aimed at evaluation of the effect of two different types of NPs, NiO and MgO, on surface chemistry and wettability of the calcite surface. The method used to evaluate the wettability of the calcite surface was the sessile drop technique. It is important to note here that the sessile drop method used for CA measurements in this research work has some limitations. For example, the accuracy of the results can be affected by factors such as size and shape of the droplet and the surface roughness. Moreover, the presence of impurities or surface heterogeneity may also affect the CA measurement results. CA measurements were conducted on different samples: a cut calcite sample, a calcite sample with asphaltene deposition, a calcite sample with asphaltene deposition in presence of MgO NPs, and a calcite sample with asphaltene deposited in presence of NiO NPs. The measurements were obtained using both Young-Laplace and modified Wenzel equations. The results of the modified Wenzel equation are better in terms of reliability as it considers the roughness of a surface as a results of wettability alteration.

Calcite is a surface that could be both water-wet and oil-wet, according to Kowalczuk et al. (2017). The CA measurement procedure and sample preparation can affect the calcite-water contacting angles. By using the sessile drop method, the receding and advancing interaction degree for every surface was calculated for the respective half of each surface. As shown in Figure 4-11, the findings of CA measurements calculated using the Young-Laplace equation for pure calcite, calcite with asphaltene deposition, and calcite with asphaltene deposition with and without NPs.

The wetting characteristic of flat surfaces cab be described using the Wenzel model. In the Wenzel model, the liquid is expected to cover all of the substrate flaws giving the appearance of a smooth surface even if the solid surface is believed to be fully rough. The Wenzel model's formula for the contact angle is:

$$cos\theta_w = r \times cos\theta_y \qquad 4\text{-}1$$

$$r = 1 + \frac{S_{dr}}{100}$$

where θ_w – Wenzel's contact angle, θ_y – Young's contact angle, r – is the roughness factor, which itself described as a ration between surface area and projected area.

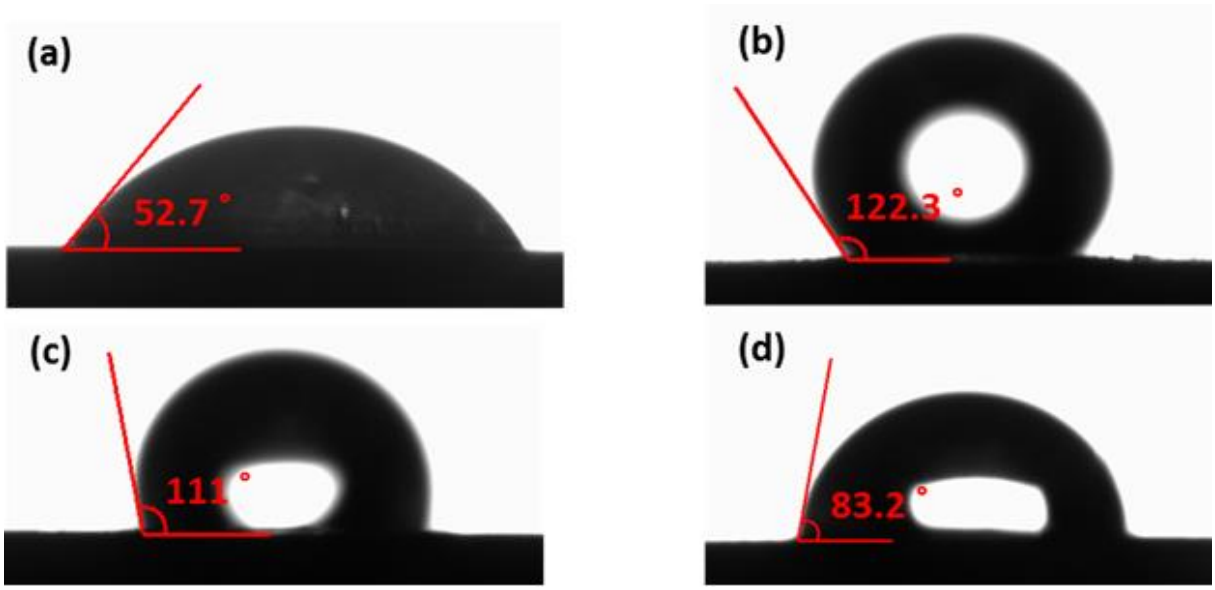

Figure 4-11. Contact angle measurement results: (a) Pure calcite; (b) Calcite with asphaltene deposition; (c) Calcite + asphaltene aged in the solution with MgO NP; (d) Calcite + asphaltene aged in the solution with NiO NP. The pure calcite surface is water-wet, initially. After the precipitation of asphaltene, the surface became oil-wet. In presence of the MgO NPs, the wettability changed to slightly oil-wet and became water-wet in presence of NiO NPs.

The results of CA measurements calculated using both Young-Laplace and modified Wenzel models are presented in Table 4-2 presents. The first sample was a cut calcite sample and the θ for this sample was 53°. This suggests that the calcite surface has moderate wettability since the contact angle is greater than 45°; which is typically considered the boundary between a water-wet and oil-wet surface. The second sample was a calcite sample precipitated with asphaltene, and the θ was determined as 122°. This suggests that the asphaltene has made the calcite surface highly oil-wet since the θ is greater than 90°; which is typically considered the boundary between a water-wet and oil-wet surface. These results are consistent with previous research that has shown that asphaltene can make surfaces highly oil-wet (Vesali et al., 2016). The third sample was a calcite sample precipitated with asphaltene and MgO NPs, and the θ was obtained as 111°. This suggests that the addition of MgO NPs has reduced the oil-wetting condition of the surface compared to the sample precipitated with asphaltene alone. The reduction was achieved due to the effect of functional groups of the MgO NPs on the interaction between liquid drop and surface and modifying the surface energy of a precipitated calcite sample. The contact angle of 111° still indicates an oil-wet surface, but it is less oil-wet than the sample with asphaltene alone. These

results are consistent with previous research that has shown that the addition of MgO NPs can reduce the oil-wetting state of glass surfaces (Daryaei et al., 2013). In essence, MgO NPs can change a surface's surface chemistry to decrease its oil-wetting condition. MgO NPs can produce a water-wet surface that is more attracted to water molecules than oil molecules when they are dispersed on a substrate. This is because the MgO NPs are reported for their high surface energy making them capable of quick interactions with other substances. In addition, the NPs' large surface areas has the potential to produce a rough surface that would capture water molecules and prohibit oil from sticking to it. Its rough surface can also narrow the contact angle between it and oil droplets increasing its hydrophobicity and decreasing its ability to absorb oil. Moreover, MgO NPs may change a molecule's surface charge, which can affect how oil droplets interact with the surface. For instance, by adding a negative surface charge, the surface might deter negatively charged oil droplets reducing the surface's oil-wetting condition. The fourth sample was a calcite sample precipitated with asphaltene and NiO NPs, and the θ was obtained as 83°. Because of high surface energy and roughness, the NiO NPs can make a surface more water-wetting. In addition to surface roughness, the NiO NPs surface energy also contributes to the improved water-wetting conditions. Compared to other materials, the NiO NPs have a higher surface energy, which increases their attraction for water atoms. Greater wetting results from the NPs' ability to capture and retain water molecules more efficiently when they are scattered across a surface. These results suggest that the addition of NiO NPs has increased the water-wetting state of the surface compared to the sample with asphaltene deposition alone. The θ of 83° indicates a moderately water-wet surface. This result is consistent with previous research that has shown that the addition of the NiO NPs can increase the water-wetting condition of silica surfaces (J. Liu et al., 2012). The experiment conducted using the sessile drop technique has demonstrated that the addition of NPs can significantly affect the wettability of the calcite surface. The addition of MgO NPs can reduce the oil-wetting state of the surface; while, addition of the NiO NPs can increase the water-wetting condition of the surface. The MgO NPs are known to have a high surface energy and a low surface tension, which can reduce the surface free energy of the material they are added to, resulting in a decrease in its oil-wetting behavior. At the same time, the NiO NPs have a high surface energy and a high surface tension, which can increase the surface free energy of the material they are added to, resulting in an increase in its water-wetting behavior.

Table 4-2. Contact angle measurement results

Sample	Wetting condition	θ	r	Wenzel model CA
Pure Calcite	Water-wet	53°	1.16	45°
Calcite with asphaltene	Oil-wet	123°	1.10	124°
Calcite with asphaltene and MgO	Slightly oil-wet	111°	1.12	114°
Calcite with asphaltene and NiO	Water-wet/neutral-wet	83°	1.10	82°

Moreover, Shojaati et al., (2017) reported that the NiO NPs, which have acidic chemical nature, are more effective in a polar interaction establishment with asphaltenes. The results obtained in this research work are consistent with previous researches that have shown addition of different types of NPs can affect the wettability of surfaces (Hemmati et al., 2018). The CA measurement results have several practical implications. For example, addition of NiO NPs can be used to modify the wettability of calcite surfaces for various applications. NiO NPs can be added to calcite surfaces to make them more water-wet, which could be useful for applications such as water treatment or oil recovery. On the other hand, addition of MgO NPs can be used to make the calcite surfaces less oil-wet, which could be useful for a variety of applications. The findings of this research work may have implications in various fields including materials science, environmental science, and biotechnology. For instance, in the field of materials science, these findings may have implications for designing surfaces for anti-fouling applications, where the surfaces are intended to be less oil-wet. In the field of environmental science, these findings may be useful for designing surfaces with higher water-wetness for water treatment applications.

The experiment conducted to evaluate the effect of NiO and MgO NPs on the wettability of a calcite surface using the CA measurement method has shown that the addition of NPs can significantly affect the surface's wettability. The results suggest that NPs can be used to modify the wettability of different surfaces for various applications. However, more research is needed to understand the underlying mechanisms responsible for the observed changes in wettability and to optimize the nanoparticle synthesis and surface modification processes for different applications.

4.4 X-ray Photoelectron Spectroscopy

The XPS surveys aimed at providing deep insights into the relationship between asphaltene adsorption, NPs, and surface to assess the role of NP in preventing asphaltene adsorption onto calcite surface, which is a crucial factor in the deposition of asphaltene. The results of the analysis can be used to optimize surface treatments and NP coatings to enhance surface wettability and prevent asphaltene deposition, which can lead to reduced efficiency and increased maintenance costs in the oil and gas industry. The surveys included four different samples and asphaltene, MgO and NiO NPs: sample 1 – a pure calcite surface, sample 2 - calcite with asphaltene deposition and heptane, sample 3 - calcite with asphaltene deposition and heptane affected by MgO NPs, sample 4 - calcite with asphaltene deposition and heptane affected by NiO NPs. The X-ray source used for the analysis was a monochromated low power Al Ka X-ray source and the standard lens mode was used. The X-ray photoelectron spectroscopy analysis revealed valuable information about the surface composition and surface chemistry of each sample. The presence of different elements, such as Ca, C, S, N_2, O_2, Mg, and Ni was determined and used to assess the effects of asphaltene precipitation and the effect of presence of NPs on surface chemistry of the calcite. The results obtained from the XPS surveys are presented and discussed in detail in this section.

4.4.1 XPS analysis of the asphaltene powder

In this research work, XPS was used to investigate the asphaltene powder, and four elements were detected, namely C, O_2, S, and N_2 (Figure 4-12). Carbon was found to have the highest atomic ratio of 84.55%. This is consistent with the fact that asphaltene is predominantly composed of carbon. The binding energy of C was measured to be 286.04 eV, which is consistent with literature values for sp2-hybridized C in aromatic rings (Guzmán et al., 2017). The high C content and sp2-hybridization indicate the aromatic nature of asphaltene, which is known to have a complex and heterogeneous molecular structure. Oxygen was the second most abundant element with an atomic ratio of 12.41% and a binding energy of 535.19 eV. The high binding energy suggests that the O_2 is present as carboxylic or carbonyl functional groups, which are commonly found in asphaltenes (Rudrake et al., 2009). These Oxygen-containing functional groups are important for the reactivity and stability of asphaltene, as they can participate in chemical reactions such as oxidation and adsorption on surfaces. S and N_2 were also detected in the asphaltene powder with atomic ratios of 1.71% and 1.33%, respectively. The binding energies of S and N_2 were measured to be 165.82

eV and 400.74 eV, respectively. These elements are known to play an important role in the properties and behavior of asphaltene as they can form heteroatomic functional groups and contribute to stability of the asphaltene molecular structure (Rudrake et al., 2009).

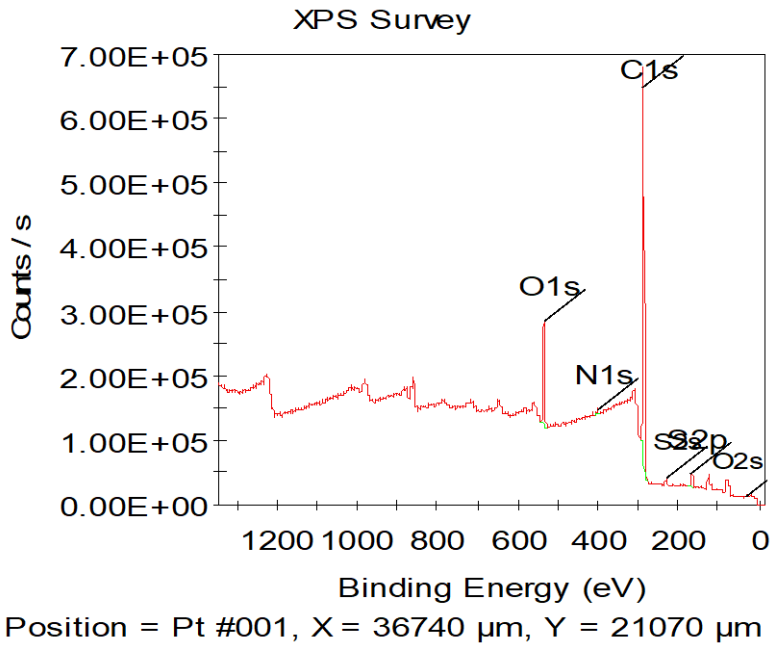

Figure 4-12. Asphaltene XPS survey

4.4.2 XPS analysis of the MgO NPs powder

XPS analysis of the MgO NPs (Figure 4-13) revealed presence of two main elements, Mg and O_2, with binding energies of 1302.44 eV and 531.28-532.3 eV, respectively. The atomic ratios of O_2 were found to be 31.19%, 47.96%, and 20.86%, indicating the presence of different O_2 species on the surface of the nanoparticle. A comparison with the literature values for MgO XPS spectra shows good agreement with the observed binding energies. For example, the binding energy for Mg 1s in MgO has been reported to be between 1301.3 and 1303.3 eV, consistent with the observed value of 1302.44 eV in this study. The binding energies for O 1s in MgO have been reported to vary between 529.5 and 533.2 eV, which also agrees with the observed values of 531.28, 530.1, and 532.3 eV. The presence of multiple O_2 species on the surface of MgO NPs has been reported in several studies. For instance, Khairallah et al. (2007) observed three O_2 species with binding energies of 531.5, 532.2, and 533.1 eV on the surface of MgO NPs using XPS analysis.

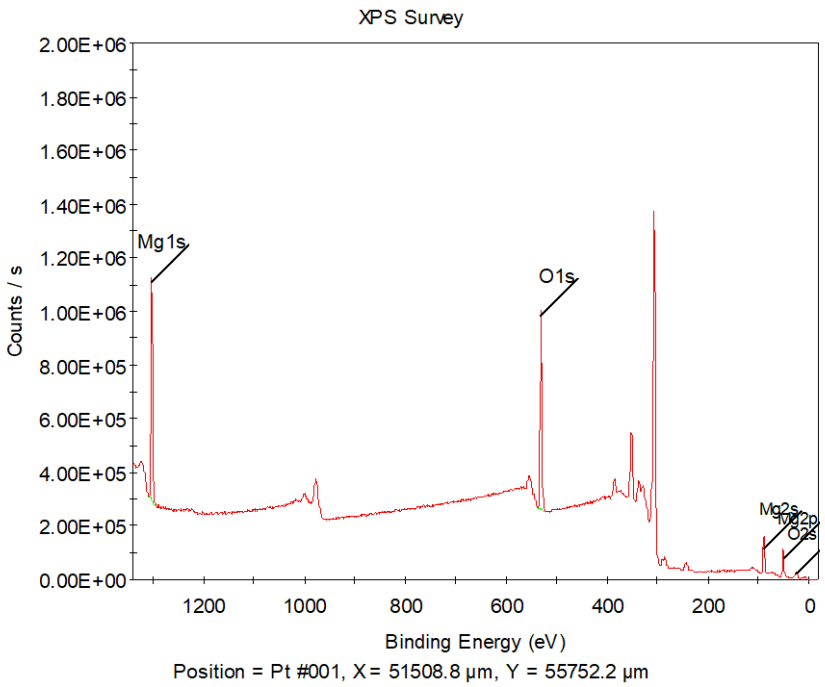

Figure 4-13. Mg1s XPS survey

4.4.3 XPS analysis of the NiO NPs powder

NiO NPs were investigated with XPS (Figure 4-14), which detected the main elements Ni2p, O1s, and C1s. The investigation included an elemental orbitals test and an overall XPS survey. The results of the XPS surveys confirmed the presence of four peaks of Ni with binding energies of 855.29, 872.37, 860.91, and 878.76 eV, indicating existence of Ni^{2+} oxidation state in the NiO NPs. The atomic ratios of the four peaks were 44.85, 19.59, 20.53, and 15.03, respectively, which suggest that the sample is slightly Ni-rich. The three peaks detected for O1s indicate presence of O_2 in different chemical environments. The binding energies of 532.44, 531.12, and 529.68 eV correspond to O_2 in Ni-O, O^{2-}, and adsorbed O_2 species, respectively. The atomic ratio of O^{2-} was the highest among the three peaks, suggesting the presence of O_2 vacancies in the NiO NPs. The XPS survey also detected presence of C1s element with a binding energy of 285.29 eV and an atomic ratio of 27.31%. The presence of C1s can be attributed to surface contamination or residual organic compounds from the synthesis process. The results of this XPS investigation are consistent with previous studies on NiO NPs. Peck et al. (2012) reported similar binding energies for Ni2p3/2 and Ni2p1/2 orbitals in NiO NPs, indicating presence of Ni^{2+} oxidation state. These researchers have also reported detection of O_2 in different chemical environments and suggested the existence of O_2 vacancies.

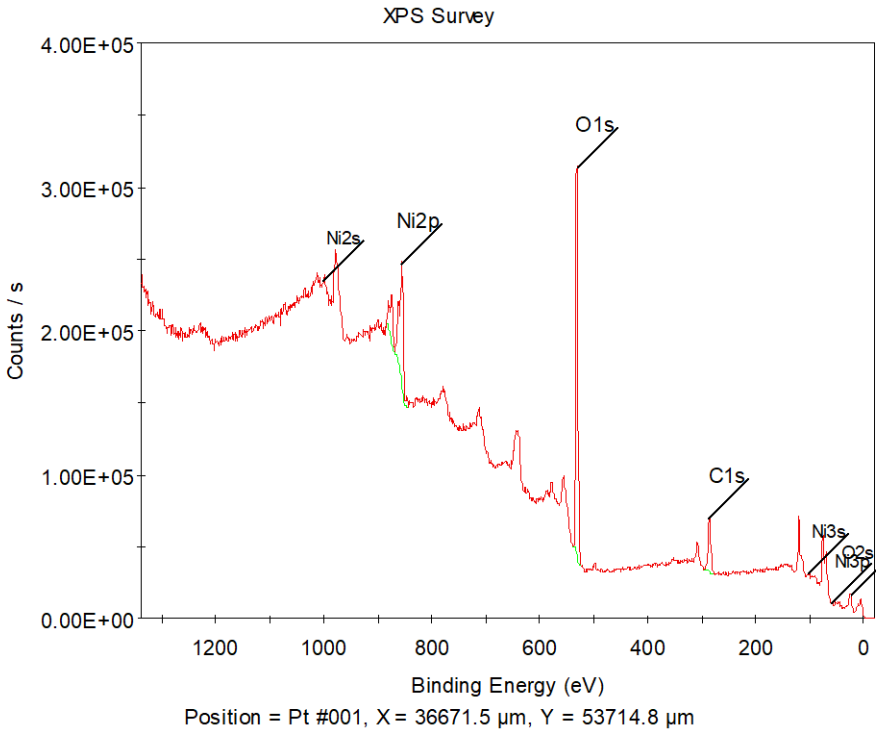

Figure 4-14. Ni2p XPS survey

4.4.4 XPS analysis of the sample 1. Pure calcite (Ca 2p3/2 O 1S C 1s)

Based on the XPS results obtained for the calcite slice sample, the elemental composition was investigated using XPS survey analysis. The XPS survey (Figure 4-15) revealed presence of four elements in the sample, namely O_2, C, Ca, and N_2. The binding energy of these elements was observed at 530.83 eV, 284.8 eV, 346.86 eV, and 400 eV, respectively. The intensity of the peaks corresponding to each element was recorded in counts per second (CPS) and the height of the peaks in the XPS graph was found to be 407298 CPS for O_2, 356869 CPS for C, 155329 CPS for calcium, and 25016 CPS for N_2. The interpretation was based on the shift of C content of the sample, which can provide information about the chemical environment of the sample. The net charge of calcite in reservoir condition (pH<8-9) is positive because of existence of Ca-OH groups (Al-Busaidi et al., 2019). Hence, the acidic groups in the asphaltene structure (i.s., hydroxyl groups, R-COO-) play a key role in asphaltene adsorption onto the calcite surface.

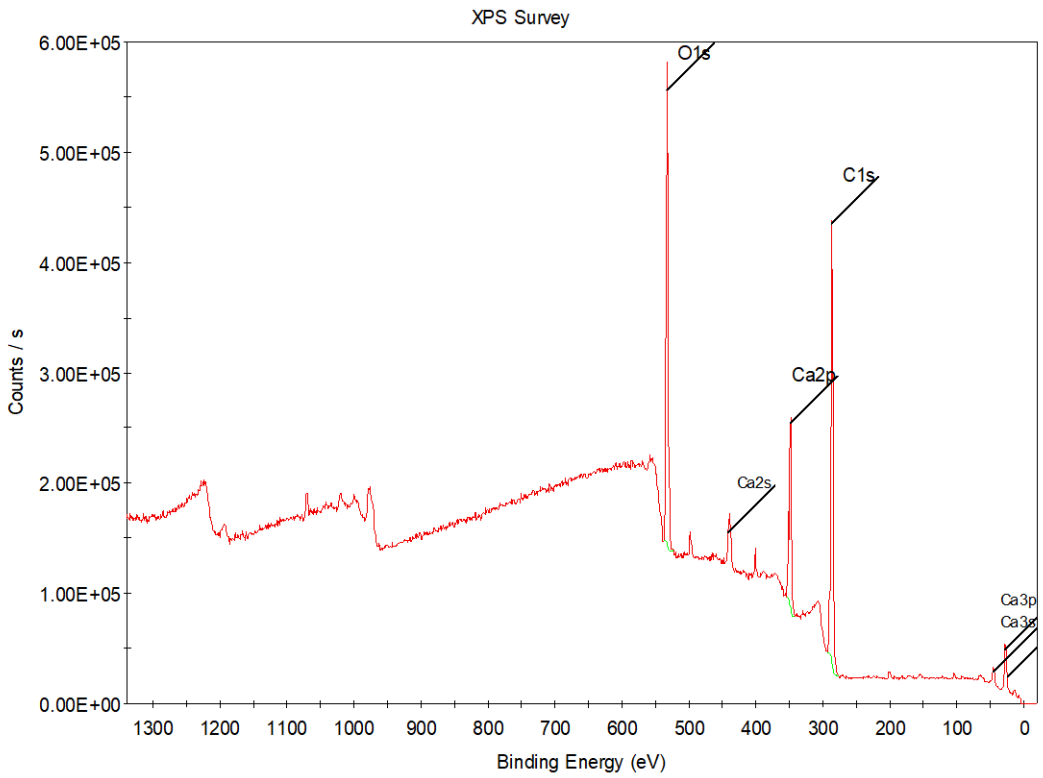

Figure 4-15. XPS survey for the calcite slice sample

4.4.5 XPS analysis of the sample 2. Calcite + asphaltene + heptane (Ca 2p3/2 O 1S C 1s S 2p3/2 N 1s)

The second sample is calcite with deposited asphaltene and subsequently diluted with heptane. XPS was used to analyze the sample, which detected four elements, including C, O_2, S, and N_2. The XPS survey (Figure 4-16) also shows five peaks of N_2, which were found to have binding energies ranging from 393.98 eV to 407.48 eV. The binding energy peak for C was observed at 284.8 eV, while O_2 had two binding energy peaks at 531.88 eV and 540.42 eV. S's binding energy peak was observed at 164.39 eV. Additionally, the XPS survey provided information on the height counts per second (CPS) for each of the detected elements. The CPS for C was observed to be 683497.92, while O_2 had a CPS of 32011.72. S's CPS was 25791.57, and N_2's CPS was 9669.17. It is worth noting that calcium was not detected at this stage of the experiment. Additionally, heptane dilution was used that effect the XPS results and should be considered. Previous studies reported that heptane dilution can affect the surface composition and depth profiling of the materials potentially altering the XPS results. Therefore, the use of heptane as a diluent may have influenced the XPS findings in this research work.

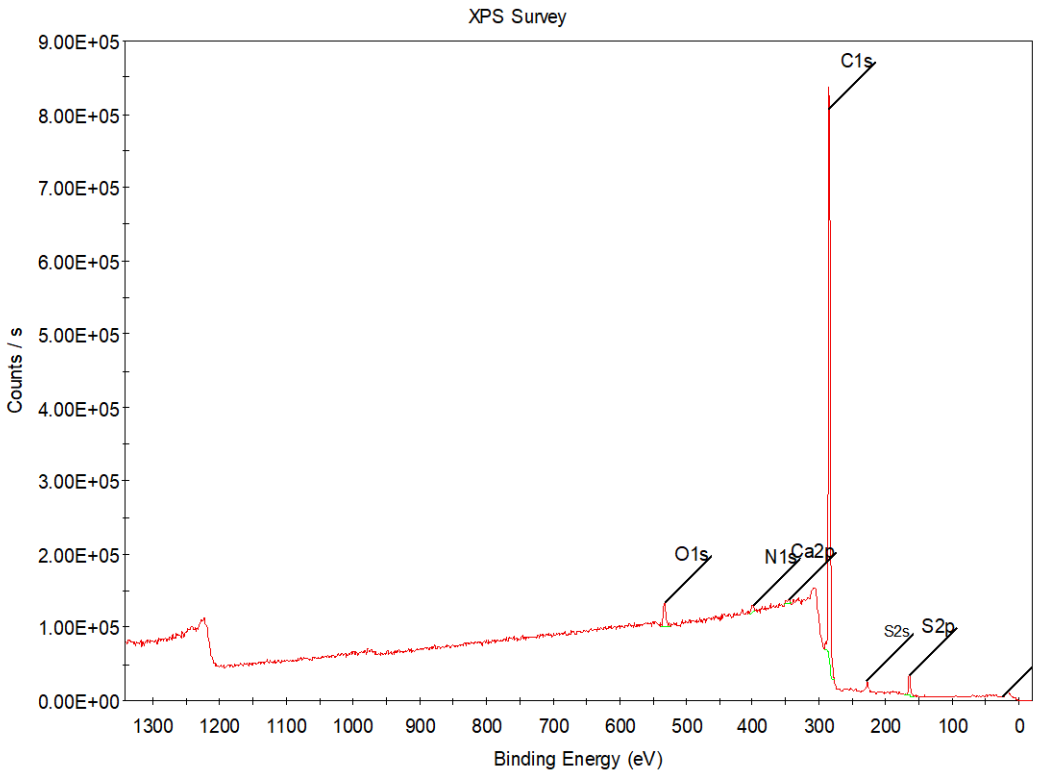

Figure 4-16. XPS survey of calcite with asphaltene deposition and diluted with heptane

In comparison, the second sample that is diluted with heptane shows a higher intensity of the C peak compared to the other samples. This suggests that the sample contains more C or organic material possibly due to presence of asphaltene or other hydrocarbons. In addition, it should be noted here that in all samples the highest atomic percentage indicates C elements. Presence of asphaltene in the sample was confirmed by the XPS analysis. Asphaltene molecules are large and complex organic molecules that contain high concentrations of S and N_2. The detection of four peaks of S and three peaks of N_2 in the XPS survey suggests that the asphaltene molecules in the sample are present in a complex mixture with different chemical environments and binding.

Heptane usage may effect on how asphaltene aggregates in oil environment and this could have an influence on how XPS data are interpreted. Because of their strong polarity and propensity to cluster in crude oil, asphaltene compounds are believed to generate enormous and complicated aggregates. By solvating the polar compounds on the substrate of the asphaltene particles, the use of heptane as a solvent can destabilize the solution and tendency to asphaltene aggregation increases. At lower asphaltene contents, when heptane content is quite large, this impact is

especially prominent (Wang et al., 2014). The dominance of heptane in the solvent combination can potentially encourage asphaltene agglomeration at greater asphaltene amounts. This is because the heptane concentrations are no longer high enough to fully dissolve all of the polar groups on the asphaltene molecules, which causes the creation of tiny groupings that can combine to create massive aggregation. Other polar solvents may also react with the asphaltene molecules and affect their aggregating tendency, which can make this impact more noticeable. As the quantity of heptane in these samples can be large enough to encourage asphaltene agglomeration, this impact would be more noticeable (Headen et al., 2009). Consequently, while interpreting XPS data, it is crucial to carefully analyze how heptane dilution affects asphaltene aggregation behavior.

4.4.6 XPS analysis of the sample 3: Calcite + asphaltene + heptane +MgO

The third sample is a calcite with asphaltene deposition in presence of MgO NPs and diluted with heptane. The XPA analysis (Figure 4-17) focused on six different elemental orbitals including C 1s, O_2 1s, S 2p, calcite 2p, N_2 1s, and Mg 2p. The binding energy of each element was detected, providing information about the chemical environment of the atoms. The highest binding energy was detected on O_2 atoms in a form of C and O_2 bonds. The lowest was on S in a form of sulfides indicating differences in chemical state of these elements. Three C and Ca peaks, 4 S peaks and N_2 peaks, three O_2 peaks, and two Mg peaks were detected by XPS indicating presence of multiple chemical species in the sample (Table 4-3). The atomic ratio analysis showed that C was the most abundant element in the sample with a percentage of 88% followed by S with 2.16%.

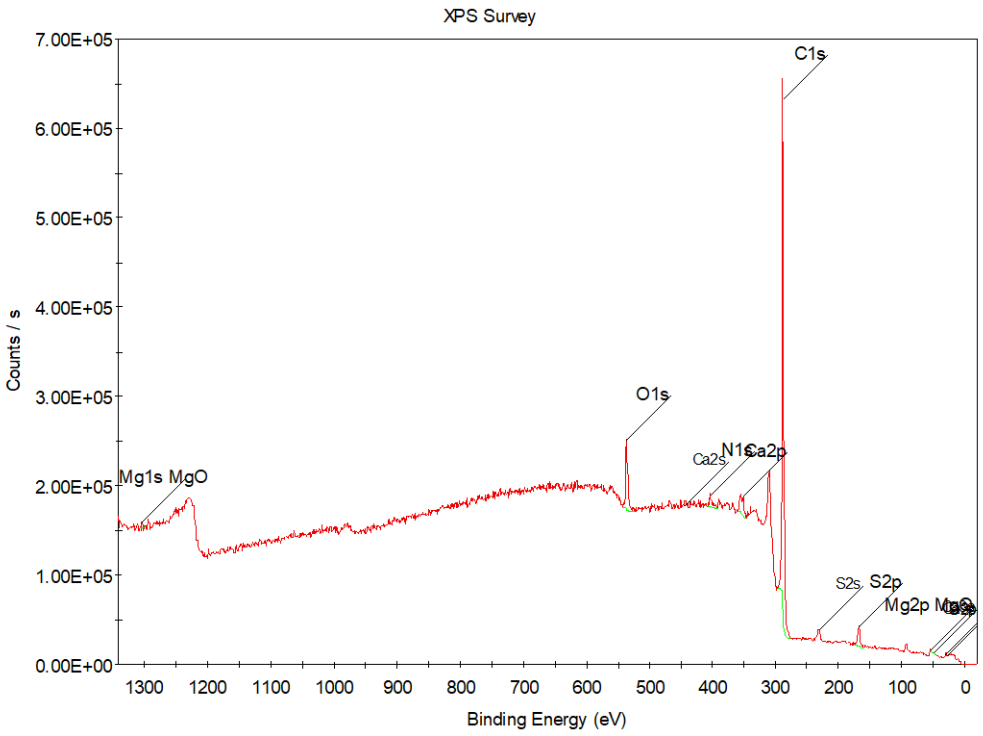

Figure 4-17. XPS survey of a sample affected with MgO NP.

4.4.7 XPS analysis of the sample 4: Calcite + asphaltene + heptane +NiO

The XPS results obtained for the fourth sample (Figure 4-18), which was a calcite surface with asphaltene deposition affected by NiO NPs, are discussed here. The XPS survey detected the presence of C, N_2, S, and O_2 in high resolution, with atomic ratios calculated from the binding energies of the respective peaks (Table 4-3). The C peaks were identified at binding energies of 284.82, 285.5, and 286.11 eV with atomic ratios of 34.64%, 55.71%, and 9.64%, respectively. These peaks are consistent with presence of C in the asphaltene in form of C-C bond and aliphatic C. Four different peaks were detected for N_2 at binding energies of 399.78, 400.34, 401.26, and 403.23 eV with atomic ratios of 58.62%, 11.03%, 16.58%, and 13.77%, respectively. These peaks suggest presence of different N_2-containing functional groups in the asphaltene, which are Pyridine-N, Amino-N, Pyrrolic-N, and Quaternary-N correspondingly. Sulfur peaks were detected at binding energies of 163.31, 164.68, 165.75, and 166.03 eV with atomic ratios of 13.07%, 56.63%, 20.41%, and 9.88%, respectively. These peaks indicate presence of sulfur-containing functional groups in the asphaltene with the highest concentration of Thiophene. Three peaks of O_2 were detected at binding energies of 531.71, 533.53, and 534.96 eV with atomic ratios of

14.04%, 84.12%, and 1.84%, respectively. The O_2 peaks suggest presence of O_2-containing functional groups, which could originate from asphaltene or heptane and confirms the single bond of O_2 and C, single bond between C and an O_2 atom with hydrogen. Notably, Ni and Ca elements were not detected in the sample by XPS. This suggests that the NiO NPs were not absorbed onto the surface or that the XPS has low sensitivity towards Ni as reported in some previous researches (Drouet et al., 2000; Grosvenor et al., 2006).

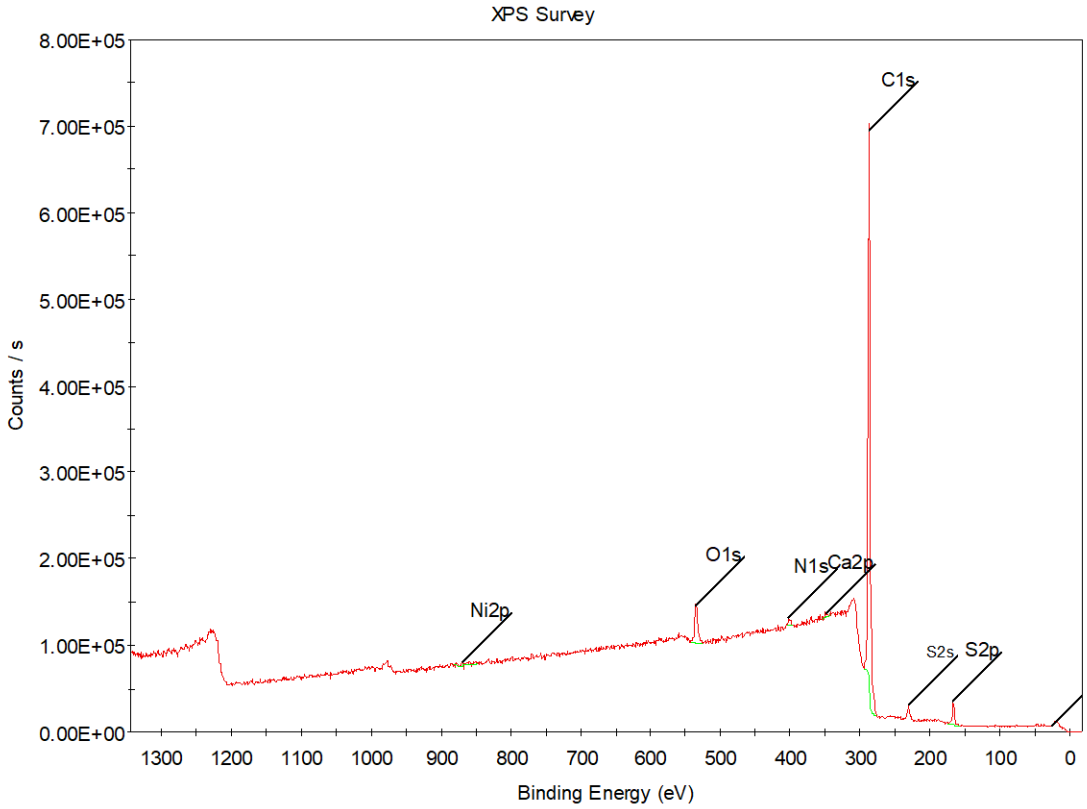

Figure 4-18. XPS survey of a sample affected with NiO NP.

The effect of NPs on asphaltene presence confirming elements, which are N_2 and S can be seen in Table 4-3. The changes in concentrations of three assignments of N_2 after application of NPs show that a chemical reaction between them has occurred. The decrease in pyrrolic assignment from 81.59% to 7.03% and 16.58% and the increase in pyridine atomic ratio form 14.31% to 88.67% and 58.62% suggest that the NPs have converted the assignments. Moreover, it can be suggested that the changes in concentrations is the results of physical adsorption of asphaltene by the NPs. As for S, concentration of sulfones decreased with the application of NPs. This is due to adsorption of sulfones onto NPs. The effect of MgO NPs was significant in terms of

conversion of sulfones to sulfoxides and Thiophene. However, the NiO NPs were not effective as previous NPs, but the atomic concentration of sulfoxides decreased and led to increase of sulfides. Overall, the atomic concentration of S and N_2 decreased particularly in presence of MgO to 0.27% and S to 1.04%, respectively; whereas, in presence of NiO NPs, the decrease for N_2 was 1.06% and for S 0.12%.

By examining O_2's impact on C spectra response of nearby C electrons, organic O_2 formations have been identified. The O1s spectra (Figure 4-19), which contains the signals belonging to the C = O, C-O-C/C-OH/C-O, and COO groups, was characterized by three peaks (Shao et al., 2018). The major forms of binding for O1s are C = O and C-O-C/C-OH/C-O, with COO- being less common. The curve resolved XPS C signals consists of three peaks for each sample at around 284.8, 285.8, and 286.5 eV.

The impact from both aromatic and aliphatic C can be seen in the 284.8 eV high point (Figure 4-20). The C molecule is connected to one O1s by a single bonding, as seen by the 285.8 eV peak. The 286.5 eV peak is the result of two O_2 connections holding C to O_2 (C=O). According to Geng et al. (2009)**,** the C1s spectra for each sample are separated into three positions: aromatic C (sp2), aliphatic C (sp3), and phenol/ether (C–O–C, C–OH, C–O). C mostly binds through sp2 and sp3 hybridization, having a little amount of C-O_2 bonding. It is clear that there are additional O-containing molecules in the asphaltene due to the high molar abundance of C-O_2 bonding in these components. A sample XPS C (1s) spectrum for curve-resolution into various organic O_2 elements is illustrated in Figure 4-20.

Table 4-3. C, O_2, N_2, and S elements in materials with concurrent states by XPS

Element	Assignment	Peak BE				Atomic ratio %			
		Calcite	Calcite +asphaltene+heptane	Calcite+asphaltene+MgO+heptane	Calcite+asphaltene+NiO+heptane	Calcite	Calcite+asphaltene+heptane	Calcite+asphaltene+MgO+heptane	Calcite+asphaltene+NiO+heptane
C1s	C-C bond	284.78	284.78	284.83	284.82	50.22	76.63	35.59	34.64
	Aliphatic C (sp^3)	286.07	285.92	285.82	285.5	17.18	22.32	61.55	55.71
	C-O-C, C-OH, C-O	286.88	286.54	286.85	286.11	32.6	1.04	2.86	9.64
	sp^2/(sp^{2+} sp^3)								
O1s	C = O	530.99	532.95	531.74	531.71	64.94	42.09	29.99	14.04
	C-O-C, C-OH, C-O	532.28	531.78	533.27	533.53	16.64	32.89	49.74	84.12
	COO–	533.07	534.13	533.88	534.96	18.42	24.4	20.27	1.84

N1s	Pyridine-N (N-6)	*	395.89	399.32	399.78	*	14.31	88.67	58.62
	Amino-N	*	399.14	400.1	400.34	*	4.1	4.3	11.03
	Pyrrolic-N (N-5)	*	400.66	400.22	401.23	*	81.59	7.03	16.58
	Quaternary -N	*	401.88	401.23	403.23	*	-	-	13.77
S 2p	Sulfides	*	163.74	162.23	163.31	*	11.03	8.93	13.07
	Thiophenes	*	164.9	164.12	164.68	*	26.3	58.45	56.63
	Sulfoxides	*	165.53	164.41	165.75	*	25.88	32.12	20.41
	Sulfones	*	166.46	165.87	166.03	*	36.44	0.5	9.08

*Note: * not investigated;*

- not detected by XPS.

O1s

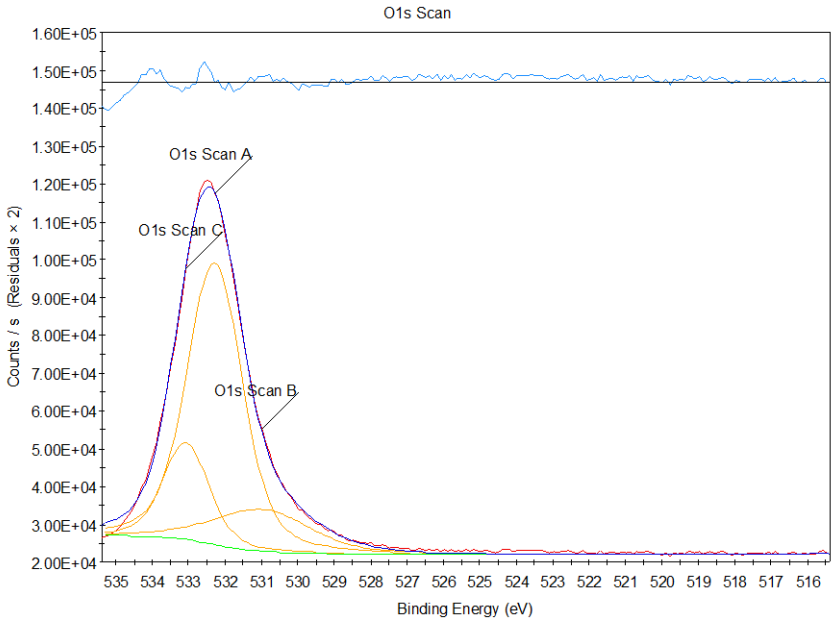

Sample 1 Calcite

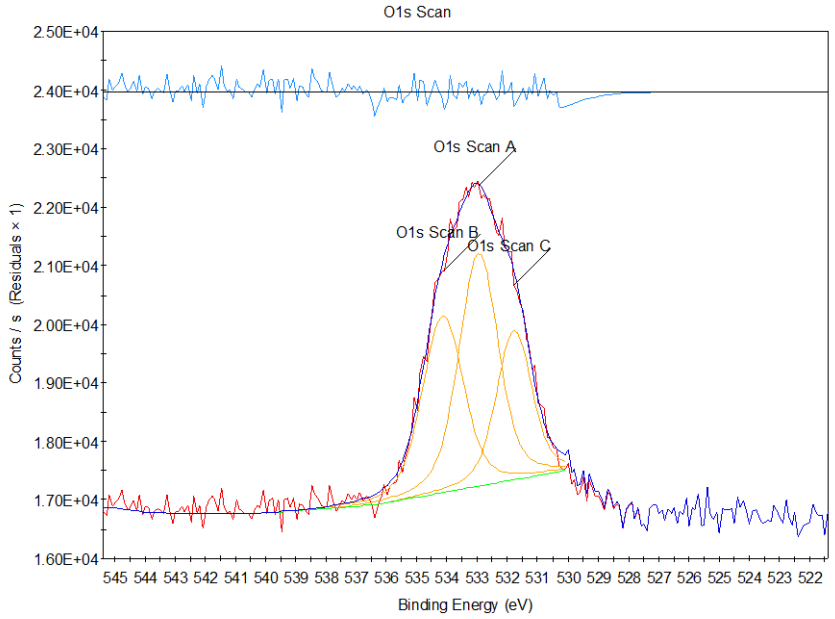

Sample 2

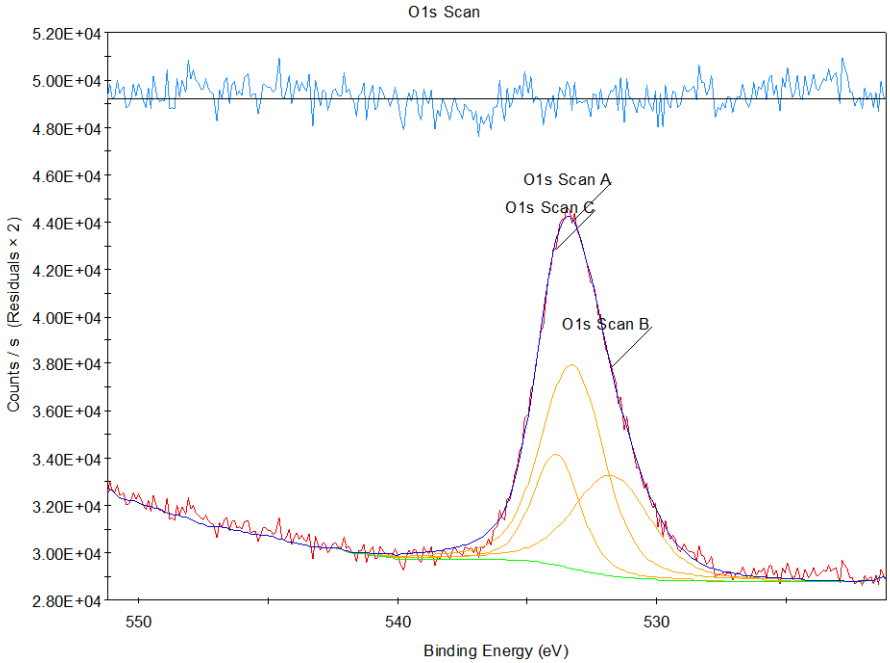

Sample 3 MgO

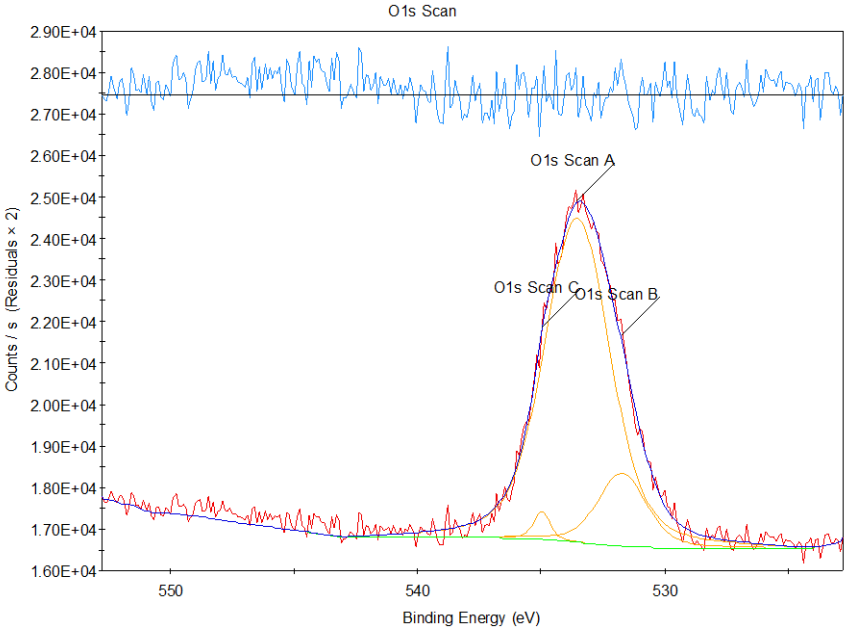

Sample 4 NiO

Figure 4-19. Oxygen 1s XPS scan

C1s

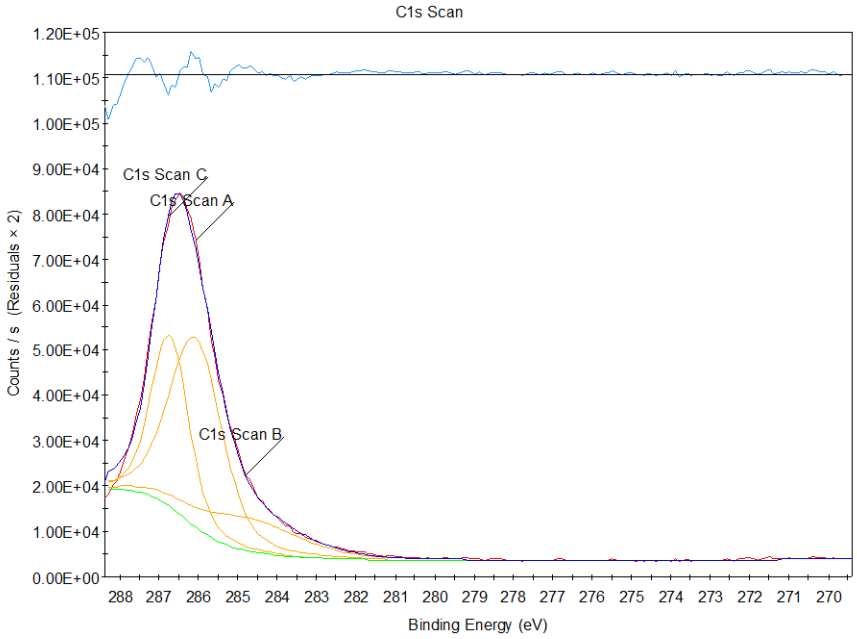

Sample 1 Calcite

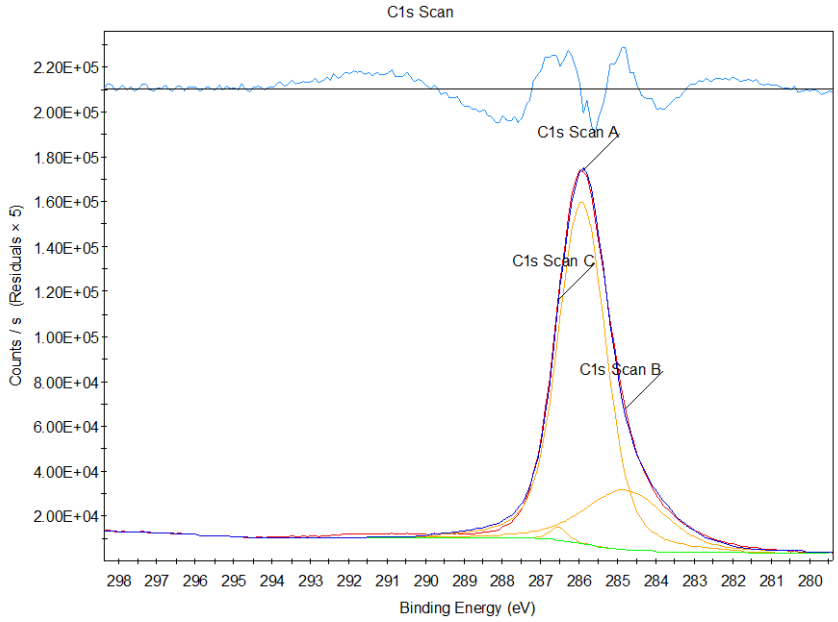

Sample 2

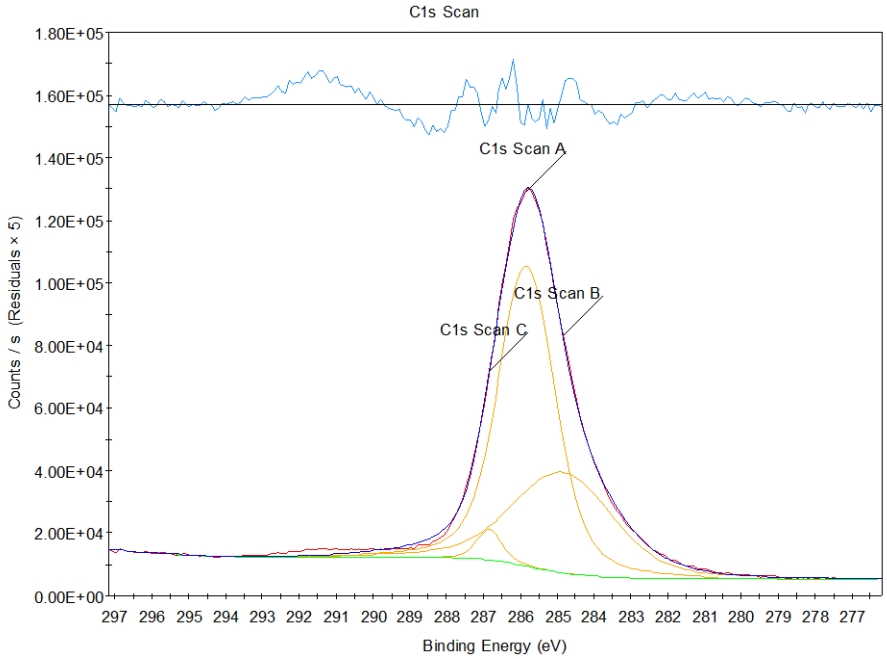

Sample 3 MgO

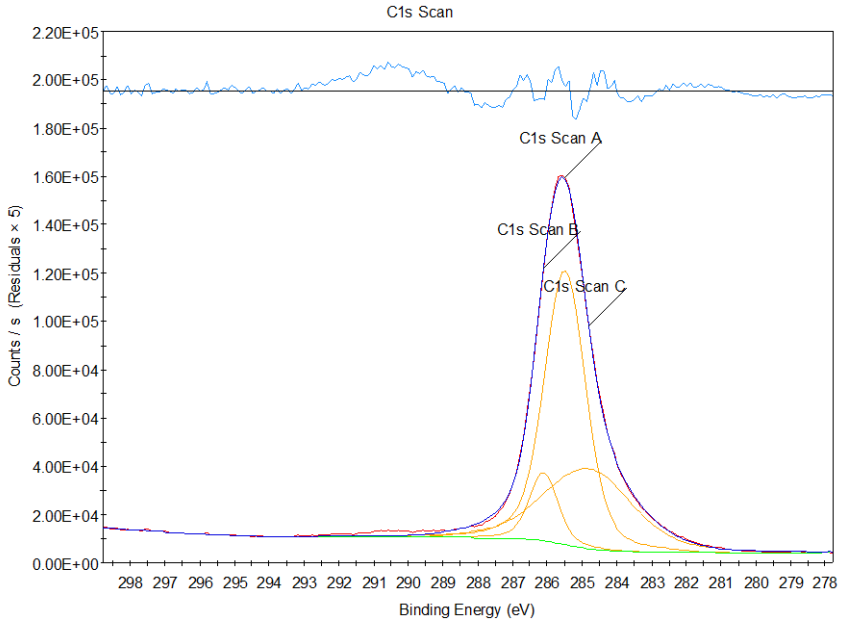

Sample 4 NiO

Figure 4-20. Carbon 1s XPS scan

Table 4-3 contains the findings of investigations of the quantity of organic O_2 connected to every C (1s) peak. The 286.5 eV C (1s) peak is thought to be related with one O_2, and the 284.8 eV C (1s) peak is thought to be linked with two O2s (for example, O=C-O). These observations are consistent with research works reported by Zhu et al. (2021), which showed that the molar composition of C bonding with O_2 is high in the asphaltene.

The procedures for N_2 XPS curve resolution is described here. Using four peaks at constant value locations of 399.3, 400.1, 400.8, and 401.4 eV, N_2 (1s) spectrum were curve-resolved. As Examples of XPS N_2 (1s) peaks and the breakdown of the curve into various elements for various assignments are presented in Figure 4-21. XPS spectra's 400.8 eV peak is ascribed to pyrrolic N_2. Similar to this, the pyrrolic N_2 forms are responsible for the 400.1 eV peak observed in other bonds. Unmistakable pyridinic and quaternary N_2 peaks were found at 399.3 eV and 401.4 eV, respectively. Another peak can be seen at 399.3 eV, which is where N_2 amine forms are predicted to be. These results are in line with Kelemen et al. (2007) findings where most of the N_2 assignments exist as pyrrolic N_2. Moreover, the hydroxyl, N-5, and N-6 groups are all connected by solid hydrogen bonding. The majority of them are found in asphaltene as hydrogen bonding compounds, which are a key factor in the agglomeration of asphaltene (Zhu YH et al., 2016).

By using the XPS, sulfur variation was also quantified (Figure 4-22). Each single element type XPS sulfur (2p) spectra consists of 2p3/2 and 2p1/2 constituents with a 2-to-1 intensity separation in energy. The complicated XPS S (2p) spectra for measurements typically consist of a signal with a lower binding energy (164 eV) and a response with a higher binding energy (167 eV). Applying parts with constant energy locations and values, all peaks were concurrently resolved along their curves. The lowest binding energy indications have 2p3/2 and 2p1/2 elements and are about 163 eV (sulfides), 164.4 eV (thiophenes), 165.2 eV (sulfoxides), and 166 eV (sulfones). Two elements with 2p3/2 and 2p1/2 components at 165.9 and 166.5 eV were used to curve-resolve the greater energy signals. Such signals overlap, but it is anticipated that sulfate will be primarily responsible for their emergence. Nevertheless, sulfite and sulfones may also have contributed. Just the total of the curve-resolved intensity for the 165.9 and 166.5 elements is thus recorded and given to sulfones.

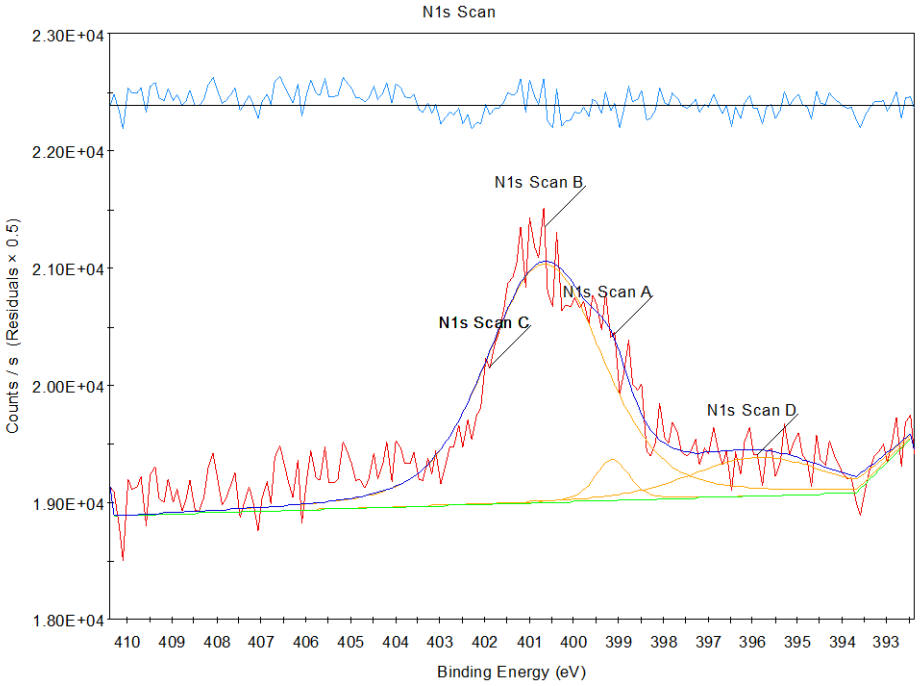

Sample 2

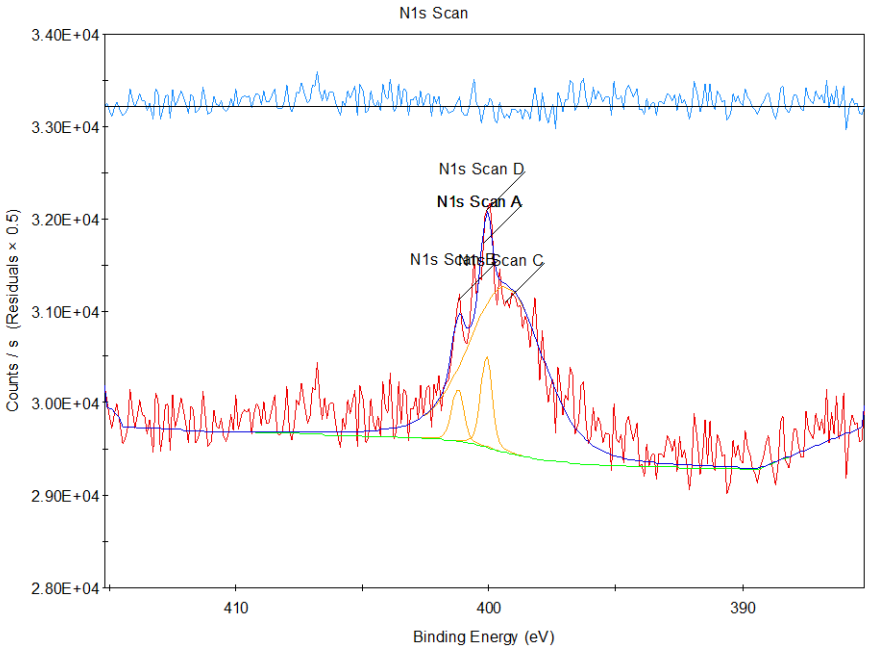

Sample 3

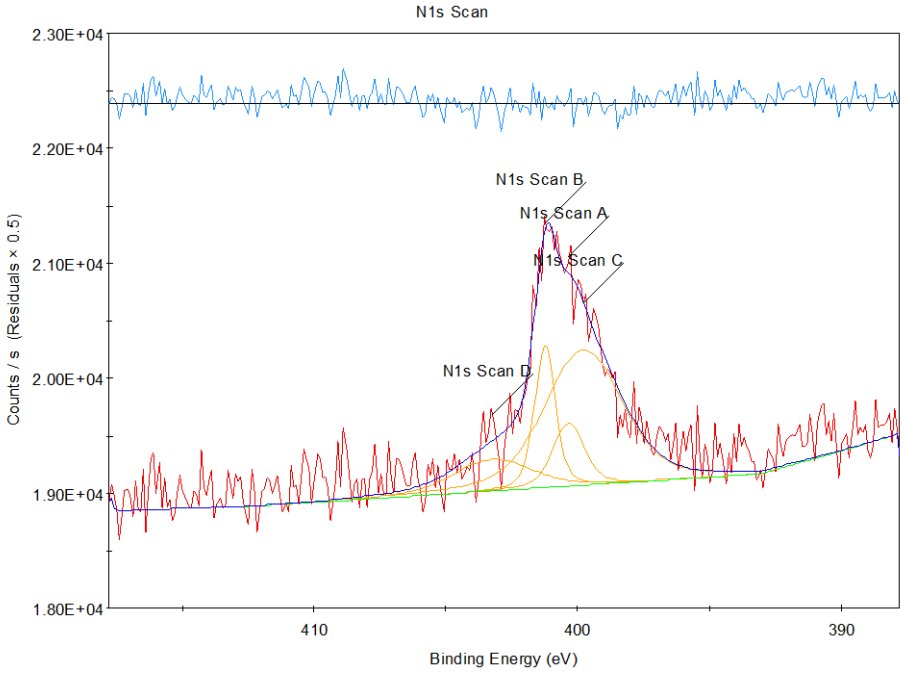

Sample 4

Figure 4-21. Nitrogen 1s XPS scan

S2p

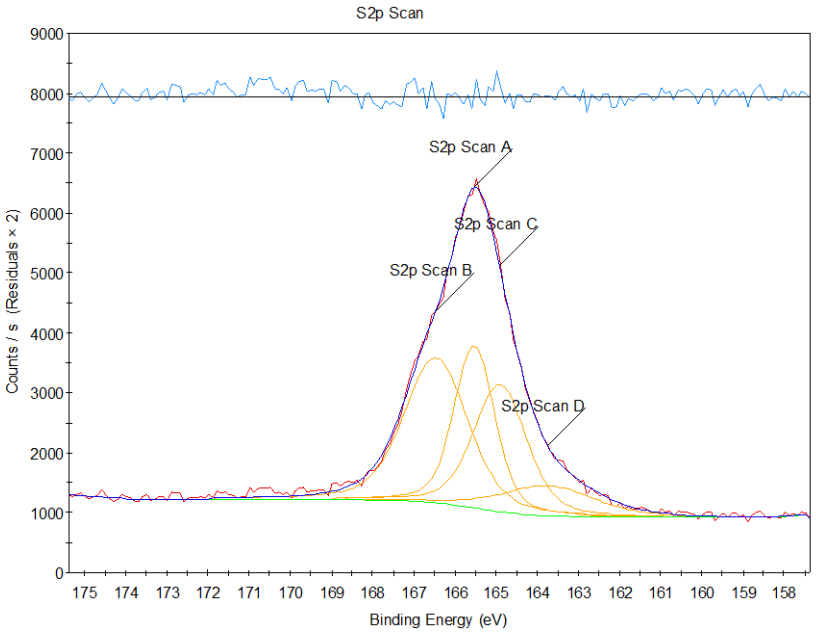

Sample 2

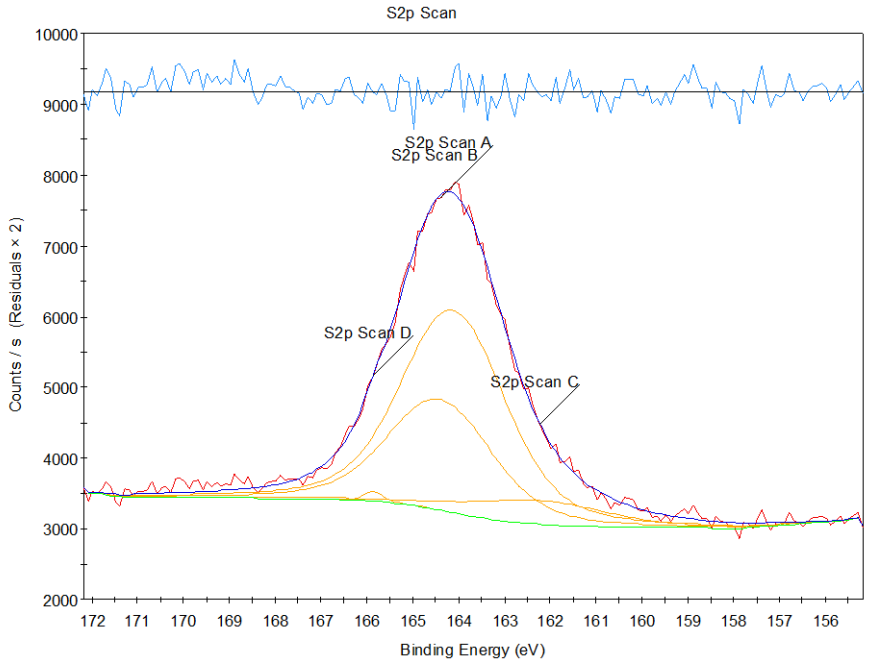

Sample 3

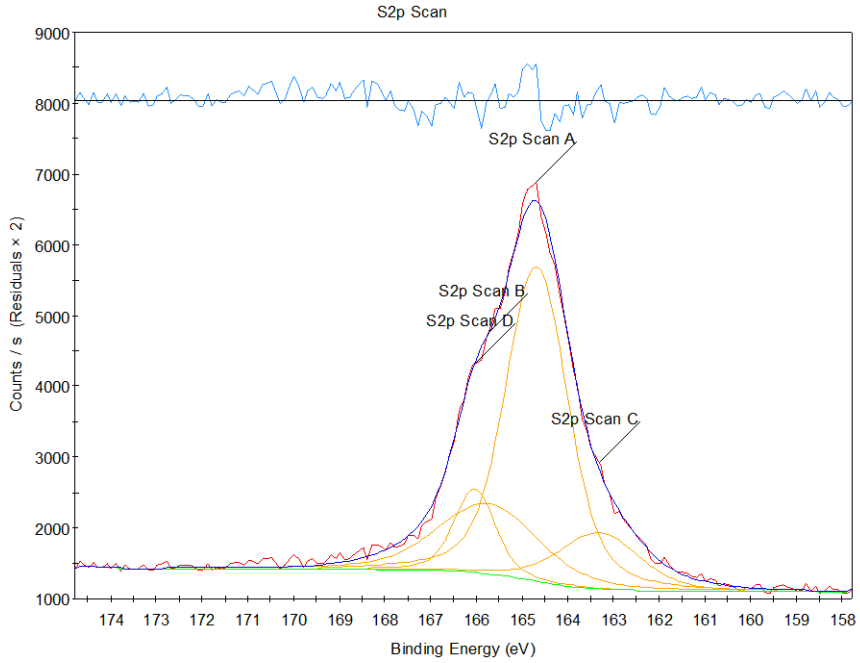

Sample 4

Figure 4-22. Sulfur 2p XPS scan

5 CONCLUSIONS AND RECOMMENDATIONS

Understanding the effect of presence of NPs on surface chemistry and morphology of calcite-asphaltene interface is crucially important for flow assurance and EOR processes involving calcite-asphaltene and NPs. The main objective of this research work was to delineate the effect of changes in surface topography, wettability alteration, and surface chemistry of calcite-asphaltene interface in presence and/or absence of NPs (NPs). A comprehensive laboratory research plan was designed and executed in three stages of NP characterization, preparation of special asphaltene deposited smooth calcite surfaces followed by X-Ray Photoelectron Spectroscopy (XPS) surveys and Atomic Force Microscopy (AFM) probes.

Asphaltene was extracted from a paraffinic Kazakhstani heavy crude oil using indirect IP-143 standard method. In the next step, NiO and MgO NPs were characterized using scanning electron microscopy (SEM), Transmission Electron Microscopy (TEM), and Energy Dispersive X-ray Spectroscopy (EDAX) to determine NPs' surface morphology, particle size and distribution, and elemental compositions. Special calcite + asphaltene + MgO + heptane and calcite + asphaltene + NiO + heptane samples were prepared according to specific sample preparation procedures for XPS and AFM surveys. Contact angle measurements were conducted in each stage to check the wettability alteration of each sample. The calcite surface samples were prepared by polishing and cutting specimens to meet the requirements of each equipment, especially the surface roughness that must be below 5 μm. XPS survey was conducted on pure asphaltene, pure calcite, calcite + asphaltene and calcite + asphaltene + MgO NP + heptane and calcite + asphaltene and calcite + asphaltene + NiO NP + heptane. Based on the method of sample preparation, elemental orbitals C1s, O1s, S2p, N1s, Mg2p, Ni2p, and Ca2p were investigated on each sample to identify the level of adsorption. Moreover, an overall XPS survey was carried out on each sample to determine the elemental composition of the sample under investigation. The following six main conclusions can be drawn based on the results obtained from this research work:

1. Based on SEM images, the MgO NPs are spherical granules with a non-uniform distribution with moderate agglomeration and the NiO NPs form strongly coalesced granules with irregular scattered grains. TEM analysis results showed that the average particle of size of the MgO and NiO NPs are 50 nm and 70-80 nm, respectively. EDAX

analysis results also confirmed complete dominance of Mg and Ni in MgO and NiO NPs, respectively, as well as O_2 in both NPs.

2. The AFM probes revealed that MgO NP reduced the height of asphaltene agglomerates from 500 nm to 200 nm and reduced the amount of aggregates on the surface, notably. NiO NPs also decreased the height of asphaltene agglomerates deposited on calcite surface from 1000 nm to 200 nm and presence of aggregates on the surface reduced, drastically.
3. The amount and agglomeration of asphaltene was reduced after application of both NPs. The height of the precipitated asphaltene was reduced by MgO NPs by more 2.5 times compared with the thickness of initial asphaltene deposition on the calcite's surface. Furthermore, this reduction after NiO NP was almost 5 times. In terms of distribution of precipitates and surface coverage on the surface of calcite, large agglomerates decreased in shape and size; whereas, the aggregates that were initially small were almost cleared.
4. The Young-Laplace equation was used to calculate the contact angles of each sample at every stage. The modified Wenzel methods was also used to correct the effect of surface roughness on calculation of contact angle. Presence of NPs at the calcite-asphaltene interface positively affected the wettability alteration. After precipitation of asphaltene onto calcite, MgO and NiO NPs changed the contact angle of the asphaltene deposited calcite surface from 122° (preferentially oil wet) to 111° (less preferentially oil wet) and 83° (preferentially water wet), respectively.
5. All of the elements of calcite + asphaltene + MgO + heptane sample were detected by XPS. The surface (Ca2p) and Mg2p NP elements were also detected at high resolution. Ca and Ni atoms were not detected at high resolution in the Calcite + asphaltene + NiO + heptane sample. This implies that Ni was not absorbed onto the calcite's surface and adsorption kinetics of NPs and calcite-asphaltene interface depends on the type of NP.
6. NiO NPs are found more effective for asphaltene precipitation inhibition and wettability alteration than MgO NPs. This can be attributed to amphoteric metal oxides origin of NiO NPs characterized by their high adsorption capacity than basic metal oxides origin of MgO NPs and particle size, which plays a crucial role in adsorption mechanism.

The following recommendations are made for further research:

- The investigation of acidic and amphoteric metal oxides as a new potential dispersants to deal with the problems related to flow assurance.
- Consideration of other rocks which makeup carbonate and limestone reservoirs.

REFERENCES

Abdallah, W. A., & Taylor, S. D. (2007). Surface characterization of adsorbed asphaltene on a stainless steel surface. *Nuclear Instruments and Methods in Physics Research, Section B: Beam Interactions with Materials and Atoms, 258*(1), 213–217. https://doi.org/10.1016/j.nimb.2006.12.171

Abdulrazag Y. Zekri. (2001). *A Novel Technique for Treating Asphaltene Deposition Using Laser Technology*.

Ahooei, A., Norouzi-Apourvari, S., Hemmati-Sarapardeh, A., & Schaffie, M. (2020). Experimental study and modeling of asphaltene deposition on metal surfaces via electrodeposition process: The role of ultrasonic radiation, asphaltene concentration and structure. *Journal of Petroleum Science and Engineering*, *195*. https://doi.org/10.1016/j.petrol.2020.107734

Al-Anssari, S., Barifcani, A., Wang, S., Maxim, L., & Iglauer, S. (2016). Wettability alteration of oil-wet carbonate by silica nanofluid. *Journal of Colloid and Interface Science*, *461*, 435–442. https://doi.org/10.1016/j.jcis.2015.09.051

Al-Busaidi, I. K., Al-Maamari, R. S., Karimi, M., & Naser, J. (2019). Effect of different polar organic compounds on wettability of calcite surfaces. *Journal of Petroleum Science and Engineering*, *180*, 569–583. https://doi.org/10.1016/j.petrol.2019.05.080

Al-Ibad, A., & Civan, F. (2013). *Experimental Investigation and Correlation of Thermal Effects on Near-Wellbore Formation Treatment by Gel Particles*.

Alimohammadi, S., Zendehboudi, S., & James, L. (2019). A comprehensive review of asphaltene deposition in petroleum reservoirs: Theory, challenges, and tips. In *Fuel* (Vol. 252, pp. 753–791). Elsevier Ltd. https://doi.org/10.1016/j.fuel.2019.03.016

Al-Yaari, M. (2011). *the SPE Saudi Arabia section Young Professionals Technical Symposium*.

Ana Varela Coelho, & Catarina de Matos Ferraz Franco. (2013). *Tandem Mass Spectrometry - Molecular Characterization.* InTech.

Anderson, W. G. (1988). *Wettability Literatu,re Survey-Part 2: Wettability Measurement*.

Aquino-Olivos, M. A., Buenrostro-Gonzalez, E., Andersen, S. I., & Lira-Galeana, C. (2001). Investigations of inhibition of asphaltene precipitation at high pressure using bottomhole samples. *Energy and Fuels*, *15*(1), 236–240. https://doi.org/10.1021/ef000136i

Asemani, M., & Rabbani, A. R. (2016). Oil-oil correlation by FTIR spectroscopy of asphaltene samples. *Geosciences Journal*, *20*(2), 273–283. https://doi.org/10.1007/s12303-015-0042-1

Bantignies, J.-L., Cartier Dit Moulin, C., & Dexpert′, H. D. (1998). Asphaltene adsorption on kaolinite characterized by infrared and X-ray absorption spectroscopies. In *Journal of Petroleum Science and Engineering* (Vol. 20).

Barrera, D. M., Ortiz, D. P., & Yarranton, H. W. (2013). Molecular weight and density distributions of asphaltenes from crude oils. *Energy and Fuels*, *27*(5), 2474–2487. https://doi.org/10.1021/ef400142v

Bénard, Q., Fois, M., & Grisel, M. (2005). Peel ply surface treatment for composite assemblies: Chemistry and morphology effects. *Composites Part A: Applied Science and Manufacturing*, *36*(11), 1562–1568. https://doi.org/10.1016/j.compositesa.2005.02.012

Benoit B. Mandelbrot. (1982). *The fractal geometry of nature*.

Bernadiner, M. (1993). *SPE 25192 Advanced Asphaltene and Paraffin Control Technology*.

Bouhadda, Y., Florian, P., Bendedouch, D., Fergoug, T., & Bormann, D. (2010). Determination of Algerian Hassi-Messaoud asphaltene aromaticity with different solid-state NMR sequences. *Fuel*, *89*(2), 522–526. https://doi.org/10.1016/j.fuel.2009.09.018

Brown, C. A., Johnsen, W. A., & Halt, K. M. (1998). Scale-sensitivity, Fractal Analysis and Simulations. In *J. Mach Tools Manufact* (Vol. 38, Issue 6).

Buckley J. (1989). *Influence of Electrical Surface Charges on the Wetting Properties of Crude Oils*. http://onepetro.org/RE/article-pdf/4/03/332/2631821/spe-16964-pa.pdf/1

Buckley, J. S. (2001). *Effective wettability of minerals exposed to crude oil*.

Buckley, J. S., Liu, Y., & Monsterleet, S. (1998). *Mechanisms of Wetting Alteration by Crude Oils*. http://onepetro.org/SJ/article-pdf/3/01/54/2593066/spe-37230-pa.pdf/1

Buckley, J. S., Liu, Y., Xie, X., & Morrow, N. R. (1997). *Asphaltenes and Crude Oil Wetting - The Effect of Oil Composition*. http://onepetro.org/SJ/article-pdf/2/02/107/2597324/spe-35366-pa.pdf/1

Buenrostro-Gonzalez, E., Andersen, S. I., Garcia-Martinez, J. A., & Lira-Galeana, C. (2002). Solubility/molecular structure relationships of asphaltenes in polar and nonpolar media. *Energy and Fuels*, *16*(3), 732–741. https://doi.org/10.1021/ef0102317

Buenrostro-Gonzalez, E., Lira-Galeana, C., Gil-Villegas, A., & Wu, J. (2004). Asphaltene precipitation in crude oils: Theory and experiments. *AIChE Journal*, *50*(10), 2552–2570. https://doi.org/10.1002/aic.10243

Castillo, J., Fernández, A., Ranaudo, M. A., & Acevedo, S. (2001). New techniques and methods for the study of aggregation, adsorption, and solubility of asphaltenes. Impact of these properties on colloidal structure and flocculation. *Petroleum Science and Technology*, *19*(1–2), 75–106. https://doi.org/10.1081/LFT-100001227

Castro, A. T. (2006). NMR and FTIR Characterization of Petroleum Residues: Structural Parameters and Correlations. In *J. Braz. Chem. Soc* (Vol. 17, Issue 6).

Collins, S. H., & Melrose, J. C. (1983). *SPE Adsorption of Asphaltenes and Water on Reservoir Rock Minerals "Member SPE-AIME*.

Cortés, F. B., Mejía, J. M., Ruiz, M. A., Benjumea, P., & Riffel, D. B. (2012). Sorption of asphaltenes onto nanoparticles of nickel oxide supported on nanoparticulated silica gel. *Energy and Fuels*, *26*(3), 1725–1730. https://doi.org/10.1021/ef201658c

Daryaei, E., Reza Rahimi Tabar, M., & Moshfegh, A. Z. (2013). Surface roughness analysis of hydrophilic SiO2/TiO 2/glass nano bilayers by the level crossing approach. *Physica A: Statistical Mechanics and Its Applications*, *392*(9), 2175–2181. https://doi.org/10.1016/j.physa.2012.11.058

Davudov, D., & Moghanloo, R. G. (2019). A new model for permeability impairment due to asphaltene deposition. *Fuel*, *235*, 239–248. https://doi.org/10.1016/j.fuel.2018.07.079

Dickie, J. P., Haller, M. N., & Teh Yen, D. F. (1969). *Electron Microscopic Investigations on the Nature of Petroleum Asphaltics.*

Drouet, C., Laberty, C., Fierro, J. L. G., Alphonse, P., & Rousset, A. (2000). X-ray photoelectron spectroscopic study of non-stoichiometric nickel and nickel-copper spinel manganites. *International Journal of Inorganic Materials*, *2*(5), 419–426. https://doi.org/10.1016/S1466-6049(00)00047-7

Dudášová, D., Simon, S., Hemmingsen, P. v., & Sjöblom, J. (2008). Study of asphaltenes adsorption onto different minerals and clays. Part 1. Experimental adsorption with UV depletion detection. *Colloids and Surfaces A: Physicochemical and Engineering Aspects*, *317*(1–3), 1–9. https://doi.org/10.1016/j.colsurfa.2007.09.023

Feninat, F. el, Elouatik, S., Ellis, T. H., Sacher, E., & Stangel, I. (2001). *Quantitative assessment of surface roughness as measured by AFM: application to polished human dentin*.

Franco, C. A., Nassar, N. N., Ruiz, M. A., Pereira-Almao, P., & Cortés, F. B. (2013). Nanoparticles for inhibition of asphaltenes damage: Adsorption study and displacement test on porous media. *Energy and Fuels*, *27*(6), 2899–2907. https://doi.org/10.1021/ef4000825

Fujisawa, N., McKenzie, D. R., James, N. L., Woodard, J. C., & Swain, M. v. (2006). Combined influences of mechanical properties and surface roughness on the tribological properties of amorphous carbon coatings. *Wear*, *260*(1–2), 62–74. https://doi.org/10.1016/j.wear.2004.12.032

G.Ali Mansoori. (2010). Remediation_of_Asphaltene. *SOCAR*.

Gan, S., Zhou, Q., Xu, X., Hong, Y., Liu, Y., & Fu, S. (2007). Study on the surface roughness of substrate with multi-fractal spectrum. *Microelectronic Engineering*, *84*(5–8), 1806–1809. https://doi.org/10.1016/j.mee.2007.01.273

Garrouch, A. A., & Al-Ruhaimani, F. A. (2005). Simple models for permeability impairment in reservoir rocks caused by asphaltene deposition. *Petroleum Science and Technology*, *23*(7–8), 811–826. https://doi.org/10.1081/LFT-200034441

Gaweł, B., Eftekhardadkhah, M., & Øye, G. (2014). Elemental composition and fourier transform infrared spectroscopy analysis of crude oils and their fractions. *Energy and Fuels*, *28*(2), 997–1003. https://doi.org/10.1021/ef402286y

Geng, W., Kumabe, Y., Nakajima, T., Takanashi, H., & Ohki, A. (2009). Analysis of hydrothermally-treated and weathered coals by X-ray photoelectron spectroscopy (XPS). *Fuel*, *88*(4), 644–649. https://doi.org/10.1016/j.fuel.2008.09.025

Gharbi, K., Benyounes, K., & Khodja, M. (2017). Removal and prevention of asphaltene deposition during oil production: A literature review. In *Journal of Petroleum Science and Engineering* (Vol. 158, pp. 351–360). Elsevier B.V. https://doi.org/10.1016/j.petrol.2017.08.062

Giraldo, J., Benjumea, P., Lopera, S., Cortés, F. B., & Ruiz, M. A. (2013). Wettability alteration of sandstone cores by alumina-based nanofluids. *Energy and Fuels*, *27*(7), 3659–3665. https://doi.org/10.1021/ef4002956

Gonzalez, G., & Middea, A. (1988). The Properties of the Calcite-Solution Interface the Presence of Adsorbed Resins or Asphaltenes. In *Colloids and Surfaces* (Vol. 33).

Goual, L., Sedghi, M., Wang, X., & Zhu, Z. (2014). Asphaltene aggregation and impact of alkylphenols. *Langmuir*, *30*(19), 5394–5403. https://doi.org/10.1021/la500615k

Grosvenor, A. P., Biesinger, M. C., Smart, R. S. C., & McIntyre, N. S. (2006). New interpretations of XPS spectra of nickel metal and oxides. *Surface Science*, *600*(9), 1771–1779. https://doi.org/10.1016/j.susc.2006.01.041

Guo, Boyun. (2014). *Offshore pipelines : design, installation, and maintenance*. Gulf Professional Publishing.

Guzmán, H. J., Isquierdo, F., Carbognani, L., Vitale, G., Scott, C. E., & Pereira-Almao, P. (2017). X-ray Photoelectron Spectroscopy Analysis of Hydrotreated Athabasca Asphaltenes. *Energy and Fuels*, *31*(10), 10706–10717. https://doi.org/10.1021/acs.energyfuels.7b01863

Hashemi, S. I., Fazelabdolabadi, B., Moradi, S., Rashidi, A. M., Shahrabadi, A., & Bagherzadeh, H. (2016). On the application of NiO nanoparticles to mitigate in situ asphaltene deposition in carbonate porous matrix. *Applied Nanoscience (Switzerland)*, *6*(1), 71–81. https://doi.org/10.1007/s13204-015-0410-1

Headen, T. F., Boek, E. S., & Skipper, N. T. (2009). Evidence for asphaltene nanoaggregation in toluene and heptane from molecular dynamics simulations. *Energy and Fuels*, *23*(3), 1220–1229. https://doi.org/10.1021/ef800872g

Hendraningrat, L., Li, S., & Torsaeter, O. (2013). *SPE 165955 Effect of Some Parameters Influencing Enhanced Oil Recovery Process using Silica Nanoparticles: An Experimental Investigation*.

Hendraningrat, L., & Torsaeter, N. (2014a). *SPE-171407-MS Understanding Fluid-Fluid and Fluid-Rock Interactions in the Presence of Hydrophilic Nanoparticles at Various Conditions*.

Hendraningrat, L., & Torsaeter, O. (2014b). *OTC Unlocking the Potential of Metal Oxides Nanoparticles to Enhance the Oil Recovery*.

Hendrickson, J. G., & Moore, J. C. (1966). Gel Permeation Chromatography. 111. Molecular Shape versus Elution. In *JOURNAL OF POLYMER SCIENCE: PART A-1* (Vol. 4).

Higaki, Y., Hatae, K., Ishikawa, T., Takanohashi, T., Hayashi, J. I., & Takahara, A. (2014). Adsorption and desorption behavior of asphaltene on polymer-brush-immobilized surfaces. *ACS Applied Materials and Interfaces*, *6*(22), 20385–20389. https://doi.org/10.1021/am505904b

Hoepfner, M. P. (2013). *Investigations into Asphaltene Deposition, Stability, and Structure*.

J. M. Li. (2003). *IMAGE-BASED FRACTAL DESCRIPTION OF MICROSTRUCTURES*. https://doi.org/10.1007/978

Joonaki, E., Buckman, J., Burgass, R., & Tohidi, B. (2018). Exploration of the Difference in Molecular Structure of n -C7 and CO2 Induced Asphaltenes. *Industrial and Engineering Chemistry Research*, *57*(26), 8810–8818. https://doi.org/10.1021/acs.iecr.8b01634

K. Ichikawa. (2004). *05•00562 Study on char deposition characteristics on the heat exchanger tube in a coal gasifier-relationship between char formation and deposition characteristics*.

Kaminsky, R., & Radke, C. J. (1997). *Asphaltenes, Water Films, and Wettability Reversal*.

Karambeigi, M. A., & Kharrat, R. (2014). Asphaltene precipitation during different production operations. *Petroleum Science and Technology*, *32*(14), 1655–1660. https://doi.org/10.1080/10916466.2011.631661

Karimi, A., Fakhroueian, Z., Bahramian, A., Pour Khiabani, N., Darabad, J. B., Azin, R., & Arya, S. (2012). Wettability alteration in carbonates using zirconium oxide nanofluids: EOR implications. *Energy and Fuels*, *26*(2), 1028–1036. https://doi.org/10.1021/ef201475u

Kashefi, S., Shahrabadi, A., Jahangiri, S., Lotfollahi, M. N., & Bagherzadeh, H. (2016). Investigation of the performance of several chemical additives on inhibition of asphaltene precipitation. *Energy Sources, Part A: Recovery, Utilization and Environmental Effects*, *38*(24), 3647–3652. https://doi.org/10.1080/15567036.2016.1198847

Kashefi, S., Shahrabadi, A., Lotfollahi, M. N., & Varamesh, A. (2016). A new polymeric additive as asphaltene deposition inhibitor in CO2 core flooding. *Korean Journal of Chemical Engineering*, *33*(11), 3273–3280. https://doi.org/10.1007/s11814-016-0199-y

Kaushik, P., Kumar, A., Bhaskar, T., Sharma, Y. K., Tandon, D., & Goyal, H. B. (2012). Ultrasound cavitation technique for up-gradation of vacuum residue. *Fuel Processing Technology*, *93*(1), 73–77. https://doi.org/10.1016/j.fuproc.2011.09.005

Kayukova, G. P., Gubaidullin, A. T., Petrov, S. M., Romanov, G. v., Petrukhina, N. N., & Vakhin, A. v. (2016). Changes of Asphaltenes' Structural Phase Characteristics in the Process of Conversion of Heavy Oil in the Hydrothermal Catalytic System. *Energy and Fuels*, *30*(2), 773–783. https://doi.org/10.1021/acs.energyfuels.5b01328

Kelemen, S. R., Afeworki, M., Gorbaty, M. L., Sansone, M., Kwiatek, P. J., Walters, C. C., Freund, H., Siskin, M., Bence, A. E., Curry, D. J., Solum, M., Pugmire, R. J., Vandenbroucke, M., Leblond, M., & Behar, F. (2007). Direct characterization of kerogen by X-ray and solid-state 13C nuclear magnetic resonance methods. *Energy and Fuels*, *21*(3), 1548–1561. https://doi.org/10.1021/ef060321h

Kelland A. (2009). *Production Chemicals for the Oil and Gas Industry*.

Khormali, A., Sharifov, A. R., & Torba, D. I. (2018). Experimental and modeling study of asphaltene adsorption onto the reservoir rocks. *Petroleum Science and Technology*, *36*(18), 1482–1489. https://doi.org/10.1080/10916466.2018.1496116

Khvostichenko, D. S., & Andersen, S. I. (2009). Electrodeposition of asphaltenes. 1. preliminary studies on electrodeposition from oil-heptane mixtures. *Energy and Fuels*, *23*(2), 811–819. https://doi.org/10.1021/ef800722g

Kokal, S. L., & Sayegh, S. G. (1995). Asphaltenes: The Cholesterol of Petroleum Presently with Saudi Aramco, Dhahran, SAUDI ARABIA. In *the SPE Middle East Oil Show held in Bahrain*. http://onepetro.org/SPEMEOS/proceedings-pdf/95MEOS/All-95MEOS/SPE-29787-MS/1965805/spe-29787-ms.pdf/1

Kokal, S., Tang, T., Schramm, L., & Sayegh, S. (1995). A Electrokinetic and adsorption properties of asphaltenes. In *CollOids and Surfaces A. Physicochemical and Engineering Aspects* (Vol. 94).

Kord, S., Soleymanzadeh, A., & Miri, R. (2019). A generalized scaling equation to predict asphaltene precipitation during precipitant dilution, natural depletion, water injection and gas injection. *Journal of Petroleum Science and Engineering*, *182*. https://doi.org/10.1016/j.petrol.2019.106320

Kowalczuk, P. B., Akkaya, C., Ergun, M., Janicki, M. J., Sahbaz, O., & Drzymala, J. (2017). Water contact angle on corresponding surfaces of freshly fractured fluorite, calcite and mica. *Physicochemical Problems of Mineral Processing*, *53*(1), 192–201. https://doi.org/10.5277/ppmp170116

Kraiwattanawong, K., Fogler, H. S., Gharfeh, S. G., Singh, P., Thomason, W. H., & Chavadej, S. (2009). Effect of asphaltene dispersants on aggregate size distribution and growth. *Energy and Fuels*, *23*(3), 1575–1582. https://doi.org/10.1021/ef800706c

L. Nabzar. (2005). *SPE 93062 Experimental Study on Asphaltene-Induced Formation Damage*.

Lambert, A. (1971). *Review of Gel Permeation Chromatography*.

Leontaritis, K. J. (1989). *SPE 18892 Asphaltene Deposition: A Comprehensive Description of Problem Manifestations and Modeling Approaches*. Write Publicefions Manager.

Li, S., Genys, M., Wang, K., & Torsaeter, O. (2015). *SPE-175610-MS Experimental Study of Wettability Alteration during Nanofluid Enhanced Oil Recovery Process and Its Effect on Oil Recovery*.

Lichaa, P. M., & Herrera, L. (1975). *Electrical and Other Effects Related to the Formation and Prevention of Asphaltene Deposition Problem in Venezuelan Crudes*.

Liu, F., Yang, H., Yang, M., Wu, J., Yang, S., Yu, D., Wu, X., Wang, J., Gates, I., & Wang, J. (2021). Effects of molecular polarity on the adsorption and desorption behavior of asphaltene model compounds on silica surfaces. *Fuel*, *284*. https://doi.org/10.1016/j.fuel.2020.118990

Liu, J., Wu, S., Zou, M., Zheng, X., & Cai, Z. (2012). Surface modification of silica and its compounding with polydimethylsiloxane matrix: Interaction of modified silica filler with PDMS. *Iranian Polymer Journal (English Edition)*, *21*(9), 583–589. https://doi.org/10.1007/s13726-012-0062-x

Liu, Y. J., & Li, Z. F. (2015). Structural characterisation of asphaltenes during residue hydrotreatment with light cycle oil as an additive. *Journal of Chemistry*, *2015*. https://doi.org/10.1155/2015/580950

Lobanov, A. A., Struchkov, I. A., Belozerov, I. P., Shulev, V. E., Yuriev, A. v., Pustova, E. J., Kovalenko, V. A., & Sergeev, G. D. (2020). Prediction of asphaltenes deposition in the Russian oilfield: Laboratory investigations and modeling. *Journal of Petroleum Science and Engineering*, *186*. https://doi.org/10.1016/j.petrol.2019.106777

Mahovic Poljacek, S., Risovic, D., Furic, K., & Gojo, M. (2008). Comparison of fractal and profilometric methods for surface topography characterization. *Applied Surface Science*, *254*(11), 3449–3458. https://doi.org/10.1016/j.apsusc.2007.11.040

Maqbool, T. (2011). *UNDERSTANDING THE KINETICS OF ASPHALTENE PRECIPITATION FROM CRUDE OILS*.

Maravilha, T. S. L., Middea, A., Spinelli, L. S., & Lucas, E. F. (2021). Reduction of asphaltenes adsorbed on kaolinite by polymers based on cardanol. *Brazilian Journal of Chemical Engineering*, *38*(1), 155–163. https://doi.org/10.1007/s43153-020-00082-2

Marczewski, A. W., & Szymula, M. (2002). Adsorption of asphaltenes from toluene on mineral surface. In *Colloids and Surfaces A: Physicochemical and Engineering Aspects* (Vol. 208). www.elsevier.com/locate/colsurfa

Maurice, P., Forsythe, J., Hersman, L., & Sposito, G. (1996). Application of atomic-force microscopy to studies of microbial interactions with hydrous Fe(III)-oxides. In *Chemical Geology* (Vol. 132).

Mclean, J. D., & Kilpatrick, P. K. (1997). *Comparison of Precipitation and Extrography in the Fractionation of Crude Oil Residua*.

Melendez-Alvarez, A. A., Garcia-Bermudes, M., Tavakkoli, M., Doherty, R. H., Meng, S., Abdallah, D. S., & Vargas, F. M. (2016). On the evaluation of the performance of asphaltene dispersants. *Fuel*, *179*, 210–220. https://doi.org/10.1016/j.fuel.2016.03.056

Meyer, E. (1992). ATOMIC FORCE MICROSCOPY. In *Progress in Surface Science* (Vol. 41).

Miadonye, A., & Evans, L. (2010). The solubility of asphaltenes in different hydrocarbon liquids. *Petroleum Science and Technology*, *28*(14), 1407–1414. https://doi.org/10.1080/10916460902936960

Mirzayi, B., & Shayan, N. N. (2014). Adsorption kinetics and catalytic oxidation of asphaltene on synthesized maghemite nanoparticles. *Journal of Petroleum Science and Engineering*, *121*, 134–141. https://doi.org/10.1016/j.petrol.2014.06.031

Mohammadi, M., Akbari, M., Fakhroueian, Z., Bahramian, A., Azin, R., & Arya, S. (2011). Inhibition of asphaltene precipitation by TiO2, SiO2, and ZrO2 nanofluids. *Energy and Fuels*, *25*(7), 3150–3156. https://doi.org/10.1021/ef2001635

Mohammed, I., al Shehri, D., Mahmoud, M., Kamal, M. S., & Alade, O. S. (2021a). Impact of Iron Minerals in Promoting Wettability Alterations in Reservoir Formations. *ACS Omega*, *6*(5), 4022–4033. https://doi.org/10.1021/acsomega.0c05954

Mohammed, I., al Shehri, D., Mahmoud, M., Kamal, M. S., & Alade, O. S. (2021b). A Surface Charge Approach to Investigating the Influence of Oil Contacting Clay Minerals on Wettability Alteration. *ACS Omega*, *6*(19), 12841–12852. https://doi.org/10.1021/acsomega.1c01221

Mohanty, B. C., Murty, B. S., Vijayan, V., & Kasiviswanathan, S. (2006). Atomic force microscopy study of thermal stability of silver selenide thin films grown on silicon. *Applied Surface Science*, *252*(22), 7975–7982. https://doi.org/10.1016/j.apsusc.2005.10.004

Monjezi, R., Ghotbi, C., Jafari Behbahani, T., & Bakhshi, P. (2019). Experimental investigation of dynamic asphaltene adsorption on calcite packs: The impact of single and mixed-salt brine films. *Canadian Journal of Chemical Engineering*, *97*(7), 2028–2038. https://doi.org/10.1002/cjce.23441

Morrow. (1990). *Wettability and Its Effect on Oil Recovery*. http://onepetro.org/JPT/article-pdf/42/12/1476/2222566/spe-21621-pa.pdf?casa_token=smXMsLKc4G0AAAAA:ViTTGlbPKlpMj9xLiP9cKncej2RzhpUZqqx-wmcyRh3luPDJ1C_3jwSykoiM9Zm-P6H5gt6D

Mullins. (2007). *Asphaltenes, Heavy Oils, and Petroleomics*.

Mullins, O. C. (2010). The modified yen model. *Energy and Fuels*, *24*(4), 2179–2207. https://doi.org/10.1021/ef900975e

Mullins, O. C., Sabbah, H., Eyssautier, J., Pomerantz, A. E., Barré, L., Andrews, A. B., Ruiz-Morales, Y., Mostowfi, F., McFarlane, R., Goual, L., Lepkowicz, R., Cooper, T., Orbulescu, J., Leblanc, R. M., Edwards, J., & Zare, R. N. (2012). Advances in asphaltene science and the Yen-Mullins model. *Energy and Fuels*, *26*(7), 3986–4003. https://doi.org/10.1021/ef300185p

Nakajima, A. (2011). Design of hydrophobic surfaces for liquid droplet control. In *NPG Asia Materials* (Vol. 3, Issue 5, pp. 49–56). https://doi.org/10.1038/asiamat.2011.55

Nassar, N. N., Hassan, A., Carbognani, L., Lopez-Linares, F., & Pereira-Almao, P. (2012). Iron oxide nanoparticles for rapid adsorption and enhanced catalytic oxidation of thermally cracked asphaltenes. *Fuel*, *95*, 257–262. https://doi.org/10.1016/j.fuel.2011.09.022

Nassar, N. N., Hassan, A., & Pereira-Almao, P. (2011a). Effect of surface acidity and basicity of aluminas on asphaltene adsorption and oxidation. *Journal of Colloid and Interface Science*, *360*(1), 233–238. https://doi.org/10.1016/j.jcis.2011.04.056

Nassar, N. N., Hassan, A., & Pereira-Almao, P. (2011b). Effect of the particle size on asphaltene adsorption and catalytic oxidation onto alumina particles. *Energy and Fuels*, *25*(9), 3961–3965. https://doi.org/10.1021/ef2008387

Nikooee. (2009). *Fractal Analysis of Surface Roughness Induced by Asphaltene Deposits: Effect of Surface Topography on Wettability Alteration*.

Othman, M. R., Mustafa, N. N. N., & Ahmad, A. L. (2006). Effect of thermal treatment on the microstructure of sol-gel derived porous alumina modified platinum. *Microporous and Mesoporous Materials*, *91*(1–3), 268–275. https://doi.org/10.1016/j.micromeso.2005.12.005

Otitoju, T. A., Ahmad, A. L., & Ooi, B. S. (2017). Superhydrophilic (superwetting) surfaces: A review on fabrication and application. In *Journal of Industrial and Engineering Chemistry* (Vol. 47, pp. 19–40). Korean Society of Industrial Engineering Chemistry. https://doi.org/10.1016/j.jiec.2016.12.016

Ovalles, C., Rogel, E., Morazan, H., & Moir, M. E. (2016). Synthesis, characterization, and mechanism of asphaltene inhibition of phosphopropoxylated asphaltenes. *Fuel*, *180*, 20–26. https://doi.org/10.1016/j.fuel.2016.03.084

Pereira, J. C., López, I., Salas, R., Silva, F., Fernández, C., Urbina, C., & López, J. C. (2007). Resins: The molecules responsible for the stability/instability phenomena of asphaltenes. *Energy and Fuels*, *21*(3), 1317–1321. https://doi.org/10.1021/ef0603333

Risović, D., Poljaček, S. M., & Gojo, M. (2009). On correlation between fractal dimension and profilometric parameters in characterization of surface topographies. *Applied Surface Science*, *255*(7), 4283–4288. https://doi.org/10.1016/j.apsusc.2008.11.028

Roach, P., Shirtcliffe, N. J., & Newton, M. I. (2008). Progess in superhydrophobic surface development. *Soft Matter*, *4*(2), 224. https://doi.org/10.1039/b712575p

Roustaei, A., & Bagherzadeh, H. (2015). Experimental investigation of SiO2 nanoparticles on enhanced oil recovery of carbonate reservoirs. *Journal of Petroleum Exploration and Production Technology*, *5*(1), 27–33. https://doi.org/10.1007/s13202-014-0120-3

Rudrake, A., Karan, K., & Horton, J. H. (2009). A combined QCM and XPS investigation of asphaltene adsorption on metal surfaces. *Journal of Colloid and Interface Science*, *332*(1), 22–31. https://doi.org/10.1016/j.jcis.2008.12.052

Samuelson, M. L., & Schlumberger, D. (1992). *SPE Alternatives to Aromatics for Solvency of Organic Deposits*.

Saraji, S., Goual, L., & Piri, M. (2013). Dynamic adsorption of asphaltenes on quartz and calcite packs in the presence of brine films. *Colloids and Surfaces A: Physicochemical and Engineering Aspects*, *434*, 260–267. https://doi.org/10.1016/j.colsurfa.2013.05.070

Sato, S., Takanohashi, T., & Tanaka, R. (2005). Molecular weight calibration of asphaltenes using gel permeation chromatography/mass spectrometry. *Energy and Fuels*, *19*(5), 1991–1994. https://doi.org/10.1021/ef049672r

Scheu, & Wayne D. Kaplan. (2012). *Part I Basics and Methods*.

Serrano, E., & Figliola, A. (2009). Wavelet Leaders: A new method to estimate the multifractal singularity spectra. *Physica A: Statistical Mechanics and Its Applications*, *388*(14), 2793–2805. https://doi.org/10.1016/j.physa.2009.03.043

Sharma, A., Groenzin, H., Tomita, A., & Mullins, O. C. (2002). Probing order in asphaltenes and aromatic ring systems by HRTEM. *Energy and Fuels*, *16*(2), 490–496. https://doi.org/10.1021/ef010240f

Shedid, S. A. (2004a). An ultrasonic irradiation technique for treatment of asphaltene deposition. *Journal of Petroleum Science and Engineering*, *42*(1), 57–70. https://doi.org/10.1016/j.petrol.2003.11.001

Shedid, S. A. (2004b). *Influences of Ultrasonic Radiation on Asphaltene Behavior With and Without Solvent Effects*.

Sheykh Alian, S., Chemicals SdnBhd, D., Singh, K., Chemicals Sdn Bhd, D., Saidu Mohamed, A., Zaki Ismail, M., Gts, P., & Liza Anwar, M. (2013). *SPE 165912 Organic Deposition: From Detection and Laboratory Analysis to Treatment and Removal*.

Shi, C., Xie, L., Zhang, L., Lu, X., & Zeng, H. (2019). Probing the interaction mechanism between oil droplets with asphaltenes and solid surfaces using AFM. *Journal of Colloid and Interface Science*, *558*, 173–181. https://doi.org/10.1016/j.jcis.2019.09.092

Shidong Li, & Luky Hendraningrat. (2013). *Improved Oil Recovery by Hydrophilic Silica Nanoparticles Suspension: 2- Phase Flow Experimental Studies*.

Shojaati, F., Riazi, M., Mousavi, S. H., & Derikvand, Z. (2017). Experimental investigation of the inhibitory behavior of metal oxides nanoparticles on asphaltene precipitation. *Colloids*

and Surfaces A: Physicochemical and Engineering Aspects, *531*, 99–110. https://doi.org/10.1016/j.colsurfa.2017.07.087

Silverstein Robert M. (2014). *Spectrometric identification of organic compounds*.

Simon, S., Jestin, J., Palermo, T., & Barre, L. (2009). Relation between solution and interfacial properties of asphaltene aggregates. *Energy and Fuels*, *23*(1), 306–313. https://doi.org/10.1021/ef800548b

Speight, J. G. (2004). Petroleum Asphaltenes Part 1 Asphaltenes, Resins and the Structure of Petroleum. In *Oil & Gas Science and Technology-Rev. IFP* (Vol. 59, Issue 5).

Speight, J. G., & Moschopedis, S. E. (1982). *On the Molecular Nature of Petroleum Asphaltenes* (pp. 1–15). https://doi.org/10.1021/ba-1981-0195.ch001

Stephenson, W., & Chemical, N. C. (1991). *SPE SPE 22783 Asphaltene Deposition: Development and Application of Polymeric Asphaltene Dispersants*.

Syunyaev, R. Z., Balabin, R. M., Akhatov, I. S., & Safieva, J. O. (2009). Adsorption of petroleum asphaltenes onto reservoir rock sands studied by near-infrared (NIR) spectroscopy. *Energy and Fuels*, *23*(3), 1230–1236. https://doi.org/10.1021/ef8006068

Tazikeh, S., Sayyad Amin, J., Zendehboudi, S., Dejam, M., & Chatzis, I. (2020). Bi-fractal and bi-Gaussian theories to evaluate impact of polythiophene-coated Fe3O4 nanoparticles on asphaltene precipitation and surface topography. *Fuel*, *272*. https://doi.org/10.1016/j.fuel.2020.117535

Vargas, F. M., Creek, J. L., & Chapman, W. G. (2010). On the development of an asphaltene deposition simulator. *Energy and Fuels*, *24*(4), 2294–2299. https://doi.org/10.1021/ef900951n

Vargas, F. M., Garcia-Bermudes, M., Boggara, M., University, R., Punnapala, S., Abutaqiya, M., Mathew, N., Prasad, S., Khaleel, A., al Rashed, M., & al Asafen, H. (2014). *On the Development of an Enhanced Method to Predict Asphaltene Precipitation*.

Vernon-Parry, K. D. (2000). *Scanning Electron Microscopy: an introduction*.

Walker, J. M., & Rapley, R. (2008). *Molecular Biomethods Handbook, Second Edition*.

Wang, S., Xu, J., & Wen, H. (2014). The aggregation and diffusion of asphaltenes studied by GPU-accelerated dissipative particle dynamics. *Computer Physics Communications*, *185*(12), 3069–3078. https://doi.org/10.1016/j.cpc.2014.07.017

Wesolowski, D. J., Machesky, M. L., Palmer, D. A., & Anovitz, L. M. (2000). Magnetite surface charge studies to 2908C from in situ pH titrations. In *Chemical Geology* (Vol. 167). www.elsevier.comrlocaterchemgeo

Xia, S., Veony, E., & Kostarelos, K. (2019). Electro-deposition for asphaltene removal during heavy oil upgrading. *RSC Advances*, *9*(12), 6596–6602. https://doi.org/10.1039/c8ra10514f

Xue, J., Yu, Y., Bai, Y., Wang, L., & Wu, Y. (2015). Marine Oil-Degrading Microorganisms and Biodegradation Process of Petroleum Hydrocarbon in Marine Environments: A Review. *Current Microbiology*, *71*(2), 220–228. https://doi.org/10.1007/s00284-015-0825-7

Yarranton, H. W. (2005). Asphaltene self-association. *Journal of Dispersion Science and Technology*, *26*(1), 5–8. https://doi.org/10.1081/DIS-200040234

Yarranton, H. W., Alboudwarej, H., & Jakher, R. (2000). Investigation of asphaltene association with vapor pressure osmometry and interfacial tension measurements. *Industrial and Engineering Chemistry Research*, *39*(8), 2916–2924. https://doi.org/10.1021/ie000073r

Zahabi, A., Gray, M. R., & Dabros, T. (2012). Kinetics and properties of asphaltene adsorption on surfaces. *Energy and Fuels*, *26*(2), 1009–1018. https://doi.org/10.1021/ef2014698

Zhang, D. R., Oh, S. W., Hong, Y. P., & Kang, Y. S. (2005). Synthesis and characterization of a new adhesion-activator for polymer surface. *International Journal of Adhesion and Adhesives*, *25*(5), 371–378. https://doi.org/10.1016/j.ijadhadh.2004.07.008

Zhu, Y., Tian, F., Liu, Y., Cui, L., Dan, Y., Du, C., & Li, D. (2021). Comparison of the composition and structure for coal-derived and petroleum heavy subfraction by an improved separation method. *Fuel*, *292*. https://doi.org/10.1016/j.fuel.2021.120362

Zhu YH, Huang DK, & Zhan MX. (2016). *Analysis and characterization of medium/low temperature coal tar asphaltene*.

Zolotukhin A., & Ursin J. (2000). Fundamentals of Petroleum-Reservoir Engineering. *Norwegian Academic Press*.

Zoveidavianpoor, M., Samsuri, A., & Shadizadeh, S. R. (2013). The clean up of asphaltene deposits in oil wells. *Energy Sources, Part A: Recovery, Utilization and Environmental Effects*, *35*(1), 22–31. https://doi.org/10.1080/15567036.2011.619630